FIBREGY

This project has received funding from the European Union's Horizon 2020 research and innovation programme under grant agreement No 952966.

Development, engineering, production and life cycle management of improved FIBRE-based material solutions for the structure and functional components of large offshore wind enerGY and tidal power platforms

D2.5 (WP2): Multifunctional materials for Structural Health Monitoring (SHM) Diagnosis and Structural Performance Assessment.

Responsible Partner: TSI

Contributor(s): TSI, INEGI, CIMNE, CORSO, IXBLUE, ENEROCEAN

This project has received funding from the European Union's Horizon 2020 research and innovation programme under grant agreement No 952966.

DOCUMENT INFORMATION TABLE

CONTRACT NUMBER:	952966	
PROJECT ACRONYM:	FIBREGY	
PROJECT COORDINATOR:	CIMNE	
DOCUMENT RESPONSIBLE	TÉCNICAS Y SERVICIOS DE INGENIERÍA S.L.	TSI
DELIVERABLE TYPE:	Report	
DOCUMENT TITLE:	D2.5 - Multifunctional materials for SHM diagnosis and structural performance assessment	
DOCUMENT ID:	D2.5	
DISSEMINATION LEVEL:	PU: Public	
FILENAME:	FIBREGY_D.2.5_Development of multifunctional materials_Master File_TSI	
STATUS:	Second version	

Authoring & Review

PREPARED / REVIEWED BY				
Name	Role	Partner	Date	Comments
Author	Cristóbal García	TSI	09/02/2021	
Author	Bárbara Fernandes	INEGI	24/11/2021	Section 3.4, 3.5
Reviewer 1	Rui Mendes	INEGI	24/11/2021	Section 3.4, 3.5
Reviewer 2	Fermin Otero	CIMNE	01/03/2022	

This project has received funding from the European Union's Horizon 2020 research and innovation programme under grant agreement No 952966.

EXECUTIVE SUMMARY

One of the major challenges of the FIBREGY project is to develop a new generation of Fibre Reinforced Polymers (FRP) smart materials that can be used to diagnose the integrity of the W2Power Offshore Wind Turbine. To achieve this goal, it has been investigated the feasibility of embedding sensors in the FRP materials used for the construction of the tower. The procedure to develop this innovative technology has been divided into three steps:

Selection of sensors for multifunctional materials

The first step consists of the selection of the most appropriate sensors to be embedded in the 1:6 scale FRP-based towers installed in the W2Power floating platform. To achieve this goal, a two-stage testing strategy was carried out in order to down-select relevant accelerometers and strain gauges for the diagnosis of the integrity of the FRP-based tower:

- Stage I: Preliminary selection of five sensors with potential to be implemented into the Structural Health Monitoring (SHM) system of the tower. The sensors preselected in this initial stage fulfill these minimum requirements: wide measurement range, high sensitivity, small size, capability to operate in aggressive sea environments, acceptable resistance to temperatures, and cost-effectiveness;
- Stage II: Final selection of sensors for their integration into the FRP multifunctional materials based on the criterion given above.

Feasibility study to evaluate the integration of sensors into FRP materials

The second step is focused on the selection of the optimum strategy for the integration of the sensors into FRP-based materials that will be used for the construction of the W2Power tower. The main objectives are twofold:

- With the aim to evaluate the feasibility of the technology, FRP multifunctional materials have been manufactured with sensors embedded in the backing of the dry coating by INEGI's research institute. The performance of this new generation of FRP multifunctional materials has been validated and verified in the TSI laboratory.
- A preliminary definition of the location of the sensor network in the structural element to be monitored (W2Power Towers) is given in the deliverable. The input of this task is of relevant importance for the definition of the SHM system of the towers in Task 4.4.

Development of SHM system for the inspection and diagnosis of the structural integrity of Floating Offshore Wind Turbines (FOWTs)

The final step deals with the development of a non-destructive SHM methodology for the inspection and diagnosis of the structural integrity of the 1:50 scale tower of W2Power Wind Turbine. The main objectives are drawn below:

- Evaluate the feasibility of a series of Key Performance Indicators (KPIs) for the damage assessment of the FRP materials based on natural frequencies, damping, and mode shapes.

This project has received funding from the European Union's Horizon 2020 research and innovation programme under grant agreement No 952966.

- To validate the non-destructive SHM methodology at the laboratory scale. For such purpose, 1:50 scale FRP towers with different types and sizes of delamination failures are tested. The integrity of the FRP-based towers will be assessed based on the comparison between the modal parameters of the medium-scaled specimens in pristine and damaged conditions.
- Evaluate the feasibility of a series of key performance indicators based on natural frequencies, damping, and mode shapes for the diagnosis of the tightening torques of the bolted joints of the W2Power tower connections. To achieve this goal, the effect of the tightening torques on the natural frequencies, and damping of the towers has been investigated by the research team using a modal analysis test.

The main output of this task is to apply this non-destructive methodology for the inspection and monitoring of the 1:6 scale FRP-based towers integrated into the W2Power Platform deployed in the PLOCAN site area at the Canary Islands. Indeed, this methodology will be used to test the integrity of one of the demonstrators built in WP6 before and after the tower has operated for a certain period of time.

This project has received funding from the European Union's Horizon 2020 research and innovation programme under grant agreement No 952966.

TABLE OF CONTENTS

This project has received funding from the European Union's Horizon 2020 research and innovation programme under grant agreement No 952966.

This project has received funding from the European Union's Horizon 2020 research and innovation programme under grant agreement No 952966.

LIST OF FIGURES

This project has received funding from the European Union's Horizon 2020 research and innovation programme under grant agreement No 952966.

This project has received funding from the European Union's Horizon 2020 research and innovation programme under grant agreement No 952966.

LIST OF TABLES

This project has received funding from the European Union's Horizon 2020 research and innovation programme under grant agreement No 952966.

NOMENCLATURE / ACRONYM LIST

Acronym	Meaning
AE	Acoustic Emission
CBM	Condition-Based Maintenance
FFT	Fast Fourier Transform
FOS	Fibre Optic Sensors
FOWT	Floating Offshore Wind Turbine
FRP	Fibre Reinforced Polymers
GPS	Global Positioning System
IP	Ingress Protection
KPI	Key Performance Indicators
OMA	Operational Modal Analysis
REOP	Renewable energy offshore platform
SHM	Structural Health Monitoring

This project has received funding from the European Union's Horizon 2020 research and innovation programme under grant agreement No 952966.

1. SCOPE OF THE DOCUMENT

One of the major challenges of the project is to develop a new generation of Fibre Reinforced Polymers (FRP) smart materials that can be used to diagnose the integrity of the W2Power Offshore Wind Turbine. To achieve this goal, it has been investigated the feasibility of embedding sensors (accelerometers, strain gauges, optical fibres, etc.) in the FRP materials used for the construction of the tower. The procedure to develop this innovative technology has been divided into three steps:

- Selection of sensors for multifunctional materials

  The first step consists of the selection of the most appropriate sensors to be embedded in the 1:6 scale FRP-based towers installed in the W2Power floating platform. To achieve this goal, a two-stage testing strategy was carried out in order to down-select relevant accelerometers and strain gauges for the diagnosis of the integrity of the FRP-based tower:

  - Stage I: Preliminary selection of five sensors with potential to be implemented into the Structural Health Monitoring (SHM) system of the tower. The sensors preselected in this initial stage fulfill these minimum requirements: wide measurement range, high sensitivity, small size, capability to operate in aggressive sea environments, acceptable resistance to temperatures, and cost-effectiveness;
  - Stage II: Final selection of sensors for their integration into the FRP multifunctional materials based on the criterion given above.

  The sensors selected operate in the sea environment that is characterized by a high level of humidity, salinity, corrosion, or fatigue due to the cyclic loads of the sea waves/wind. With the aim to guarantee the correct operation of the sensor through its entire life cycle, the sensors will be protected from the aggressive environmental conditions of the sea through the application of dry coatings and protective paints. Eventually, the Ingress Protection (IP) scale of the sensors will be sufficient to avoid the sensors being damaged due to the penetration of solid and liquid particles. The information of this task will be used for the definition of the protection requirements of the dry coatings in Task 2.2.

- Feasibility study to evaluate the integration of sensors into FRP materials

  The second step is focused on the selection of the optimum strategy for the integration of the sensors into FRP-based materials that will be used for the construction of the W2Power tower. The main objectives are twofold:

  - With the aim to evaluate the feasibility of the technology, FRP multifunctional materials have been manufactured with sensors embedded in the backing of the dry coating by INEGI's research institute. The performance of this new generation of FRP multifunctional materials has been validated and verified in the TSI laboratory;
  - A preliminary definition of the location of the sensor network in the structural element to be monitored (W2Power Towers) is given in the deliverable. The input of this task is of relevant importance for the definition of the SHM system of the towers in Task 4.4.

This project has received funding from the European Union's Horizon 2020 research and innovation programme under grant agreement No 952966.

- Development of SHM for the inspection and diagnosis of the structural integrity of Floating Offshore Wind Turbines (FOWTs)

The final step deals with the development of a non-destructive SHM methodology for the inspection and diagnosis of the structural integrity of the 1:50 scale tower of W2Power Wind Turbine. The main objectives are drawn below:

- Evaluate the feasibility of a series of Key Performance Indicators (KPIs) for the damage assessment of the FRP materials based on natural frequencies, damping, and mode shapes.
- To validate the non-destructive SHM methodology at the laboratory scale. For such purpose, 1:50 scale FRP towers with different types and sizes of delamination failures are tested. The integrity of the FRP-based towers will be assessed based on the comparison between the modal parameters of the medium-scaled specimens in pristine and damaged conditions.
- Evaluate the feasibility of a series of key performance indicators based on natural frequencies, damping, and mode shapes for the diagnosis of the tightening torques of the bolted joints of the W2Power tower connections. To achieve this goal, the effect of the tightening torques on the natural frequencies, and damping of the towers has been investigated by the research team using a modal analysis test.

The main output of this task is to apply this non-destructive methodology for the inspection and monitoring of the 1:6 scale FRP-based towers integrated into the W2Power Platform deployed in the PLOCAN site area at the Canary Islands. Indeed, this methodology will be used to test the integrity of one of the demonstrators built in WP6 before and after the tower has operated for a certain period of time.

This project has received funding from the European Union's Horizon 2020 research and innovation programme under grant agreement No 952966.

2. SELECTION OF SENSORS FOR MULTIFUNCTIONAL MATERIALS

A sensor can be defined as an electronic device that converts ambient energy (e.g. pressure load, temperature, etc.) into an electrical signal, which is proportional to the magnitude of the input. A well-known classification of sensors consists of their operating principle that can be ranked into the following categories: piezoelectric (1), capacitive (2), optical (3), triboelectric (4), and resistive sensors (5). Since a long time ago, these devices have been used in multiple everyday applications as per example vehicle safety (6), structural health monitoring (7), patient monitoring in medical applications (8), and inspection of machinery and industrial equipment (9), among others.

The main purpose of subtask 2.5.1 is to carry out the selection of the most appropiate sensors for the diagnosis of the structural integrity of the 1:6 scale FRP-based towers of the W2Power floating platform deployed at the PLOCAN testing site area in the Canary Islands. To achieve this goal, a two-stage testing strategy was carried out in order to down-select relevant sensors for the diagnosis of the integrity of the FRP-based tower:

- Stage I: Preliminary selection of five sensors with potential to be implemented into the SHM system of the tower. The sensors preselected in this initial stage fulfill these minimum requirements: wide measurement range, high sensitivity, small size, capability to operate in aggressive sea environments, acceptable resistance to temperatures, and cost-effectiveness;
- Stage II: Final selection of sensors for their integration into the FRP multifunctional materials based on the criterion given above. A strain gauge and accelerometer are selected at this final stage for their integration into the FRP multifunctional materials.

The criteria for the selection of the most appropiate sensors to be integrated into the FRP multifunctional materials is described below:

- From the sensor's performance point of view, the sensors selected possess a high sensitivity, linearity, and fast response time in a wide measurement range;
- From the enviromental perspective, it is of paramount importance to guarantee that the sensors can operate in the most extreme weather conditions "humidity, salinity, cyclic sea wave impacts";
- From the manufacturing side, it is essential to select small-size sensors that can be easily embedded in the interior of the fiber-based polymeric materials without inducing undesirable delamination failures and higher stress levels;
- From the economic point of view, the sensors selected for the consortium should be cost-effective in order to make this inspection technology affordable for their commercial implementation in the market.

The rest of Section 2 is arranged as follows: Section 2.1 provides an internal guide of the conventional sensors used for the SHM community for the inspection and maintenance of FOWTs. Section 2.2 sheds light on the considerations to be taken for the selection of sensors to be integrated into the interior of the FRP multifunctional materials. Special emphasis should be paid to the selection of sensors with an appropriate Ingress Protection (IP) scale to withstand the aggressive environmental conditions of the sea (e.g., sea-waves cyclic loads salinity, humidity, etc.). Section 2.3 shows a comparison of the performance of the sensors selected in terms of sensitivity, measurement range,

This project has received funding from the European Union's Horizon 2020 research and innovation programme under grant agreement No 952966.

mounting method, resistance to high temperatures, and other KPIs. Eventually, the accelerometers and strain gauges selected for their integration into the FRP laminar materials are presented.

This project has received funding from the European Union's Horizon 2020 research and innovation programme under grant agreement No 952966.

2.1. GUIDE FOR SELECTION OF SENSORS FOR SHM AND CBM OF FOWTs

The focus of Section 2.1 is to provide a guide to carry out an appropriate selection of sensors to diagnose the structural condition of floating offshore wind turbines (FOWTs). All of this is done to proportionate to the readers of this deliverable the first view of relevant sensor systems that can be of interest for the maintenance of the W2Power Wind Offshore Platform owned by EnerOcean. The sensors that can be of interest to carry out the continuous monitoring of the drive train, floating platform, blades, tower and mooring lines of FOWTs are detailed in Figure 1.

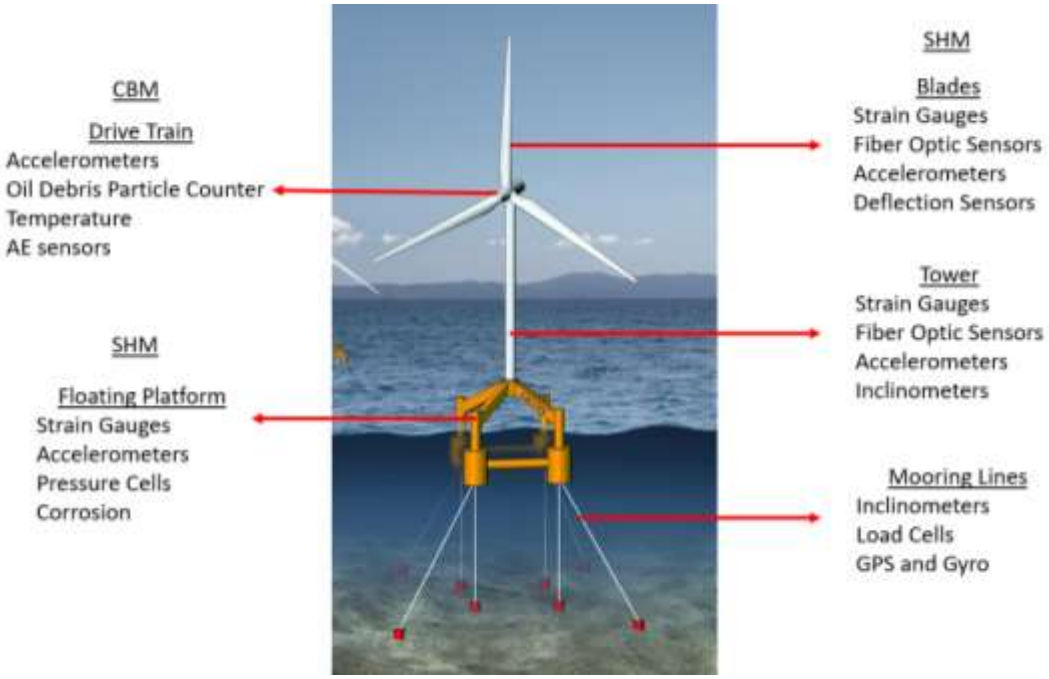

Figure 1 – Definition of sensors for the CBM and SHM of FOWTs.

2.1.1. CBM of Drivetrain

It is well known that the most popular commercially SHM systems applied for the Condition-Based Maintenance (CBM) of the rotating components of the drivetrain (bearings, shafts, or gearwheels) are vibration-based. The early detection of changes in the vibration signature of the critical components is essential to get a deeper understanding of the condition of the rotative machinery and FRP structural components of the FOWTs. Therefore, there are available a large number of commercial vibration-based systems to monitor the condition of the drivetrain in wind onshore turbines. The fundamental principle for the detection of mechanical defects is based on the fact that the failures of rotating machinery lead to excessive vibrations levels that are characterized by singular vibration Fast Fourier Transform (FFT) patterns.

Oil-based systems are also frequently applied for the inspection and maintenance of the gearbox with a dual purpose: 1st) the assessment of the quality of the lubricant oil, and 2nd) the quantification of the amount of wear debris that is a clear indicator of mechanical faults in the gearbox and thus, provided valuable information about their damaged state.

Another monitoring approach that is very popular among the SHM community for the early detection of detection and propagation of faults in the drivetrain is the technique of Acoustic Emission (AE).

This project has received funding from the European Union's Horizon 2020 research and innovation programme under grant agreement No 952966.

This approach of based on the use of high-frequency transient elastic waves that are typically in the range 20 kHz-1MHz.

2.1.2. SHM of Wind Blades

A very popular approach that is predominantly applied for the SHM community in Wind Onshore Platforms focused on the assessment of stress/strains. For such purposes, strain gauges and fibre-optical strain gauges are installed in the most loaded points of the FOWT like the route of the blades or the tower base.

Vibration-based SHM techniques like Operational Modal Analysis (OMA) have been frequently applied for the maintenance of towers and wind-blades. These vibration-based methods are fundamentally based on the fact that the shift of the modal parameters can be used as an efficient method to detect the stiffness properties of a component and therefore, its damage state.

Another commercial system for the inspection of blades lies on the basis of the deflection of the blade that can be utilized for monitoring the bending stiffness of the blade.

2.1.3. SHM of Tower

A conventional technology used for the structural inspection of Towers is based on the use of Strain Gauges. These types of sensors are installed in the critical parts as the base of the tower (the most loaded point of the tower). Alternatively, another popular monitoring approach is based on the use of Optical-Fibre sensors for strain measurement which present important advantages in terms of environmental resistance, but the limitation of being significantly more expensive than strain gauge sensors.

Vibration-based systems have been commonly used to monitor the vibration levels of the tower. This technique is based on the fact that the dynamic properties (eigen-frequency, damping, mode shapes) of these structural components are altered. Generally, small damages could be correlated to high frequency local modes, while large damages have an influence on the global modes.

Inclination sensors can be also potentially implemented as an additional measurement to monitor the stability of the tower.

2.1.4. SHM of Floating Platform

The Floating Platform is subjected to corrosion and fatigue phenomena due to the permanent impact of sea waves along with the harsh environmental conditions of the sea. Eventually, the most common sensors to monitor the Floating Platform are Strain Gauges, Accelerometers, Pressure Cells, and Corrosion. The cyclic impacts of the sea waves can be monitored by pressure cells to assess the impact of breaking waves. In parallel, the phenomenon of fatigue monitoring can be potentially inspected using strain or vibration measurements.

2.1.5. SHM of Mooring Lines

This project has received funding from the European Union's Horizon 2020 research and innovation programme under grant agreement No 952966.

A critical point of the Floating Offshore Wind Turbines is the mooring lines. Nowadays, the most common sensors installed for the inspection of the mooring lines are load cells, inclinometers and Global Positioning Sensors. A very straightforward approach to detect mooring line failures consists of the use of load cells, however this technology has not been found to be reliable when the mooring line load is not very high. Regarding the inclinometers, a direct measurement of a line angle can be directly used to estimate the mooring line tensions, with the advantages of easy implementation and affordable cost. Alternatively, the use of a Global Positioning System (GPS) has been proven as an efficient technology to identify failures in the mooring lines. However, the effectiveness of this technology depends upon many factors like the characteristics of the mooring system, water depth, or environmental conditions of the sea.

Please note that a complete study of relevant Key Performance Indicators for the inspection and maintenance of FOWT platforms will be included in the context of D4.8 “Report on recommendations for predictive maintenance of FRP-based OWTP platforms” (M30).

This project has received funding from the European Union's Horizon 2020 research and innovation programme under grant agreement No 952966.

2.2. CONSIDERATIONS FOR EMBEDDING OF SENSORS IN THE FRP TOWER OF THE W2POWER WIND TURBINE

The main objective of this paragraph is to lay the foundations for the selection of the right sensors to carry out the diagnosis of the condition of the FRP multifunctional materials used in the construction of the FRP tower. The following parameters are considered for the selection of the sensors that will be part of the SHM system: sensitivity, mounting method, range of measurement, possibility to operate in extreme environments, size and geometric shape of the sensors and ingress protection rating scale. All of this is done to proportionate to the readers an interesting guide for the selection of the most appropriated sensor devices for offshore applications.

2.2.1. Sensitivity

The sensitivity is usually defined as the ratio between the output signal with respect to a specific physical quantity (input). The sensitivity given by the accelerometers suppliers is commonly expressed as mV/g. The sensitivity recommended to carry out measurements in rotative machinery is around 100 mV/g.

2.2.2. Mounting Method

The sensitivity of the sensor is strongly influenced by the mounting method of the sensor. In general, the mounting methods recommended for permanent mounting are “studs”, “adhesives”, and “cementing pads”, while the mounting methods suggested for walkaround monitoring programs are “magnets” and “probe tips”. Below, the different typologies of mounting set-ups are listed in order of greater to lesser measurement frequency response.

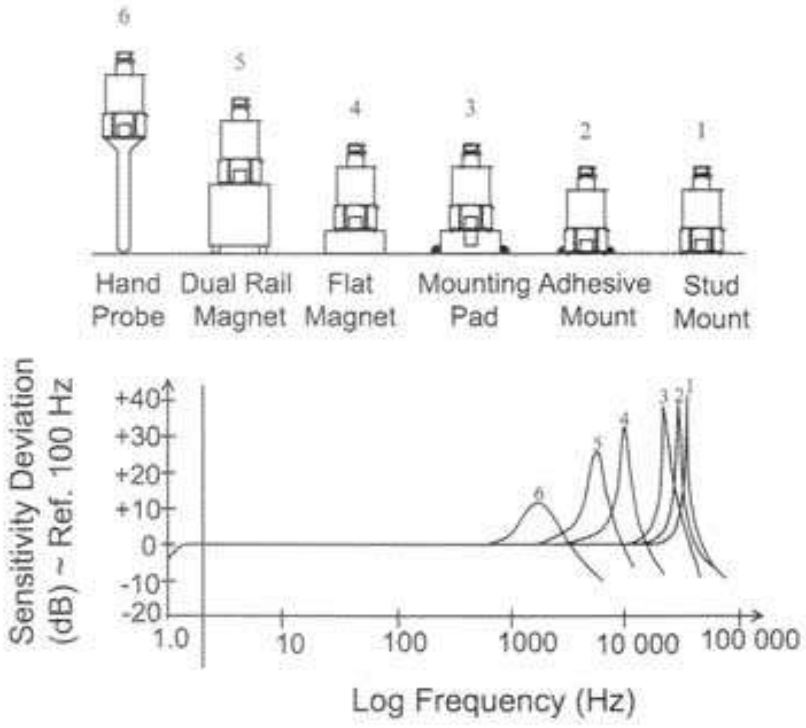

Figure 2 – Effects of the mounting method on resonant frequency.

This project has received funding from the European Union's Horizon 2020 research and innovation programme under grant agreement No 952966.

Figure 2 provides a representation of the six mounting methods (hand probe, flat/dual magnet, mounting pad, adhesive/stud mount) of the sensors along with their corresponding resonant frequency. From the figure, it can be appreciated that the hand probe tip (6) has the lowest natural frequency and therefore, the lower operating range. On the contrary, if we look at the right side of the figure, it is noticed that the stud mount (1) has the highest resonant frequency and widest measurement range. As a general conclusion, it can be said that the criteria for the selection of the mounting configuration depend primarily on the measurement requirements (e.g. frequency, operating range, etc.) of the test.

- Threaded stud mounting is the option that allows the widest dynamic measurement range, high-frequency testing, and better resistance to harsh environments as for example the aggressive climate conditions of the sea environment. The mounting with studs is the best option for permanent monitoring systems. However, it should be pointed out that the delamination is an inter-ply failure phenomenon induced by drilling, which has been recognized as an expected major damage when drilling composite.

- Adhesive is the best alternative to stud mounting for the cases where the structure/machinery can not be drilled. For this particular case, the adhesive plays a key role to guarantee good adhesion in the long term, and therefore it is of vital importance to select durable adhesives that can be applied in the most hostile environmental conditions (e.g. extreme temperatures, vibration, impact and shock). The main disadvantage is that the removal of the adhesive for the re-use of the sensor will usually damage the sensors if removal is required. The range of frequencies is slightly inferior to the one foreseen in the stud mountings.

- Cementing pads present interesting advantages as for example the high-frequency capabilities of stud mounts without the need for drilling into the structure. The range of frequencies is high but inferior to stud and adhesive mountings.

- Magnets tips are the best option for temporary mounting. Another interesting aspect of magnet tips is that allow the possibility to carry out the measurement on flat surfaces (e.g. bulkhead), but also for measuring in curved surfaces by using two-pole magnetic mounting bases (e.g. tower, pipes, etc.). The limitation of this technology is that the frequency range is reduced when compared to stud or adhesive mounts.

- Probe tips are an interesting alternative for walkaround monitoring programs and it is highly recommended for measurements in hard-to-reach areas, where it is not possible to install permanent mountings such as threaded studs, or cementing pads. The probe tip should be made of steel and be no longer than six inches. The major inconvenience is that the frequency range of this mounting method is dramatically reduced when compared to stud or adhesive mounts.

This project has received funding from the European Union's Horizon 2020 research and innovation programme under grant agreement No 952966.

The immediate conclusion is that closer contact between the sensor and the FRP structural component will lead to an enhanced ability of the sensor to couple and measure the signals. Therefore, it will be required versatile accelerometers and strain gauges with an appropriate frequency response for the inspection and maintenance of the FRP tower. The sea trials in the 1:6 prototype W2Power turbine at Canary Islands (WP6) will be based on the use of permanent mountings such as "stud", "adhesives", and "cementing pads", which show the best durability for the long-term period measurements in the aggressive conditions of the sea. Among the above-mentioned options, the use of "stud mountings" is highly recommended for steel-based components, while "adhesives / cementing pods" are the best alternative to stud mounting for the cases where the structure/machinery can be damaged by drilling (e.g. FRP structural components).

2.2.3. Range of measurement

Accelerometers with a broad frequency range are suitable for the inspection and maintenance of the rotative components of FOWTs as rotors, gearboxes, generators, as well as for the inspection of wind turbine blades/towers.

- The low-frequency signals do not show a good damage resolution for the detection of internal defects. This can be explained by the fact that low-frequency excitations give spatial wavelengths which are far larger than the extent of the damage as detailed in Figure 3. For this reason, low-frequency waves are quite insensitive to the damage because the signal does not interact with the defect.
- The high-frequencies range (above 300 Hz) has a good damage-detection resolution for the detection of defects. Therefore, it is highly recommended the use of ultrasonic frequencies as a practical tool for the identification of damages at the early and intermediate stages (small- and medium-size defects). This is well represented in Figure 3, where it can be easily deduced that the high-frequency range gives spatial wavelengths which are smaller than the extent of the damage, and hence, this type of high-frequency waveform has the capabilities to penetrate the interior of the damage and excite it.

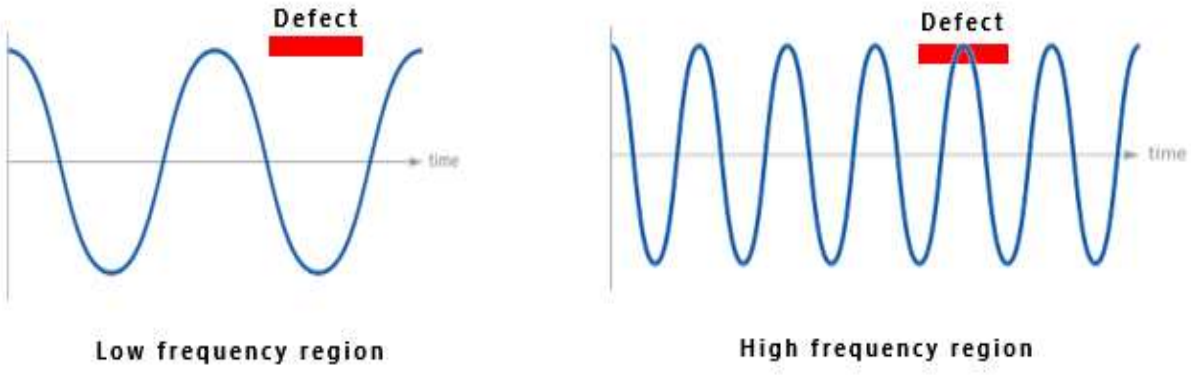

Figure 3 – Effect of low frequency and high frequency waves on the defects.

This project has received funding from the European Union's Horizon 2020 research and innovation programme under grant agreement No 952966.

If we look at the vibration tests to be scheduled during the sea trials (WP6) of the W2Power wind turbine, we can expect the following behaviour:

- The low-frequency region of the FFT spectrum is mainly affected by the climate conditions of the sea and does not provide valuable information on the defects of the FRP structural components. Generally, the periodic excitations of the wind excitations are found on the range of frequencies below 0.2 Hz, while the impacts of the sea waves with the wind turbine will be found on the low-frequency range of frequencies between 0.2 and 0.5 Hz. As mentioned above, the information given in the low-frequency region of the FFT spectrum is not sensitive to the presence of defects.
- The information given in the high-frequency region of the FFT spectrum provides valuable information about the rotation of the blades, shift, and other rotative components of the wind turbines. The high-frequency modes of the FRP structure provide more precise information about the presence of defects, and therefore it is recommended for the detection of internal defects as for example delamination damage, cracks, connections breakages, etc.

Through the ocean sea tests carried out in the 1:6 prototype of the W2Power, the vibration signals induced by the impact of the sea waves as well as the rotation of the rotor blades will be recorded using a large number of accelerometers distributed over the length of the FRP-based towers.

To carry out the experimental trials in the prototype 1:6 of the W2Power turbine at Canary Islands (WP6), the sensors selected should have a broad range of frequencies. Therefore, it will be required the implementation of sensors with appropriate resolution in the low-frequency range to enable the detection of the low-frequency motions of the FRP tower due to the cyclic loads of the sea waves and wind as well as a good resolution in the high-frequency range (up to 2000 Hz) in order to maximize the possibilities for the detection of defects.

2.2.4. Possibility to operate in extreme environments

The “temperature range” of the sensor is commonly defined as the temperature span, given by the temperature extremes, over which the sensor will perform without failure. With the aim to guarantee the correct operation of the sensor through its entire life cycle, a wide temperature response is required in the sensors to be embedded into the new multifunctional materials. For the selection of the ideal temperature range, we recommend looking at these two aspects:

- The high temperatures applied during the manufacturing process of the FRP materials may damage the internal electronic systems of the sensor devices due to several reasons as for example misalignment of the piezoelectric crystal dipoles, breakage of the connectors, electrical wires, etc. To avoid undesirable failures, the sensor selected should be able to withstand the curing temperature of the polymer resin during the infusion process. It is possible to find sensors in the market with superior resistance to high-temperature that are designed specifically for their use in extremely high-temperature environments such as high-temperature furnaces and gas turbines. A good example of this can be the model 6245 provided by Meggitt which has a temperature resistance of up to 815 °C. This typology of sensors with extended temperature range is significantly more expensive than other commercial sensors due to the superior level of protection required for the sensor to withstand high temperatures, which

limits the massive application of these commercial sensors in structural health monitoring systems.

- In parallel, it is also pointed out that the sensors applied for the monitoring of the Floating Offshore Tower will be subjected to the aggressive sea environment that it characterized by a high level of humidity, salinity, corrosion, or fatigue due to the cyclic loads of the sea waves/wind.

As a general rule, the sensors selected should be able to operate in a large range of temperatures. The sensors selected to be embedded into the FRP multifunctional materials are within the temperature threshold from -50 ºC to 120 ºC. Special attention should be paid to the curing and exothermic reaction (resulting in increased temperature) of the resin during the infusion procedure that can damage the electronic systems integrated into the sensor devices.

2.2.5. Size of the sensor

The size of the sensors is a critical factor that needs to be carefully considered by the materials team during the infusion of the sensors. If we referred to the size, it is important to bear in mind that the sensors selected should be small enough to be successfully integrated into the FRP materials without breaking the external dry coating. **Figure 4** displays different sorts of accelerometers applied for the inspection of machinery/structures in the market. The smallest size sensor shown in the front row is a good representation of the maximum sensor size device proposed for their integration into the FRP multifunctional materials. On the contrary, the rest of the sensors shown in **Figure 4** are not suggested for this task due to their large size, which generates mechanical discontinuities in the laminar material to lead to a reduction of the mechanical performance of the FRP laminar materials.

In conclusion, the sensors to be embedded into the FRP multifunctional materials are only limited to small-size sensors with the main objective to avoid discontinuities that may affect the mechanical performance of the composite laminate material.

Figure 4 – Most commonly used accelerometers for inspection of machinery/structures in the market (10).

This project has received funding from the European Union's Horizon 2020 research and innovation programme under grant agreement No 952966.

2.2.6. Geometric shape of the sensor

Another aspect of interest for the selection of the sensors is their geometric shape that can be classified as sharp and rounded. It is evident that sensors with sharp shapes will create large tensional stresses that can damage the integrity of the dry coatings, while sensors with curved shapes are expected to generate lower tensional stress reducing the possibility to damage the dry coatings during the manufacturing process.

As a general rule, it can be said that the sensors with sharp shapes are not recommended for their integration into the FRP multifunctional materials owing to their capacity to generate large tensional stresses, and therefore a requirement of the sensors is the rounded/spherical geometry.

2.2.7. Ingress Protection (IP) rating

It is widely known that the electrical systems of the sensors can be damaged due to the penetration of solid and liquid particles. Thus, another factor of interest to be considered for the selection of the sensors to be installed in the W2Power towers is the IP scale, which defines how well the sensors will be protected from contact with dust and water. The code of the IP scale is based on two numbers, which are provided as follows: IP-XX.

- The first digit number designates the level of protection of the sensors against solid objects on a scale of 0 (no protection) to 6 (dust-tight protection);
- The second number designates the device's protection against liquids, where the minimum level of protection is referred to as 0 (no protection) and the maximum level of protection stands for 8 (protection against long periods of immersion).

For the sake of clarification, **Table 1** summarizes the levels of protection required against solids and liquids defined in the IP Rating table. This information is of critical importance for the acquisition of the sensors to be installed in the SHM system.

First Digit Number	Protection provided against solids	Second Digit Number	Protection provided against liquids
0	No protection	0	No protection
1	Protection against objects > 50 mm (e.g. bird strike)	1	Protection against vertically dripping water
2	Protection against objects > 12.5 mm (e.g. fingers)	2	Protection against angled dripping water
3	Protection against objects > 2.5 mm (e.g. hailstone)	3	Protection against sprayed water.
4	Protection against objects > 1.0 mm (e.g. wires)	4	Protection against splashed water.
5	Partial protection against dust	5	Protection against low pressure water jets.

This project has received funding from the European Union's Horizon 2020 research and innovation programme under grant agreement No 952966.

6	Full protection against dust	6	Protection against high pressure water jets.
		7	Protection against the effects of immersion at a depth of 1 m.
		8	Protection against the effects of immersion for a long time period

Table 1 – Level of protection required against solids and liquids (Ingress Protection Rating Table).

The IP scale of the sensors recommended for the sensor devices applied for the structural health monitoring system of the FRP tower is IP 67 which provides full protection against dust and the effects of immersion at a depth of 1 m. The selection of the IP scale is attributed to the aggressive environmental conditions of the open sea like wind, rain, sea waves, humidity, salinity, among others.

This project has received funding from the European Union's Horizon 2020 research and innovation programme under grant agreement No 952966.

2.3. CONSIDERATIONS FOR SELECTION OF CABLES AND CONNECTORS OF SHM/CBM SYSTEM

Selecting the right cable assembly is highly dependent on the environment in which the sensor will operate. With a view to the inspection structural health monitoring systems to be installed at W2Power tower, cables with good resistance to the aggressive environmental conditions of the sea (e.g. high humidity, salinity, water, dust, etc.) and acceptable chemical and oil resistance are required. The technical aspects to be considered during the selection of the cables and connectors are defined below:

- In terms of the IP scale, the minimum ingress protection rating recommended for the sensor devices applied for the monitoring of the FRP tower is IP 67 which provides full protection against dust and the effects of immersion at a depth of 1 m.
- Another aspect of interest is the cable length, the signal losses due to the length of the cable need to be considered by the engineering team during the definition of the structural health monitoring system of the tower. Figure 5 displays the maximum cable length as a function of the frequency of interest/supply current. From the figure, it can be deduced that the higher is the frequency of interest, the greater are the signal losses in the cable, and therefore, the use of long cables can be problematic for high-frequency signals. Besides that, it can be observed that the increment of the supply current from 2mA to 10 mA enables the application of longer cables in the structural health monitoring system, and it is therefore a possible solution for the problem of the cable length.

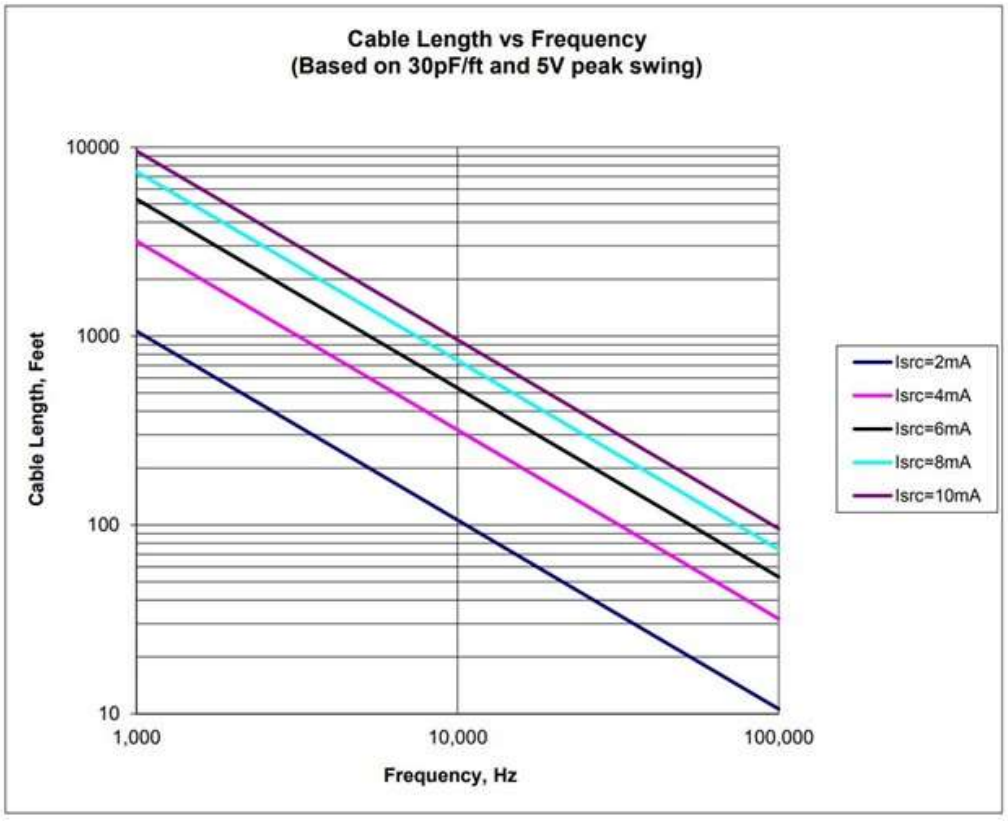

Figure 5 – Cable Length as a function of the frequency of interest and supply current.

This project has received funding from the European Union's Horizon 2020 research and innovation programme under grant agreement No 952966.

The following three aspects are to be considered during the definition of the SHM system of W2Power towers: 1st) the degree of protection of the sensors should be at least IP 67 with the aim to obtain adequate protection to the aggressive environmental conditions of the sea (e.g. high humidity, salinity, water, dust, etc.). 2nd) The cables for the instrumentation of the monitoring system need to be securely attached using flanges, cable covers, etc. in order to avoid technical problems during the instrumentation of the tower. 3rd) The length of the cables should be appropriated to ensure an appropriate transmission of the signals recorded by the sensors to the acquisition system.

This project has received funding from the European Union's Horizon 2020 research and innovation programme under grant agreement No 952966.

2.4. SENSOR SELECTION CHART

As stated in the introduction, a two-stage testing strategy was carried out in order to down-select relevant sensors for the diagnosis of the integrity of the FRP-based tower:

- Stage I: Preliminary selection of five sensors with potential to be implemented into the SHM system of the tower. The sensors preselected in this initial stage fulfill these minimum requirements: wide measurement range, high sensitivity, small size, capability to operate in aggressive sea environments, acceptable resistance to temperatures, and cost-effectiveness;
- Stage II: Final selection of one sensor for their integration into the FRP multifunctional materials based on the criterion given above. A strain gauge and accelerometer are selected at this final stage for their integration into the FRP multifunctional materials.

Table 2 lists the accelerometers that have been pre-selected in the first stage to investigate their potential implementation into the SHM system of the tower. From the sensor's performance point of view, we will look at sensors with high sensitivity and a wide measurement range that provide information about the dynamic behaviour of the structure not only in the low-frequency range but also in the high-frequency range. From the environmental point of view, we require sensor devices with acceptable resistance to the most extreme weather conditions in the open sea and therefore, the minimum ingress protection rating allowable for the sensors is IP 67. From the manufacturing point of view, we will consider small-size and cost-effective sensors that can be easily embedded in the fiber polymeric materials of the tower. The sensor model "12M1B" was selected for their integration into the FRP multifunctional materials due to their small size and weight that will facilitate the embedding process.

Model	Sensitivity	Sensitivity Tolerance (%)	Mounting Method	Frequency Response (Hz)	Temperature Range (°C)	Thickness (mm)	Weight (g)
7591A	40 mV/g	5	Board Mount	0-1000	-54 to 121	3.43	7
2222D	1.1 pC/g		Adhesive	0.1-12000	-55 to 175	4.1	1
12M1B	1.9 pC/g	5	Adhesive	1-2000	-65 to 150	1.4	0.12
7290EM5	66 mV/g	5	4-40 Screw	0-1000	-55 to 121	7.6	10
7293A	40 mV/g	5	4-40 Screw	0-1000	-55 to 121	7.6	14
7290A	66 mV/g	5	4-40 Screw	0-800	-55 to 121	7.6	12
7290E	40 mV/g	5	4-40 Screw	0-2000	-55 to 121	7.6	10
7290D	75 mV/g	5	4-40 Screw	0-800	-55 to 121	9.1	15
787A	100 mV/g	5	¼-28 Screw	0.5-10000	-55 to 120	26.42	145
787T	100 mV/g	5	¼-28 Screw	0.5-12000	-50 to 120	26.42	145

Table 2 – Sensor selection chart for the accelerometers.

This project has received funding from the European Union's Horizon 2020 research and innovation programme under grant agreement No 952966.

Table 3 provides a list of strain gauges that have been pre-selected for the engineering team to evaluate their sensing capabilities to monitor the condition of the tower. A number of factors such as Strain Gauge Dimensions, Strain Range, Temperature Range have been considered for the preliminary selection of the gauges. The definition of the parameters are detailed below:

- Strain Gauge Dimensions: The length is a parameter of relevance for the strain gauge selection, and therefore, it is usually the first parameter to be defined. The dimensions are commonly provided in the Technical Data Sheet of each sensor through the Gauge Lenght, Overall Lenght, Grid Width, and Overall Width;
- Strain Gauge Factor: The Gauge Factor (GF) or Strain Factor can be defined as the ratio of relative change in electrical resistance R, to the mechanical strain ε. The GF is affected somewhat by the pattern size, geometry, and Temperature;
- Range of Temperatures: The range of temperatures for the sensor is commonly defined as the temperature span, given by the temperature extremes, over which the sensor will perform without failure;
- Strain Gauge Range: The range of measurement appropriate for the measurement;
- Selection of the right adhesive: When installing a strain gauge, it is important to select the right adhesive to bond the strain gauge, since a strong union is critical to ensure the sensing performance of the strain gauge system.

Model	Overall Length (mm)	Overall Width (mm)	Thickness (mm)	Strain Range (%)	Temperature Range (°C)
500 BH	18.29	4.45	0.069	± 5 %	-75 - 175
375 UW	14.61	4.57	0.069	± 5 %	-75 - 175
250 UNA	10.54	3.05	0.069	± 5 %	-75 - 175
187UW	9.83	4.57	0.069	± 5 %	-75 - 175
250 LW	9.22	2.54	0.069	± 3 %	-75 - 120
125 UN	6.99	2.54	0.069	± 5 %	-75 - 175
125 AC	6.35	3.18	0.069	± 5 %	-75 - 175
125 BB	6.22	2.24	0.069	± 5 %	-75 - 175
125 BZ	5.59	1.57	0.069	± 5 %	-75 - 175
062EN	1.93	1.57	0.069	± 3 %	-75 - 175

Table 3 – Sensor selection for the strain gauges.

The nature of the material is a factor to be considered in the selection of the appropriate strain gauge. When measuring an inhomogeneous material, such as composite, wood or concrete, the measuring grids recommended for FRP materials are in the range of 10-15 mm, while short measuring grids are recommended for homogenous materials like steel. The main reason behind this is that a large measuring grid will bridge the inhomogeneities of the material. In this research work, the 250 UNA strain gauge was selected for the inspection and maintenance of the FRP-based tower of the W2power for these two reasons: 1st) It has an appropriate size to measure in inhomogeneous FRP-based materials, and 2nd) Their dimensions, strain range and temperature range are appropriated to carry out measurements in this sort of materials.

This project has received funding from the European Union's Horizon 2020 research and innovation programme under grant agreement No 952966.

3. FEASIBILITY STUDY TO EVALUATE THE INTEGRATION OF SENSORS INTO FRP MULTIFUNCTIONAL MATERIALS

Two approaches – surface-mounted sensors and embedded sensors – described hereafter have been proposed by the FIBREGY consortium for the integration of sensors into the SHM system:

- Surface-mounted sensors: These sensors are commonly mounted on the external parts of the FRP laminar materials using adhesives, studs or screw connections. The main advantage of this sensor configuration is that allows an ease of access and maintenance for the network of sensors during the operational life of the FOWT;
- Embedded sensors: These types of sensors are embedded in the interior of the composite laminar materials. On the positive side, the integration of the sensors into the FRP materials offers a superior protection level from adverse environmental climate conditions, which is of remarkable interest for the case of wind and tidal energy offshore platforms. On the negative side, the discontinuity generated due to the integration of the sensor can be a precursor of delamination damages with the potential to degrade the structural integrity of the host composite material.

The major challenge of subtask 2.5.2 is to propose an optimum strategy for the integration of the sensors into FRP-multifunctional materials that will be used for the construction of the W2Power tower. The main objectives of subtask 2.5.2 are twofold:

- With the aim to evaluate the feasibility of the technology, FRP multifunctional materials have been manufactured with sensors embedded in the backing of the dry coating by INEGI's research institute. The performance of this new generation of FRP multifunctional materials has been validated and verified in the TSI laboratory;
- A preliminary definition of the location of the sensor network in the structural element to be monitored (W2Power Towers) is given in the deliverable. The input of this task is of relevant importance for the definition of the SHM system of the towers in Task 4.4.

The rest of Section 3 is arranged as follows: Section 3.1 provides a preliminary definition of the SHM system to be part of the FRP-based Towers of W2Power Floating Platform. Section 3.2 proposed three potential strategies for embedding the sensors into the FRP multifunctional materials. With the aim to prove the feasibility of the technology, the sensors selected for the consortium have been embedded in the backing of the dry coating of the FRP multifunctional materials and their functional performance has been evaluated via pressure and vibration tests (see Section 3.3).

This project has received funding from the European Union's Horizon 2020 research and innovation programme under grant agreement No 952966.

3.1. PRELIMINARY DEFINITION OF THE SHM SYSTEM OF THE W2POWER TOWER

The initial maintenance plans of wind turbines were based on the assumption that the structural components of wind turbines were required limited or even no maintenance. However, it has been observed that the tower/blades of the wind turbines also fail due to lightning, impacts, delamination, manufacturing defects, cracks, and other sorts of defects. Hence, it is urgent to develop structural health monitoring systems capable to monitor the integrity of these structural components.

The SHM system of the FRP-based tower is based on a network of fibre optic sensors (FOS), strain gauges, accelerometers and inclinometers distributed in strategical positions of the tower. The location of the sensors in the tower to be monitored is represented in **Figure 6**. The tower is divided into 4 different levels (x_1, x_2, x_3 , x_4) with two accelerometers per level which makes a total of eight accelerometers. The accelerometers deployed at the four levels of the tower are oriented towards the forward and starboard direction of the tower as detailed in the compass. The localization of the strain gauges is given in the inset of the tower. An array of strain gauges will be installed in the base of the tower with the fundamental purpose to inspect the integrity of the two tower-halves connections, the FRP-steel hybrid connection, as well as the base of the tower to be subjected to a high level of stress. Eventually, the stability of the W2Power platform will be monitored by a set of inclinometers oriented towards the forward and starboard direction of the tower.

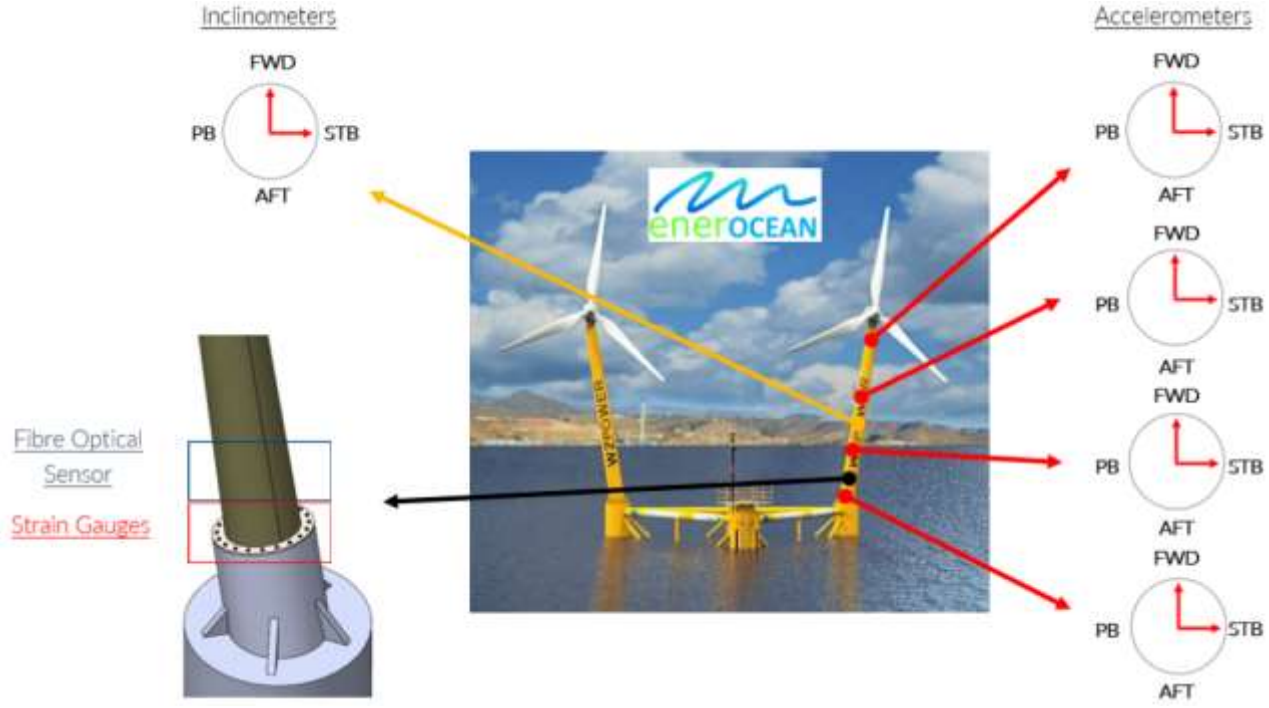

Figure 6 – Disposition of the sensors in the FRP-based tower of the W2Power wind turbine. Source: TSI.

A large variety of SHM systems have been utilized by the scientific and industrial community for continuous monitoring of FOWTs. Among the possible solutions for SHM, fibre optic-based systems have been emerging as an increasingly interesting technology due to their distinctive advantages such as superior resistance to aggressive environments, immunity to electromagnetic interference and the possibility to operate for long periods of time. For all these reasons, the SHM community envisages fibre optic sensors as a technology with a high potential for continuous real-time monitoring of

This project has received funding from the European Union's Horizon 2020 research and innovation programme under grant agreement No 952966.

FOWTs. The SHM system will also include a network of fibre optic sensors (FOS) embedded in the FRP-based materials of the towers in the positions indicated in the blue inset of Figure 6, which plays a critical role to guarantee a superior environmental protection level from adverse environmental climate conditions of the sea.

This project has received funding from the European Union's Horizon 2020 research and innovation programme under grant agreement No 952966.

3.2. SELECTION OF OPTIMUM STRATEGY FOR EMBEDDING SENSORS

The visual inspection of Floating Offshore Wind Turbines (FOWT) is dangerous, expensive and impractical due to the non-possibility to access the platform by workboat in certain sea state conditions as well as the high costs derived from the transportation of maintenance technicians to offshore platforms located far away from the coast, especially if helicopters are involved. Consequently, the energy offshore sector is demanding the development of innovative structural health monitoring solutions capable to monitor the structural condition of FWOTs during their life cycle.

The consortium of the FIBREGY project has investigated the potential of three strategies to embed the sensors selected in task 2.5.1 into the FRP-multifunctional materials that will be used for the construction of the W2Power Platform. The three strategies for the integration of the sensors are well represented in Figure 7.

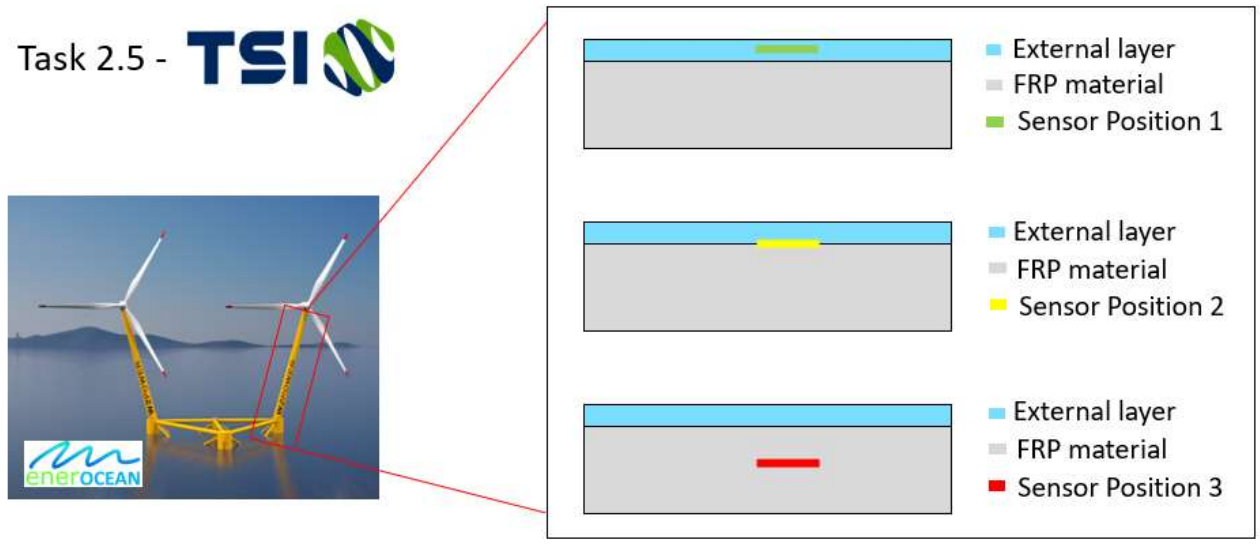

Figure 7 – Strategies for embedding the sensors in the FRP laminates. Source: TSI.

The first strategy is mainly based on the inclusion of the sensors into the dry coating (see sensor position 1). This option was discarded by the consortium for the following two reasons: 1st) The external layer is very thin and therefore, this approach is only valid for small-size sensors with thickness below 0.5 mm. 2nd) The elastic modulus of the dry coating and FRP tower is not the same and this can be affecting to the readings of the sensors.

The second strategy consists of the integration of the sensor in the interface FRP tower-Dry Coating (see sensor position 2). This option is the simplest approach from the manufacturing perspective; however, it is critical to ensure that the dry coating firmly adheres to the FRP tower during the complete sea testing in the campaign in the W2Power prototype.

The third strategy focused on the integration of the sensor device into the ply interfaces of the composite material (sensor position 3). The main problem of this approach is that the discontinuity created by the sensor is expected to create tensions that decrease the mechanical performance of the material.

This project has received funding from the European Union's Horizon 2020 research and innovation programme under grant agreement No 952966.

In conclusion, TSI, CIMNE, INEGI, and CORSO selected the second approach for embedding the sensors into the tower prototype for two reasons: 1st) It is a simple approach from the manufacturing point of view. 2nd) The integration of the sensor device will not affect the mechanical performance of the FRP tower.

This project has received funding from the European Union's Horizon 2020 research and innovation programme under grant agreement No 952966.

3.3. FEASIBILITY STUDY TO EVALUATE THE INTEGRATION OF SENSORS INTO FRP MULTIFUNCTIONAL MATERIALS

Within the scope of WP2, it was defined that different samples must be produced in order to test and validate the feasibility of the integration of sensors and dry coating in the FRP composite material. Two different options were outlined (see Table 4 and Figure 8); however, in both options the dry coating must be integrated in the vacuum infusion process. In Option A, the objective is to bond the sensor to the surface of the FRP, after curing, and apply a liquid coating on the exposed area. In Option B, the aim is to embed the sensor in the vacuum infusion process. Therefore, six samples (three using strain gauges, and three using accelerometers) of each option were produced to test the delineated approaches.

Option	Description	Number of samples
A	Application of the sensor after infusion process	6
B	Embedment of the sensor within the infusion process	6

Table 4 – Type of tests to be performed

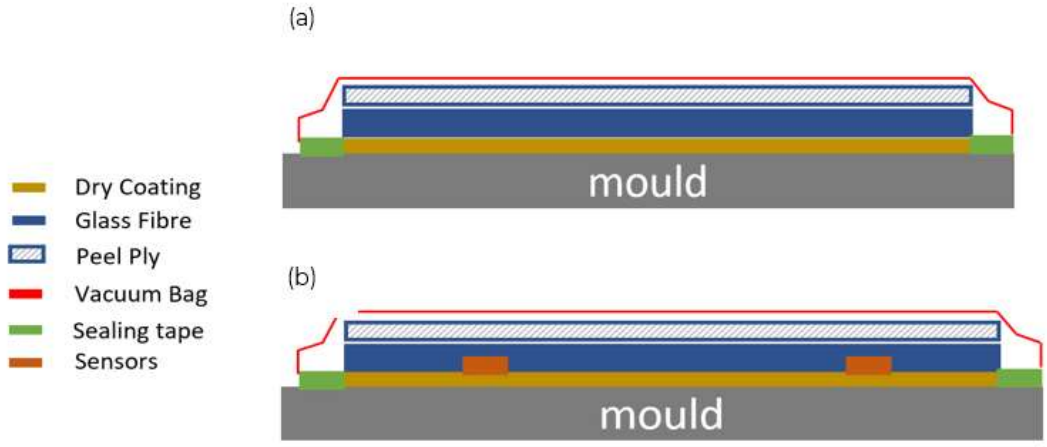

Figure 8 - Representation of the setup (a) without the sensors and (b) with embedded sensors.

It is worth noting that two more samples were firstly produced with the aim of testing the setup and response of the selected materials, which are presented in Table 5. The epoxy resin used is the same as the one selected in Task 2.1. The orientation of the glass fibres is not the most relevant parameter for this type of assessment, where the main objective is to determine the feasibility of the embedment of the sensors and of the dry coating, thus it was used ± 45º glass fibres, as they were readily available at INEGI's facilities.

Materials	
Epoxy Resin	SR InfuGreen 810
Hardener	SD 4771
Glass fibres	± 45°

Table 5 – List of materials.

This project has received funding from the European Union's Horizon 2020 research and innovation programme under grant agreement No 952966.

Figure 9 – SR InfuGreen 810 and SD 4771.

Regarding the type of sensors to be tested, TSI, within the scope of Task 2.5.1, selected a strain gauge and an accelerometer, which most relevant characteristics are presented in Table 6. Table 7 shows information on the two different sorts of dry coating provided for FIBREGY by CORSO.

Sensors	Reference	Width	Length	Thickness	Maximum Temperature
Strain Gauge	CEA-06-250UNA-350	3.05 mm	10.54 mm	60 - 75 µm	175 °C
Accelerometer	Model 12M1B	3.81 mm	4.57 mm	1.4 mm	150 °C

Table 6 – Sensors selected by TSI

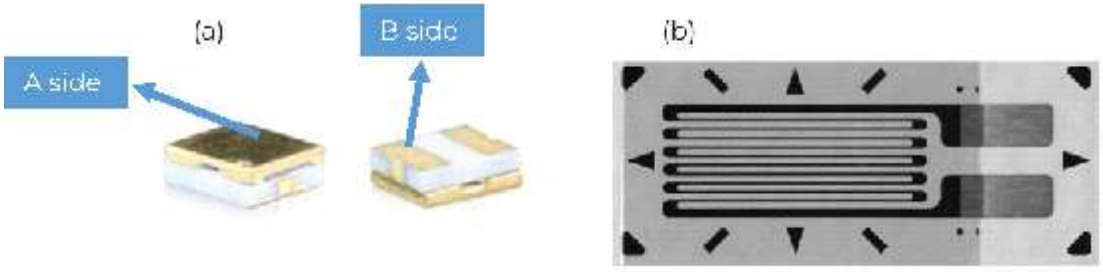

Figure 10 – Sensors. (a) Accelerometer (b) Strain gauge

This project has received funding from the European Union's Horizon 2020 research and innovation programme under grant agreement No 952966.

Dry Coating	Colour	Thickness	Chemistry
Hempathane 55210	Yellow	200 - 250 µm	Acrylic / Polyurethane
Interthane 870	White	200 - 250 µm	Acrylic / Polyurethane

Table 7 - Dry coatings selected by CORSO

Concerning the setup, it was used a prismatic steel mould, which representation is displayed in **Figure 11**, along with its respective dimensions. **Figure 12** depicts the complete setup, including the resin container, the resin inlet and outlet hoses, the resin trap and the vacuum pump.

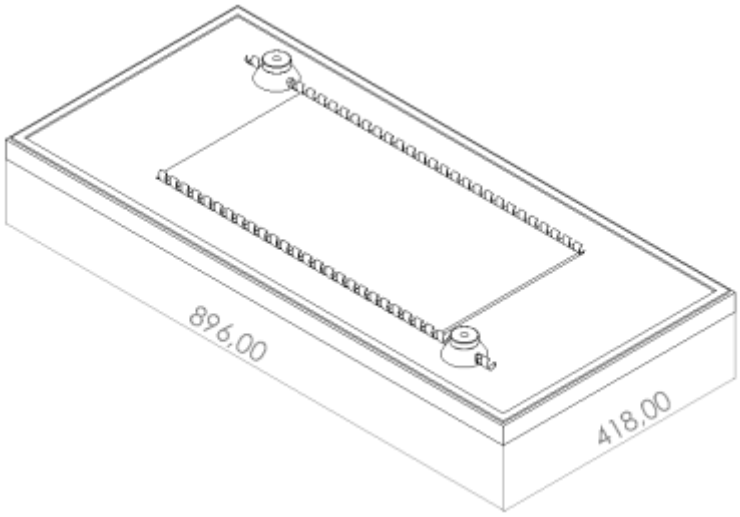

Figure 11 – Representation of the mould.

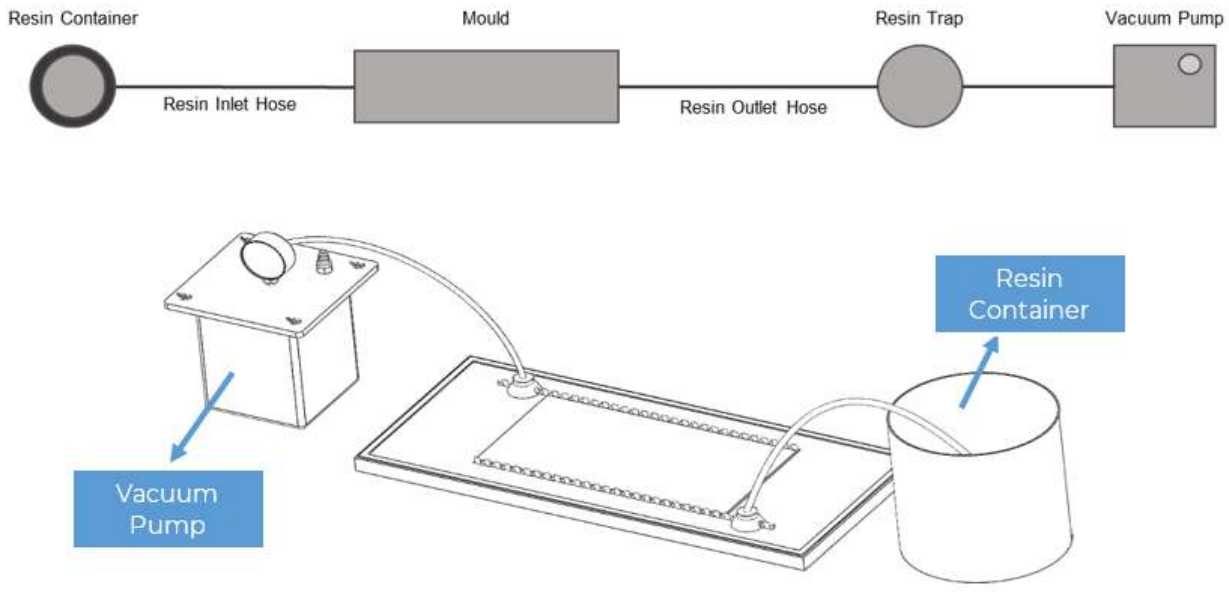

Figure 12 - Representation of the used vacuum infusion setup

This project has received funding from the European Union's Horizon 2020 research and innovation programme under grant agreement No 952966.

After gathering the necessary components to perform the vacuum infusion process, the steps presented in Table 8 were followed. Firstly, the mould has been degreased with acetone, then it was cleaned with a mould cleaner and a cotton cloth. Subsequently, it was applied a mould sealer and a release agent. Next, the dry coating was placed on the surface of the mould and sealed with Airtech Flashbreaker 1 Tape, as can be observed in Figure 13.

	Procedure
1.	Preparation of the mould
2.	Placement and sealing of the dry coating
3.	Placement of the spiral wraps and T-fittings
4.	Cutting and stacking of the glass fibres layers
5.	Placement of the peel ply and flow distribution mesh
6.	Preparation and sealing of the vacuum bag
7.	Connection of the resin inlet and resin outlet hoses
8.	Clamping off the resin line and switch on the vacuum pump
9.	Check for leaks and their correction
10.	Open the resin line
11.	Resin flow until it impregnates the full length and width of the GF layers
12.	Clamping off the resin line
13.	Cure of the FRP composite
14.	Demoulding of the specimen

Table 8 – Procedure steps of the vacuum infusion process

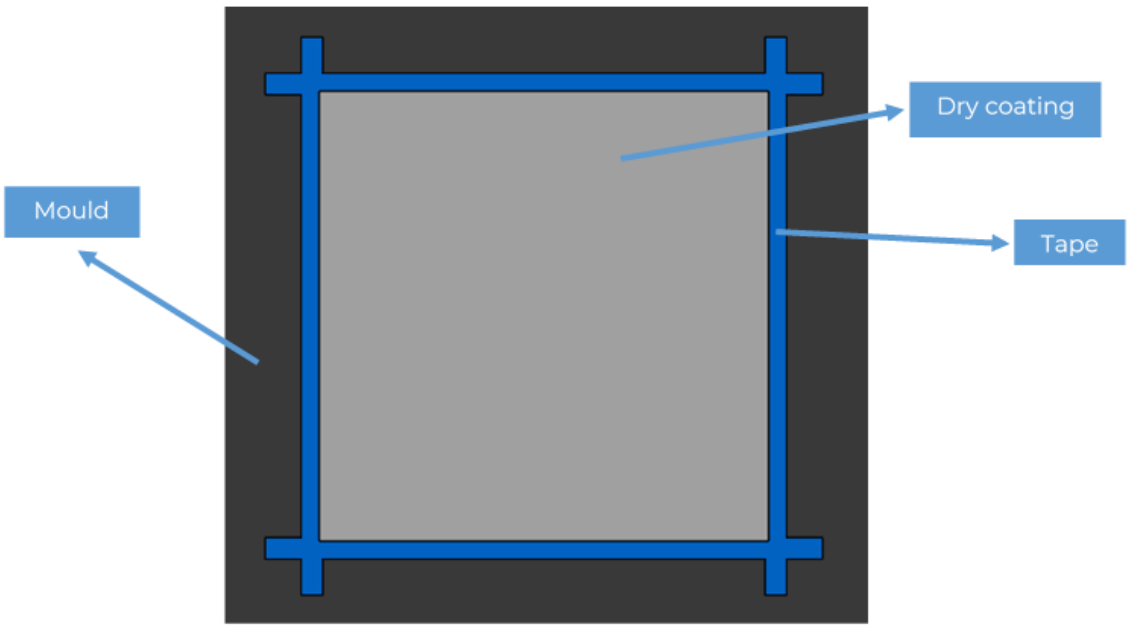

Figure 13 – Representation of the sealing of the dry coating.

The following step was to place the spiral wrap and T-fittings, as they are responsible for allowing and facilitating the resin flow. Next, the GF layers were cut using a scissor and stacked above the free area of the dry coating. A peel ply and a mesh were also placed above, in this order, above the stacked layers. Afterwards, sealant tape was bonded to the vacuum bag, which was then placed above all the assembled system. Carefully, the tape was pressed against the mould to avoid potential leaks. The system was connected to a vacuum pump, which was switched on to compact the components and fix present leaks.

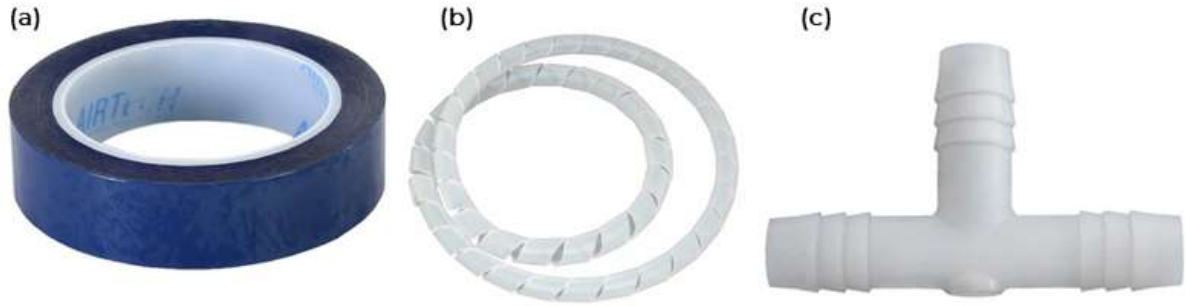

Figure 14 – (a) Airtech Flashbreaker 1 Tape. (b) Spiral Wrap. (c) T-fitting.

Next step concerns the preparation of the resin. As the first two samples were produced using a 250 x 250 mm dry coating and 9 layers of GF, it was recommended to use approximately 320 g of resin, with a mix ratio (epoxy to hardener) of 100/29. It is worth mentioning that the number of layers were calculated based on the formula presented in Table 9. Once the mixture was prepared, the resin inlet hose was immersed in the resin container and the vacuum pump was switched on, leading to the begin of the impregnation of the fibres by the resin.

When the resin impregnated the full length and width of the specimen, the resin inlet was ceased and the sample was left to cure. According to the datasheet of SR InfuGreen 810 and SD 4771, at room temperature, the composite cures in 24 hours, nonetheless, its demoulding time corresponds to nearly 66 hours. After demoulding, the excesses were cut off using an abrasive disc.

	Formulas
Number of layers	[Fibre Fraction Volume x Fibre Density x Desired Thickness] / Areal Weight
Resin Weight	[Resin Ratio / (Resin Ratio + Hardener Ratio)] x Desired Weight
Hardener Weight	[Hardener Ratio / (Resin Ratio + Hardener Ratio)] x Desired Weight

Table 9 - Formulas.

Regarding the final samples to be tested at TSI, it is expectable for them to have a square shape and 250 x 250 mm, as schematized in Figure 15. Their thickness may vary between 3 and 5 mm, depending on the number of GF layers, quantity of resin and applied pressure. As aforementioned, the dry coating is going to be integrated within the vacuum infusion process, being expected to obtain a specimen similar to the one represented in Figure 16.

This project has received funding from the European Union's Horizon 2020 research and innovation programme under grant agreement No 952966.

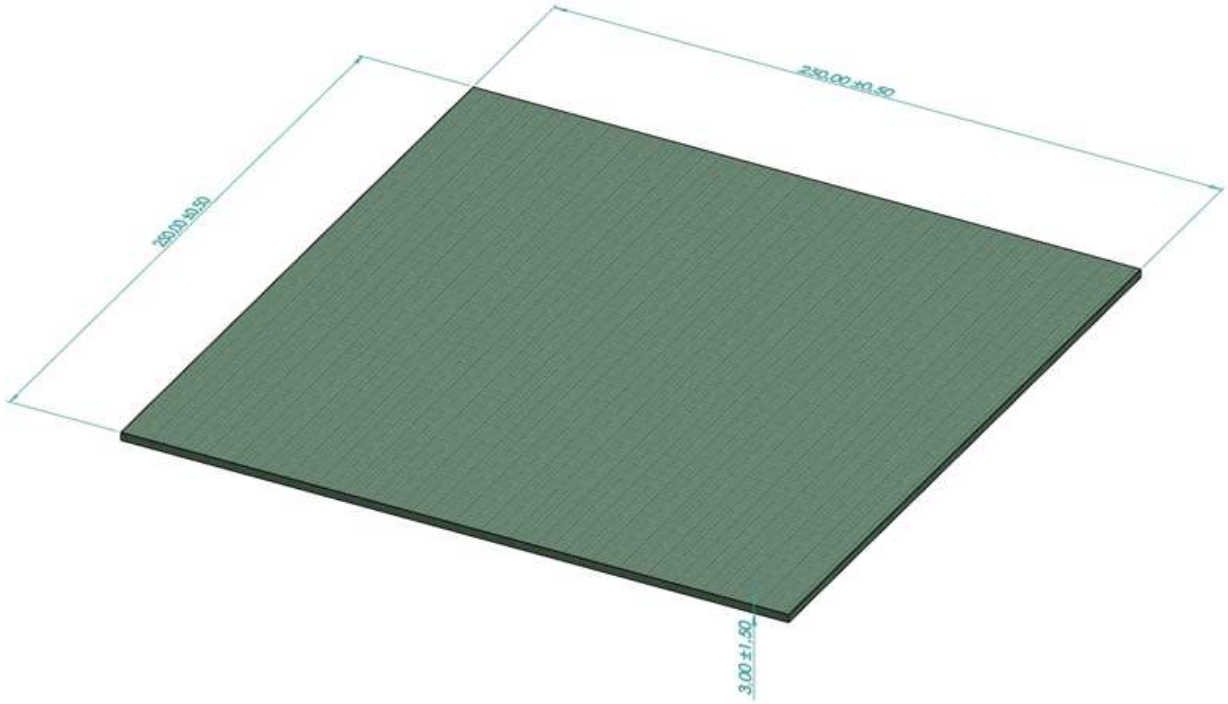

Figure 15 - CAD representation of the expectable sample.

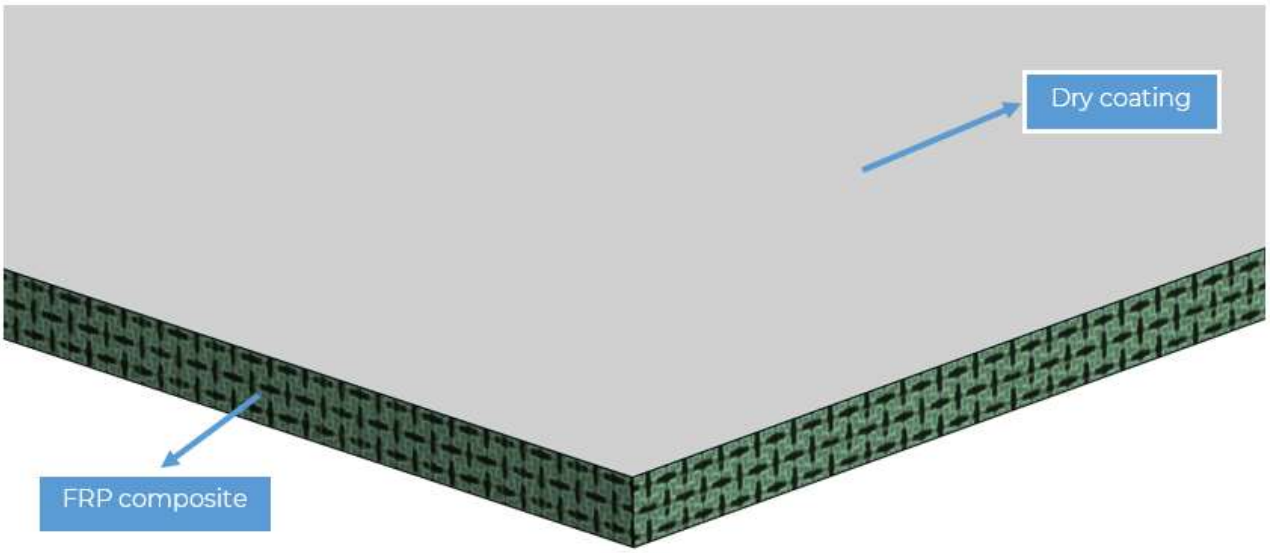

Figure 16 - Dry Coating.

After the production of the samples of option A (see **Table 4**), there is the need for open a small window on the dry coating to allow the bonding of the sensor to the FRP's surface. Three different solutions were thought:

- Using a box cutter (**Figure 17** (a));
- Using a Dremel or a small pneumatic grinding machine (**Figure 17** (b));
- Programming a NC code and machining (**Figure 17** (c)).

This project has received funding from the European Union's Horizon 2020 research and innovation programme under grant agreement No 952966.

Figure 17 – Cutting equipment (a) Box cutter. (b) Dremel. (c) CNC machine.

The sensors were bonded to the exposed FRP's surface using an epoxy adhesive, especially recommended for this type of application – M-Bond AE-10 (**Figure 18**). In order to obtain an adequate bond connection, the preparation steps recommended by the manufacturer must be carefully followed, along with a correct handling of the sensors.

Figure 18 – M-Bond AE-10.

This project has received funding from the European Union's Horizon 2020 research and innovation programme under grant agreement No 952966.

In the case of the sensors' embedment within the vacuum infusion process (Option B), it is demanded to guarantee their correct position and to glue them to avoid their dragging along the resin flow line. Thus, the sensors were glued to the dry coating using a spray adhesive (see Figure 19). The accelerometer was glued with the B side turned towards the dry coating and the strain gauge with its shiny side. The setup was the same as the one previously described. Nevertheless, in the same sample was also tested a different approach: bonding a small area of tape to the dry coating, in order to facilitate the cutting of the window for the insertion of the sensor after infusion.

Figure 19 – Airtac.

3.4. FIRST EXPERIMENTAL TRIALS

T1

As mentioned before, it is necessary to seal the dry coating layer, in order to avoid the flow of resin between the coating and the mould. Thus, as shown in **Figure 20**, the edges of the dry coating sent by CORSO were bonded to the mould and sealed with Airtech Flashbreaker 1 Tape.

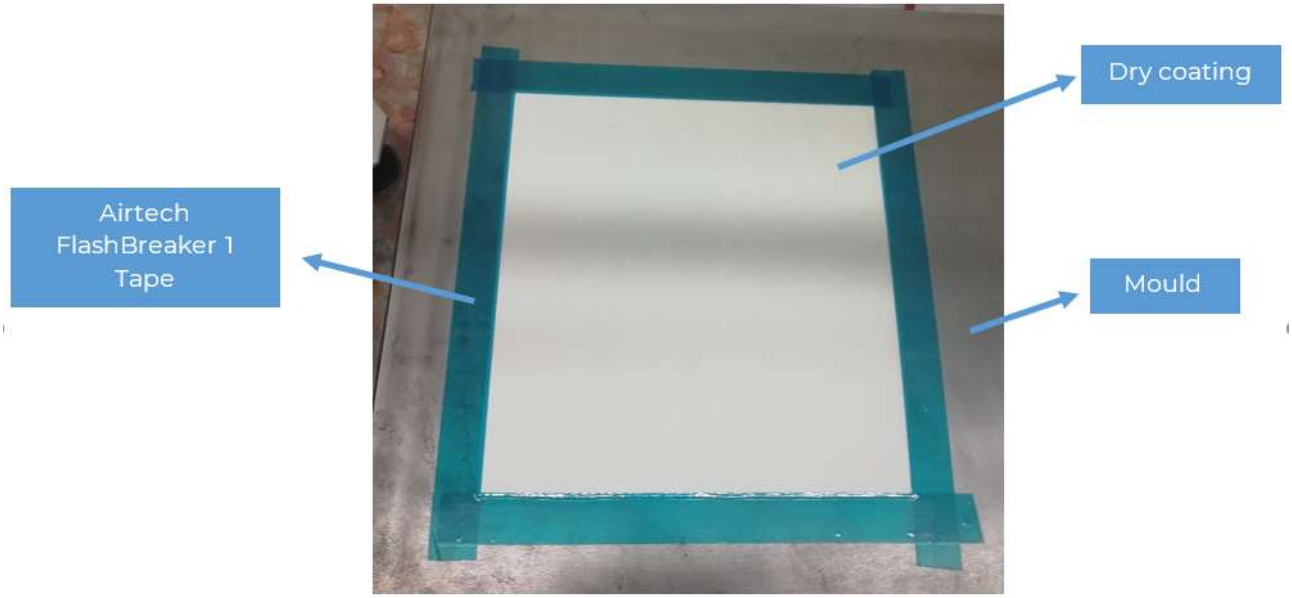

Figure 20 – Sealing of the dry coating.

This project has received funding from the European Union's Horizon 2020 research and innovation programme under grant agreement No 952966.

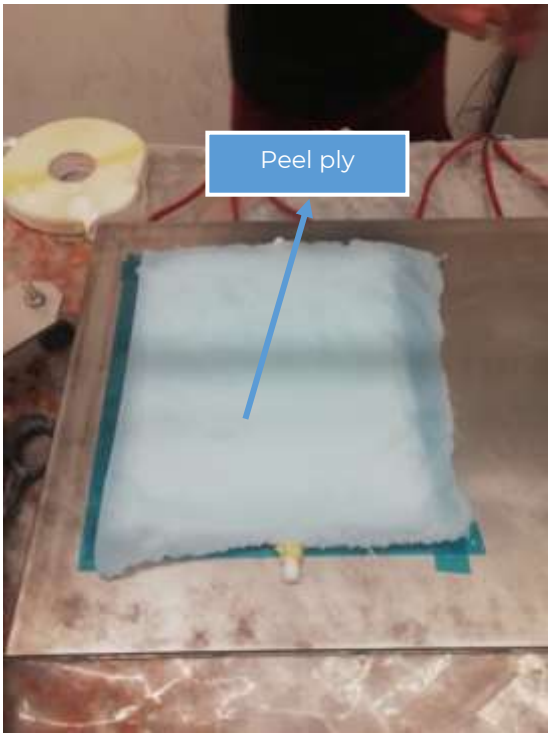

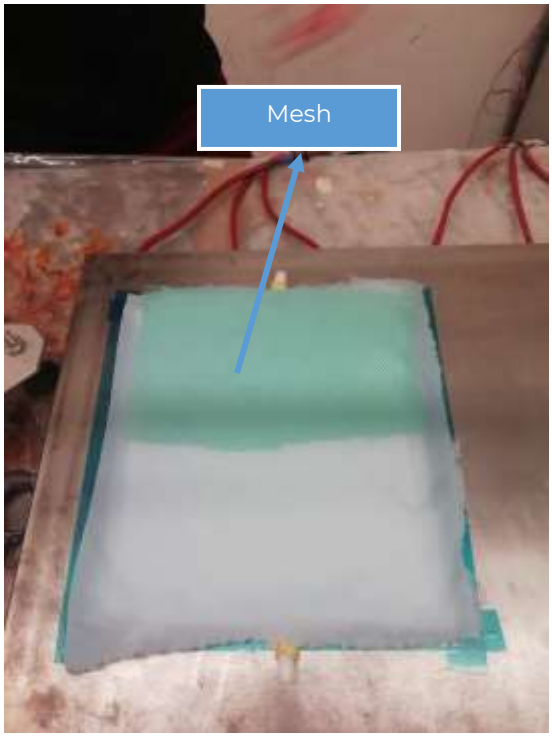

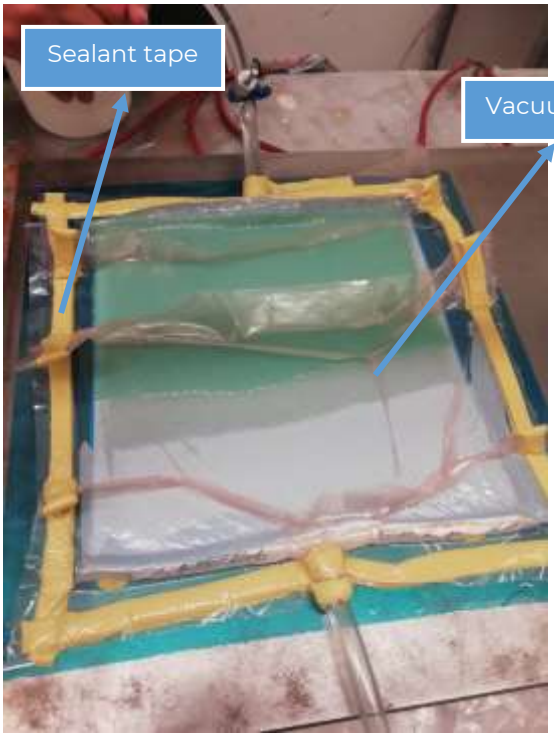

This project has received funding from the European Union's Horizon 2020 research and innovation programme under grant agreement No 952966.

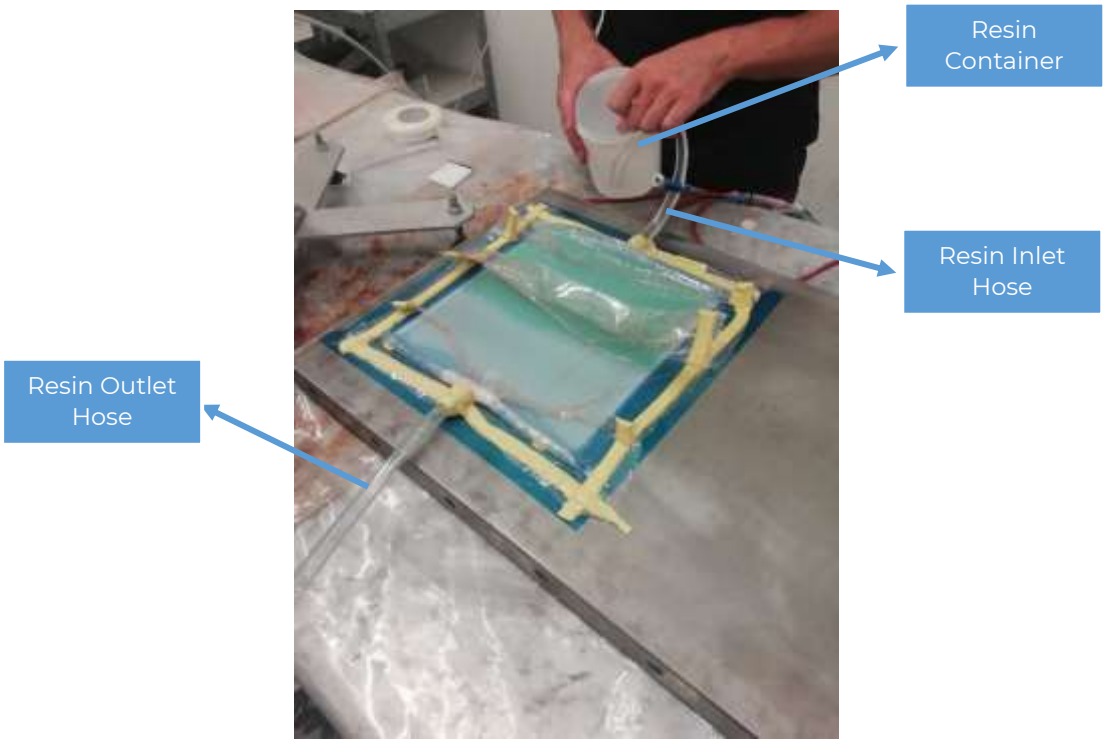

Figure 21 – Setup of the resin infusion process for the production of T1.

Subsequently, the spiral wraps and T-fittings were placed, the GF layers were stacked, followed by the peel ply and mesh. The vacuum bag was sealed and the vacuum pump was switched on (**Figure 21**). As soon as the system was compacted and free of leaks, the resin inlet hose was opened and the impregnation started.

T2

In comparison with the production of T1, the main difference of T2 relies on the embedment of the sensors in the vacuum infusion process (see **Figure 22**) and the bonding of a small area of tape on the dry coating, as described in Chapter 2.1. **Figure 23** displays the setup during the vacuum infusion process.

This project has received funding from the European Union's Horizon 2020 research and innovation programme under grant agreement No 952966.

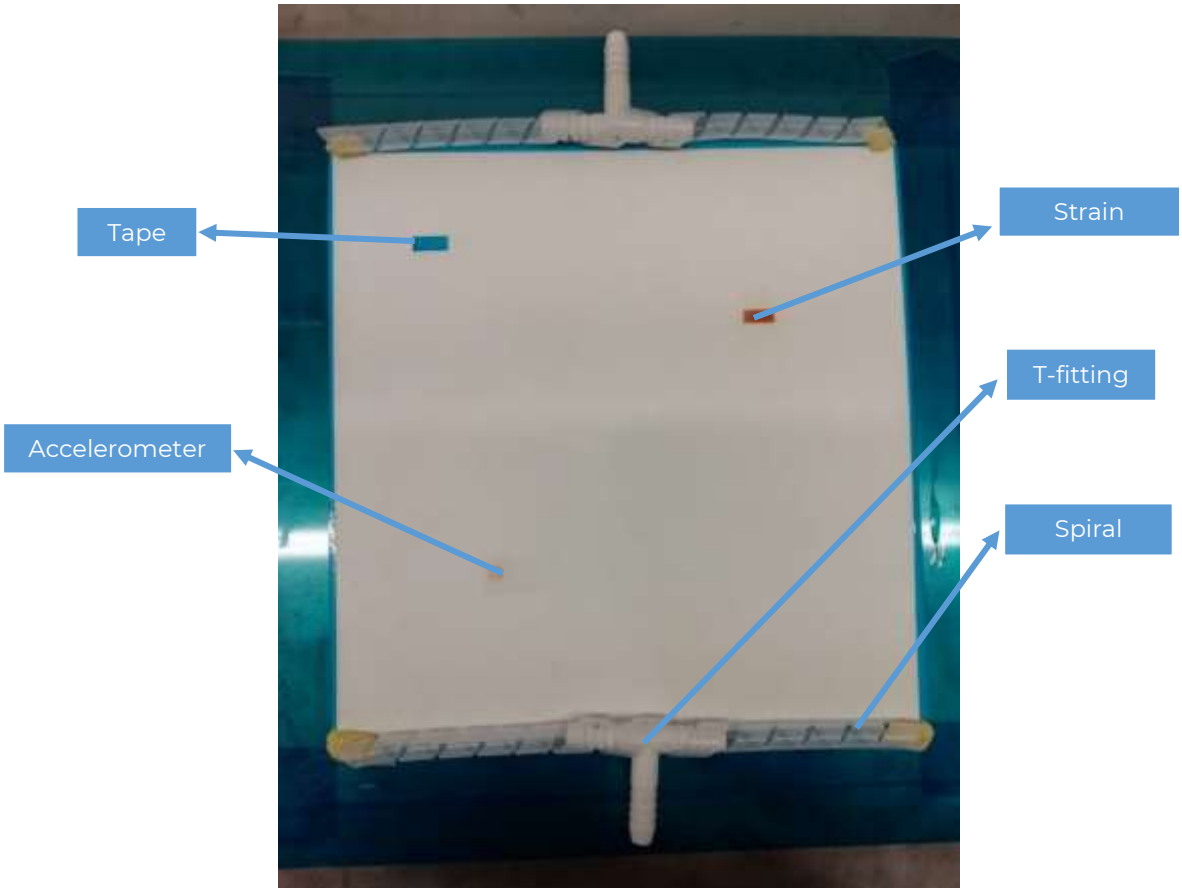

Figure 22 – Placement of the sensors and tape for posterior cutting.

Figure 23 – Vacuum infusion of T2.

This project has received funding from the European Union's Horizon 2020 research and innovation programme under grant agreement No 952966.

T3

The same process conditions as the infusion of T1 and T2 were used for the production of T3. However, in this sample were embedded four sensors. Two sensors (one strain gauge and an accelerometer) were simply placed on the dry coating using Airtac, in order to verify the results of T2, see Figure 24. However, it was also decided to test if the placement of a portion of tape between the dry coating and the sensor would facilitate the removal of the coating to access the surface of the strain gauge and accelerometer after manufacturing. Figure 25 displays the infusion process of T3.

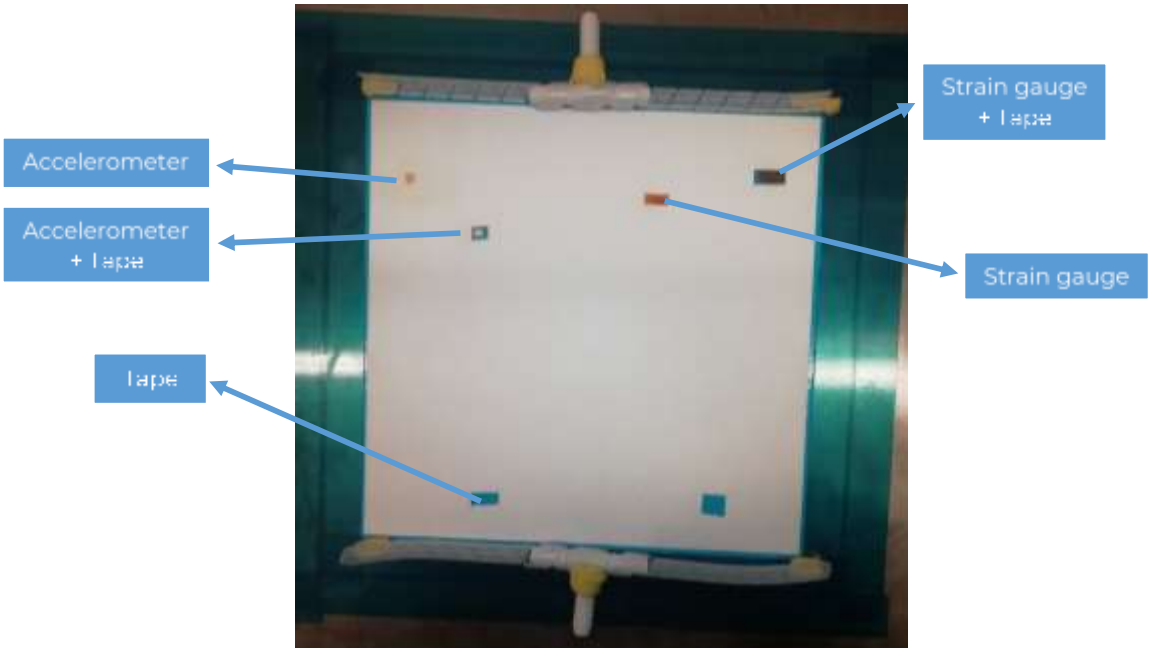

Figure 24 – Placement of the sensors and tape in T3.

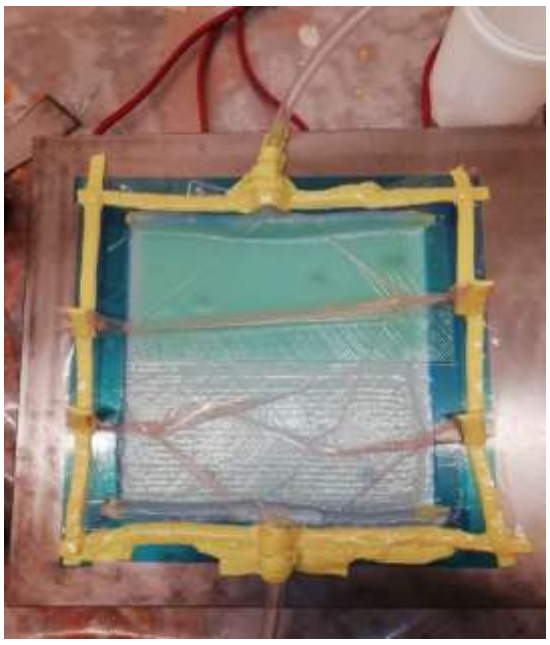

Figure 25 – Vacuum infusion of T3

This project has received funding from the European Union's Horizon 2020 research and innovation programme under grant agreement No 952966.

Results

T1

After demoulding and cutting the excesses, the S1 sample presents the visual aspect displayed in Figure 26 and the characteristics shown in Table 10.

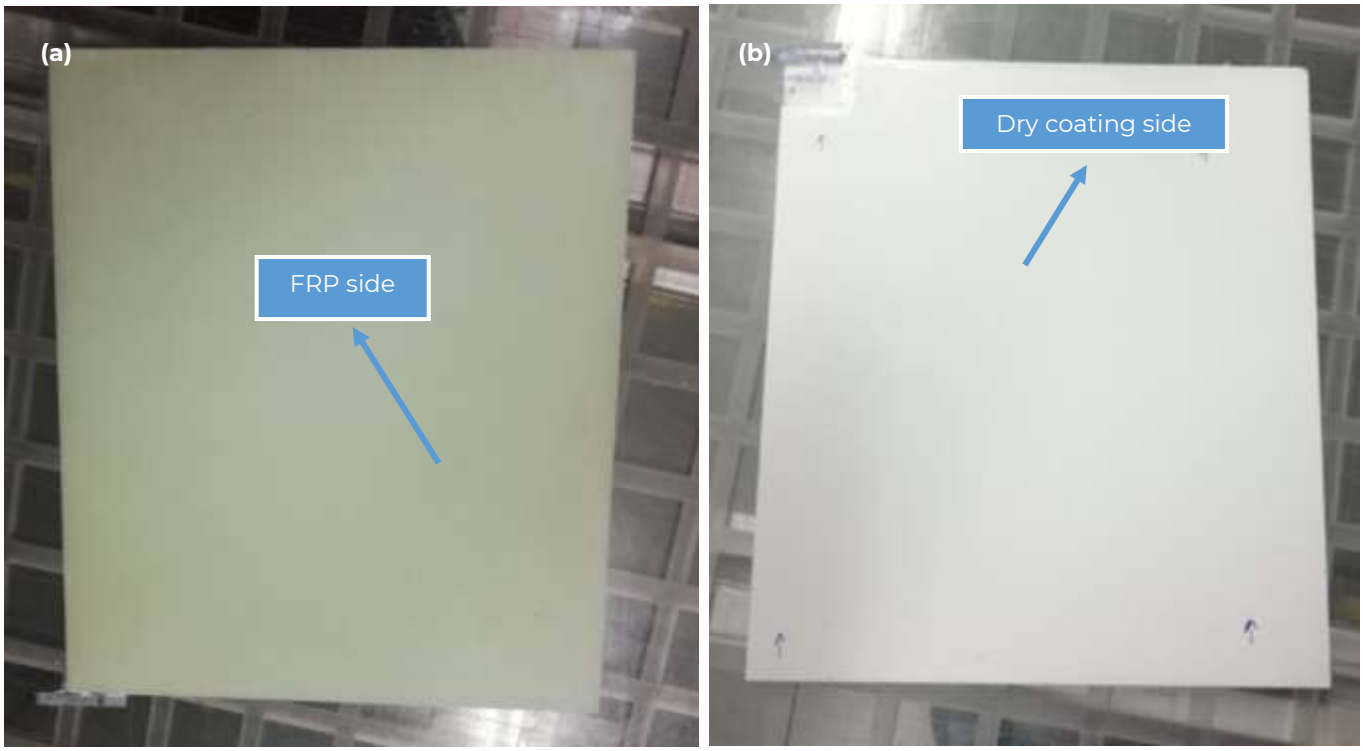

Figure 26 – T1. (a) FRP composite side. (b) Dry coating side.

Sample	Infusion Date	Demoulding Date	Thickness (mm)	Length (mm)	Width (mm)
T1	2021-09-07	2021-09-10	4.4	208	225

Table 10 – Characteristics of T1.

The sample T1 was cut in four parts (see Figure 27), which were used to test a different approach to cut a window in the dry coating. As can be seen in Figure 27, T1B was used to open two windows resourcing to an adaptable 3D printer machine. A head with a drill was mounted in the machine and the programmed NC code was run. In T1C, the windows were opened using the Dremel and a pneumatic grinding machine. T1D was cut using a box cutter.

This project has received funding from the European Union's Horizon 2020 research and innovation programme under grant agreement No 952966.

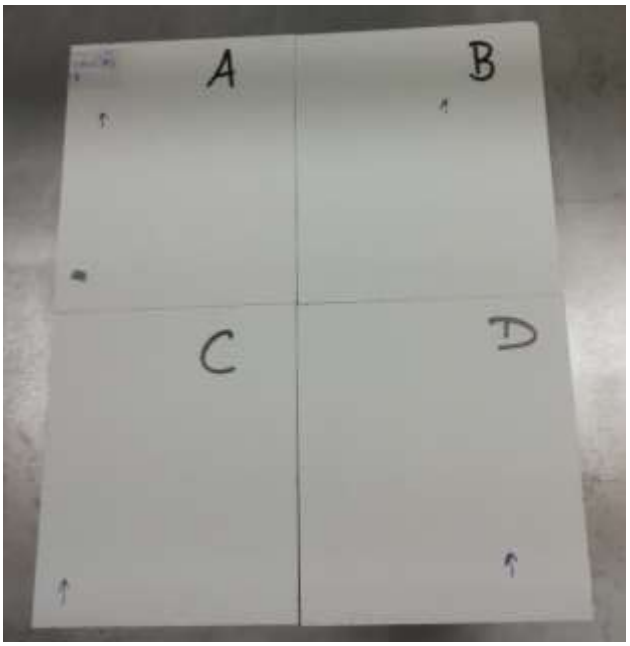

Figure 27 – Division of T1 in four parts.

The results of cutting the windows on the dry coating are shown in Figure 28. As can be observed, T1B presents a more precise and cleaner cut, as it was obtained in a CNC machine. The use of the Dremel and pneumatic grinding machine results in a less precise cut and is extremely dependent on the operator's skill. In addition, this solution can lead to an excessive removal of material. The cut on T1D is more controlled than the one attained in T1C, however, in order to reach the FRP's surface, there is the need for scrapping the dry coating - it is more time consuming.

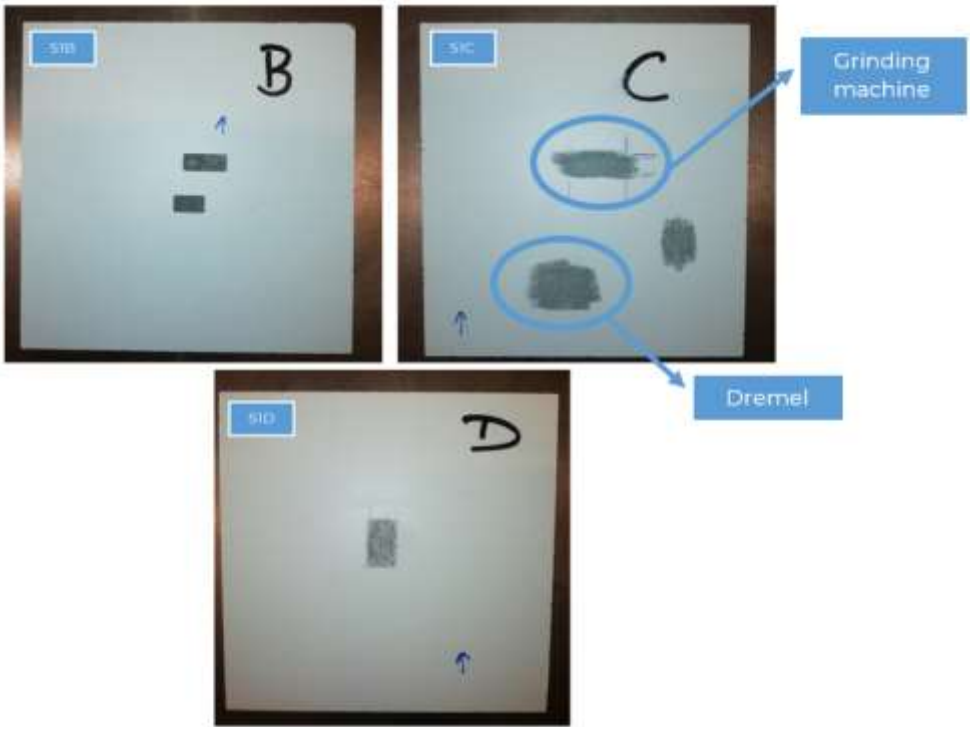

Figure 28 – T1 divided in T1B, T1C and T1D.

This project has received funding from the European Union's Horizon 2020 research and innovation programme under grant agreement No 952966.

Afterwards, with the aim of testing the adhesion of the sensors to the FRP surface, a strain gauge and an accelerometer were bonded using M-Bond AE-10 (Figure 29). The cure of the adhesive takes approximately 6 hours under a pressure of 0.03 to 0.14 MPa. After curing, it was concluded that must be used a smaller quantity of adhesive, as, under pressure, the adhesive flowed to the strain gauge's surface. On the other hand, it worked well for the bonding of the accelerometer.

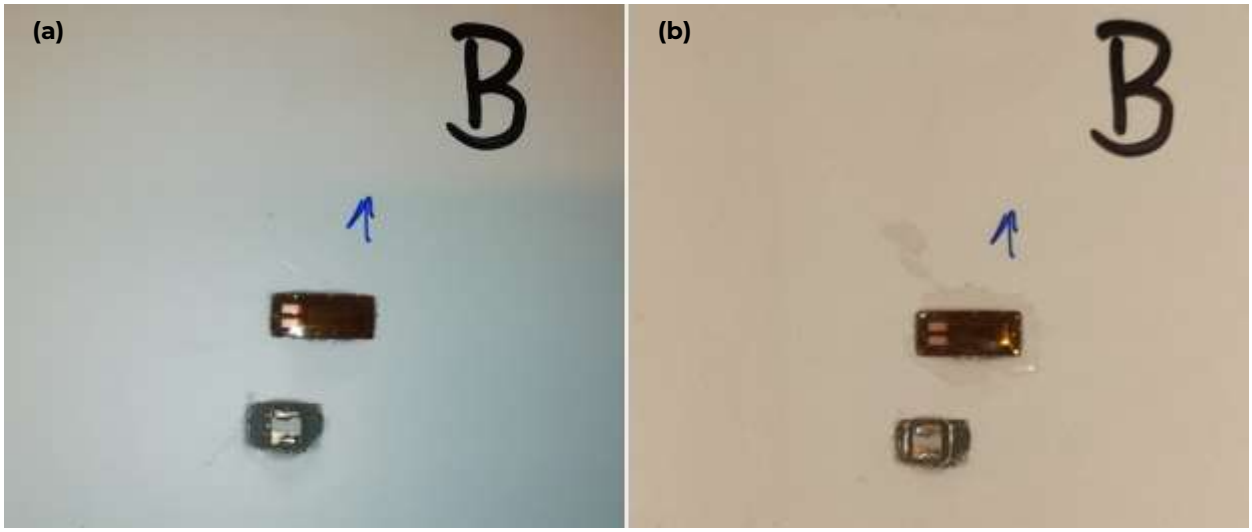

Figure 29 – (a) Adhesive application and sensor bonding. (b) After curing the adhesive

T2

The sample T2 displayed the aspect presented in Figure 30 and the characteristics in

Sample	Infusion Date	Demoulding Date	Thickness (mm)	Length (mm)	Width (mm)
T2	2021-09-14	2021-09-20	4.7	210	223

Table 11. The excesses were then cut off using an abrasive disc. Subsequently, using the same equipment, the sample was divided in four parts. T2A contained the small rectangle of tape, T2B and T2C included the embedded strain gauge and accelerometer, respectively.

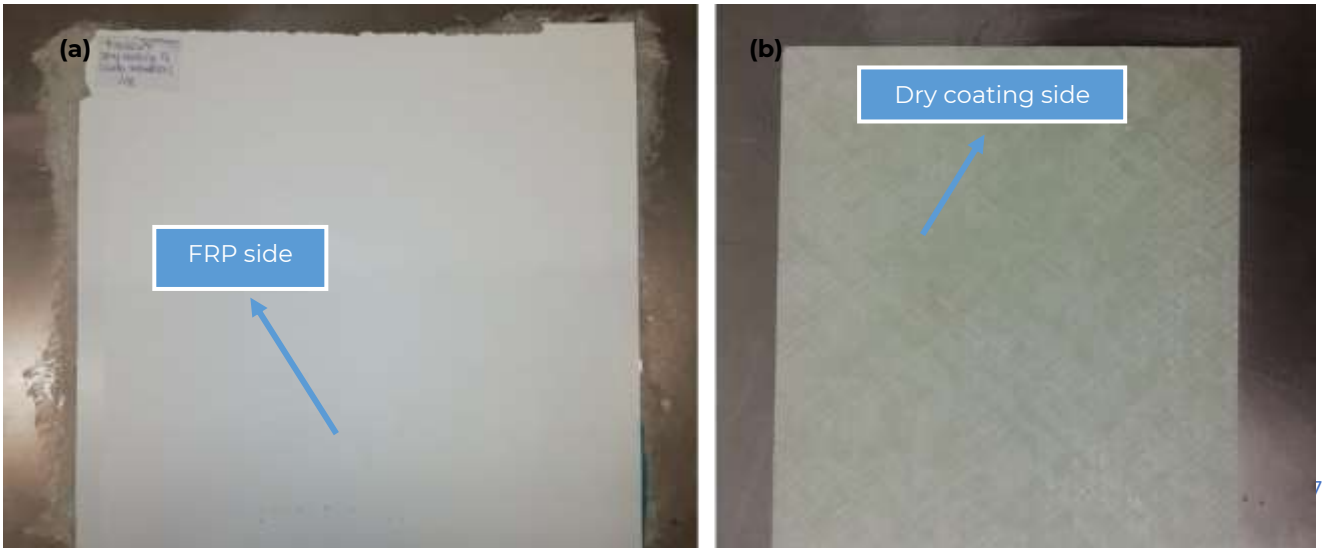

This project has received funding from the European Union's Horizon 2020 research and innovation programme under grant agreement No 952966.

Sample	Infusion Date	Demoulding Date	Thickness (mm)	Length (mm)	Width (mm)
T2	2021-09-14	2021-09-20	4.7	210	223

Table 11 – Characteristics of T2.

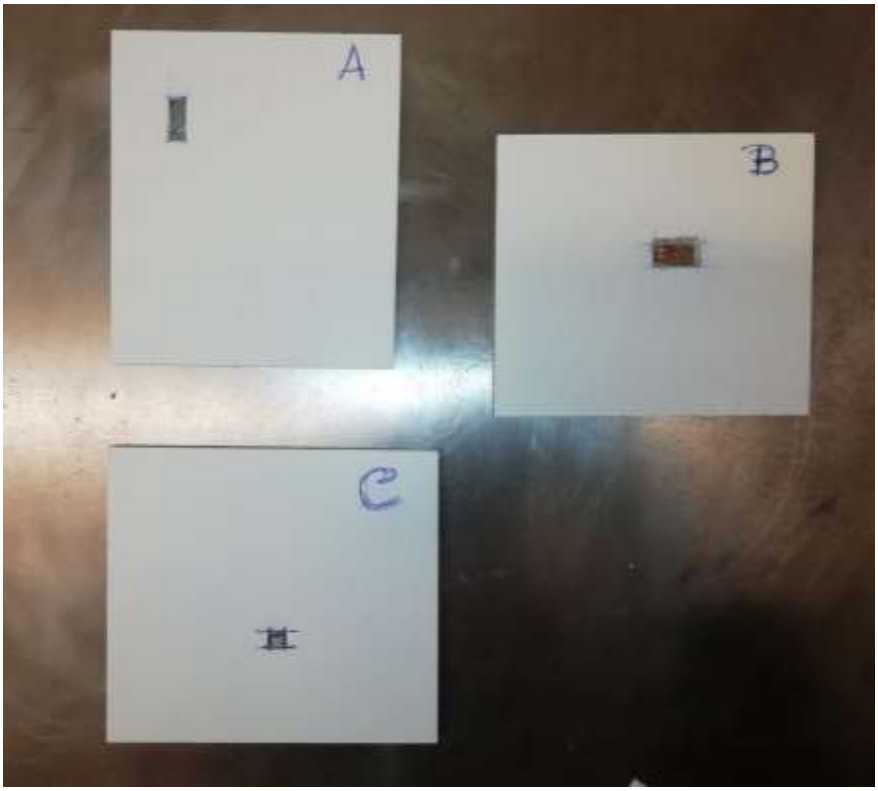

Figure 31 – T2 divided into T2A, T2B and T2C.

The following step was to open the window on T2A. Firstly, it was delineated, using a pen, the shape of the small rectangle of tape on the dry coating. Secondly, with a box cutter, the window was open and the coating was easily pulled off, without being needed to scrap it as in T1D. The main advantage of this approach is that it can be easily applied to larger parts and does not damage the FRP. The result of T2A can be observed in Figure 32.

This project has received funding from the European Union's Horizon 2020 research and innovation programme under grant agreement No 952966.

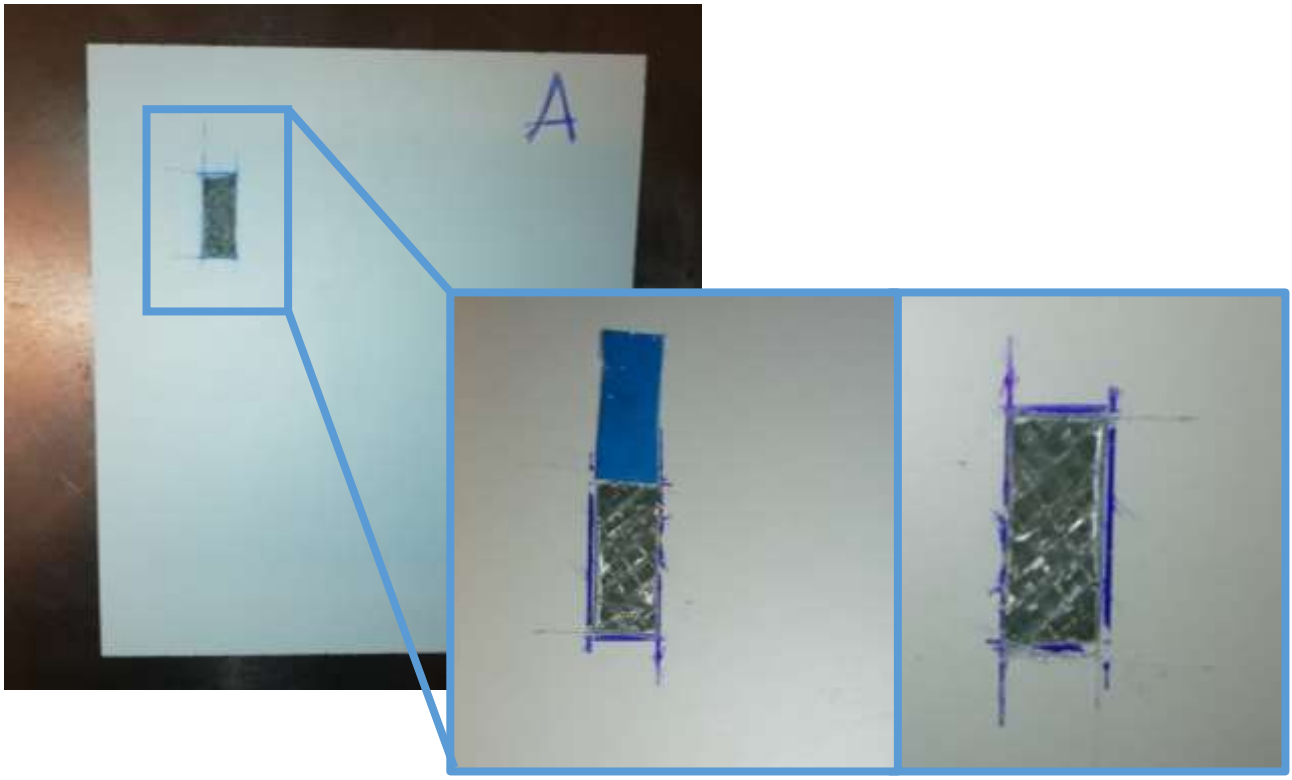

Figure 32 – T2A.

This project has received funding from the European Union's Horizon 2020 research and innovation programme under grant agreement No 952966.

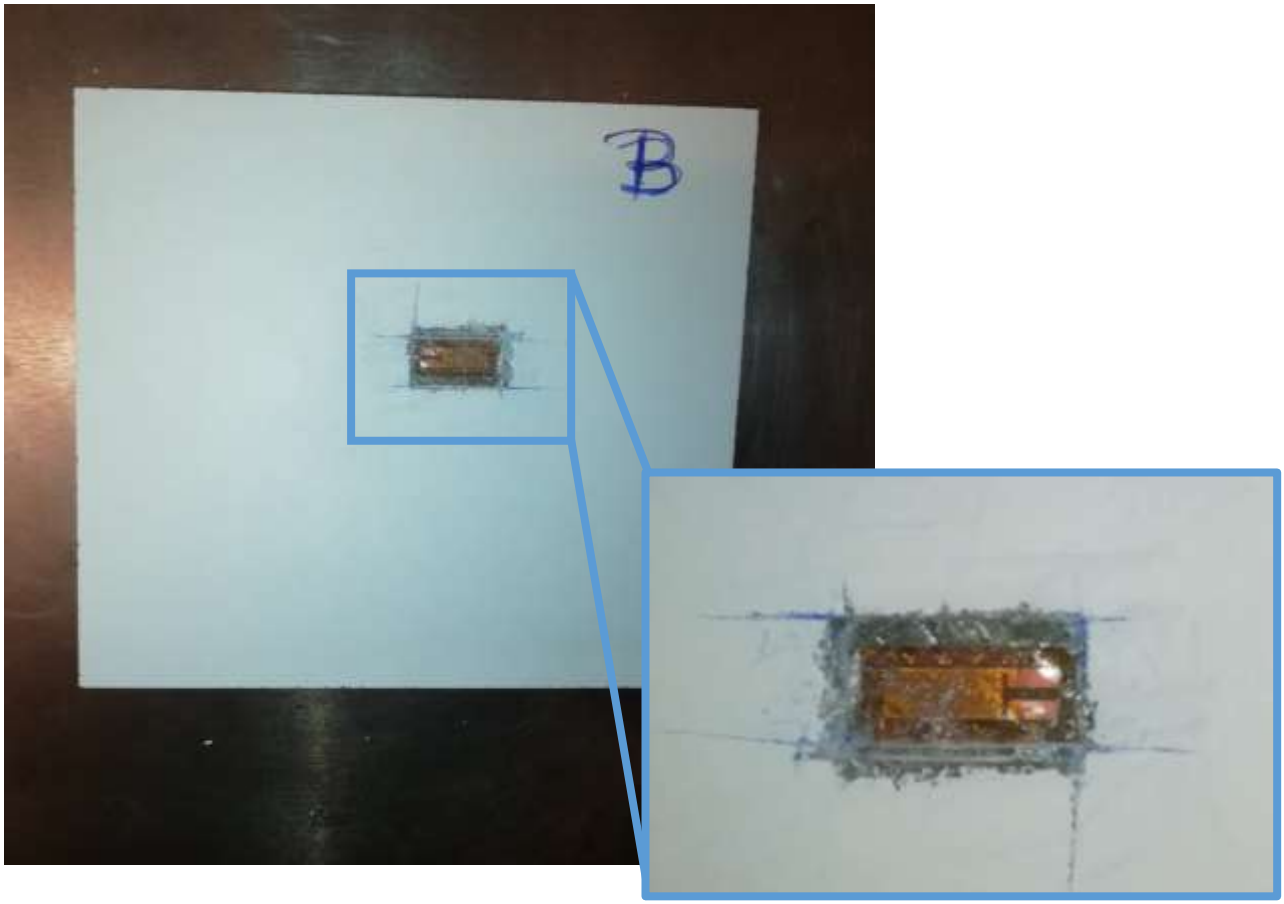

Figure 33 – T2B.

T2B (Figure 33) contained the embedded strain gauge. In order to access its surface, which is required to connect the wires, the area around the sensor was cut with a box cutter. However, the dry coating and the resin adhered to the surface of the strain gauge, which hindered the removal of dry coating and exposure of the surface. In addition, the scrapping of the dry coating led to the damage of the device. Thus, this seems not to be a feasible solution.

On the other hand, in sample T2C – see Figure 34 –, the access to the accelerometer surface was easy and there wasn't resin on it. However, as can be seen in Figure 35, the accelerometer caused a disruption of the fibres' alignment, what must be avoided, as it can affect the mechanical properties of the FRP composite. Furthermore, the presence of the accelerometer results in the formation of a void around the sensor. Consequently, this approach seems not to be feasible for a structural application, due to the thickness of the accelerometer.

This project has received funding from the European Union's Horizon 2020 research and innovation programme under grant agreement No 952966.

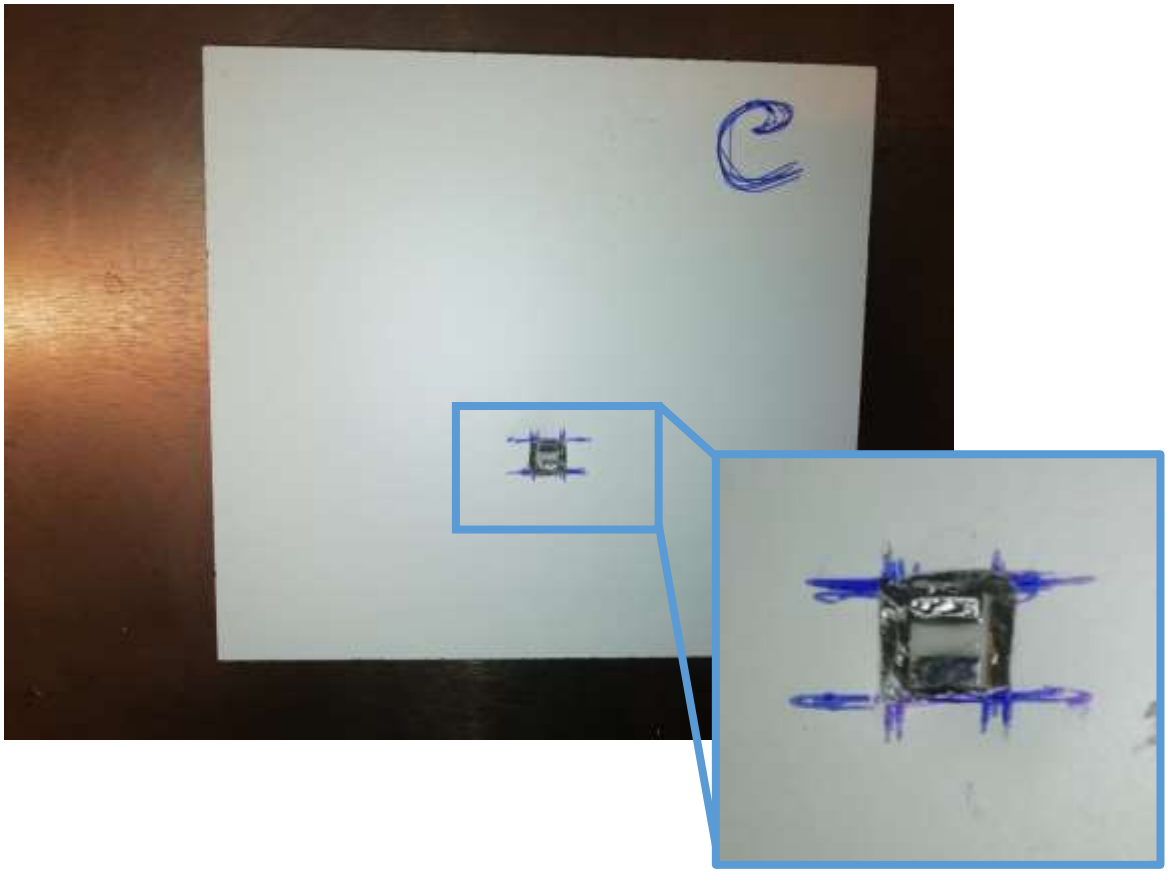

Figure 34 – T2C.

Figure 35 – Disruption of the fibres' alignment caused by the accelerometer in T2C.

T3

Figure 36 represents the aspect of sample T3 after demoulding and cutting the excesses with an abrasive disc and Table 12 comprises some of its characteristics. Subsequently, the sample was subdivided in four specimens: T3A, T3B, T3C and T3D, as can be seen in Figure 37.

Table 12 – Characteristics of T3.

Sample	Infusion Date	Demoulding Date	Thickness (mm)	Length (mm)	Width (mm)
T3	2021-09-23	2021-09-27	4.2	208	224

This project has received funding from the European Union's Horizon 2020 research and innovation programme under grant agreement No 952966.

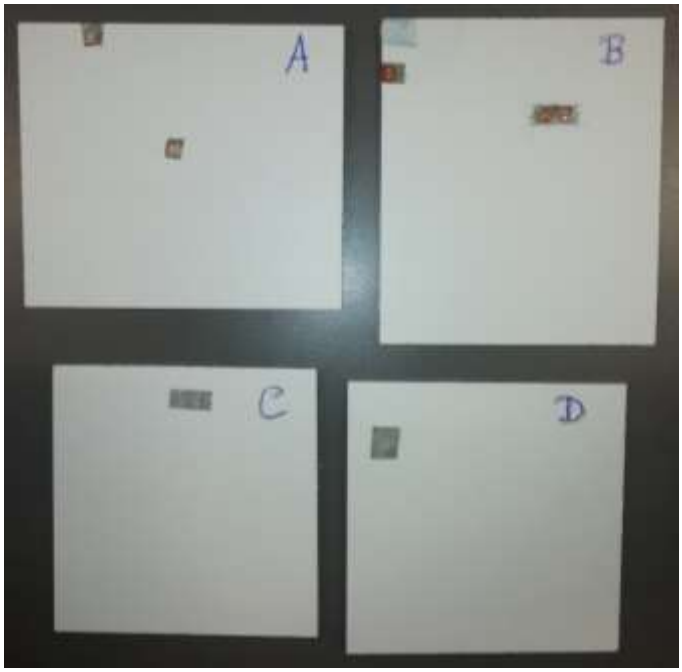

Figure 36 – T3 divided into T3A, T3B, T3C and T3D.

In sample T3A it was placed two accelerometers (A1 and A2): A1 was directly bonded to the dry coating, in order to validate the test performed in sample T2C; and A2 was bonded to a small rectangle of tape, with the aim to test if it would be easier to remove the dry coating after the manufacturing process. Therefore, resourcing to a box cutter, two windows were cut on the dry coating to access the accelerometers. Figure 38 displays the results. It is worth mentioning that, one again, the presence of the accelerometer led to the distortion of the fibres around them. Nonetheless, it was very easy to cut the windows in both approaches, essentially because the void formation round the sensors.

Sample T3B contained two strain gauges (SG1 and SG2): to validate the experimental trial of T2B and to perform a new test, using a small portion of tape between the sensor and the dry coating. As expected, it was very difficult to cut the window and access the surface of the SG2, since the dry coating and resin adhered to the surface of the sensor. Thus, it was necessary to scrap off the dry coating, which results in the damage of the strain gauge. On the other hand, in SG1 the use of the tape unhindered the cutting of the dry coating, being easier to access its surface. Nonetheless, the resin flowed between the tape and the surface of the strain gauge. Figure 38 displays the results achieved for T3B.

This project has received funding from the European Union's Horizon 2020 research and innovation programme under grant agreement No 952966.

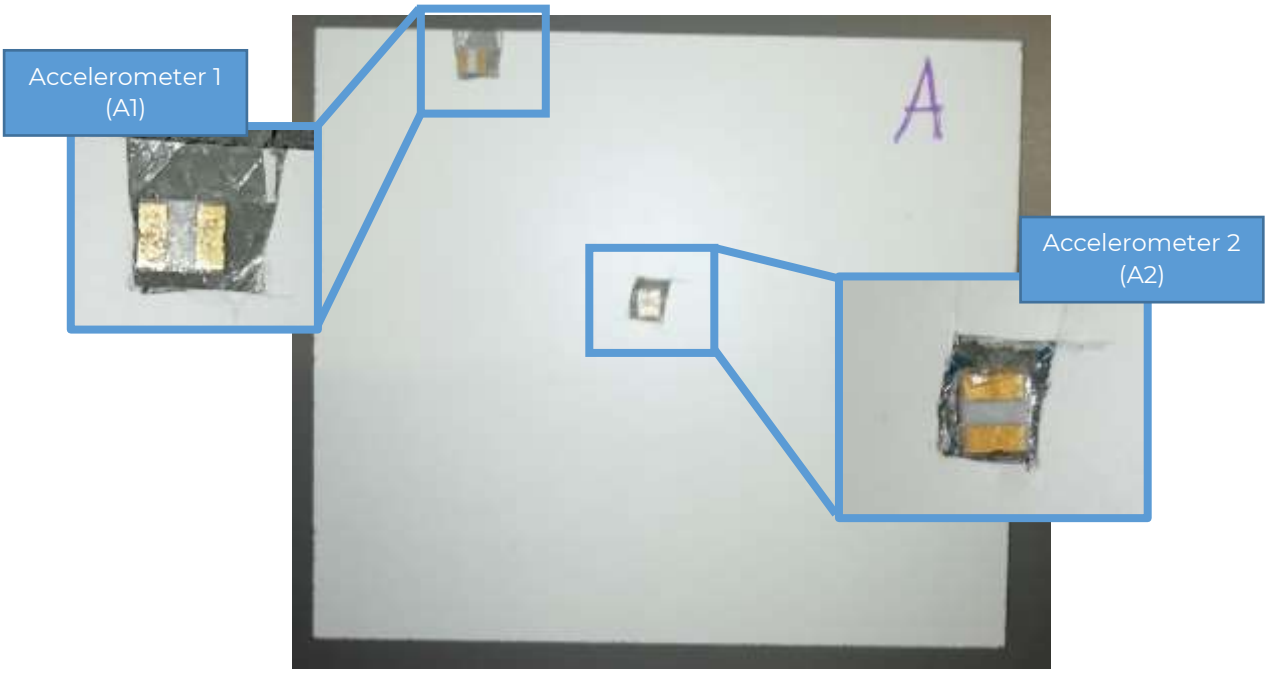

Figure 37 – T3A.

Figure 38 – T3B.

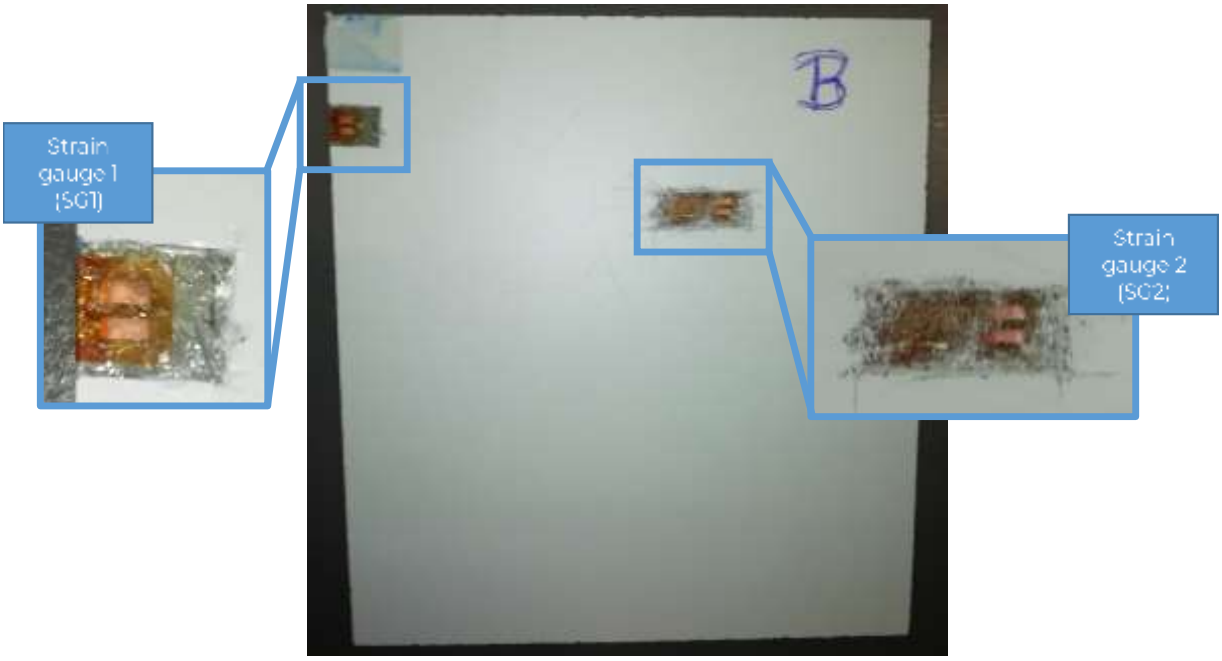

Samples T3C and T3D represent the same test and they were performed to validate the results of T2A. It was proved that the use of tape in the infusion process facilitates the removal of the dry coating, without leaving residues on the surface of the FRP composite (resultant of scrapping of the dry coating) and without causing damage to the material. Also, this approach can be used as a marker of the sensors' positioning. Figure 39 and Figure 40 show the outcomes of T3C and T3D, respectively.

This project has received funding from the European Union's Horizon 2020 research and innovation programme under grant agreement No 952966.

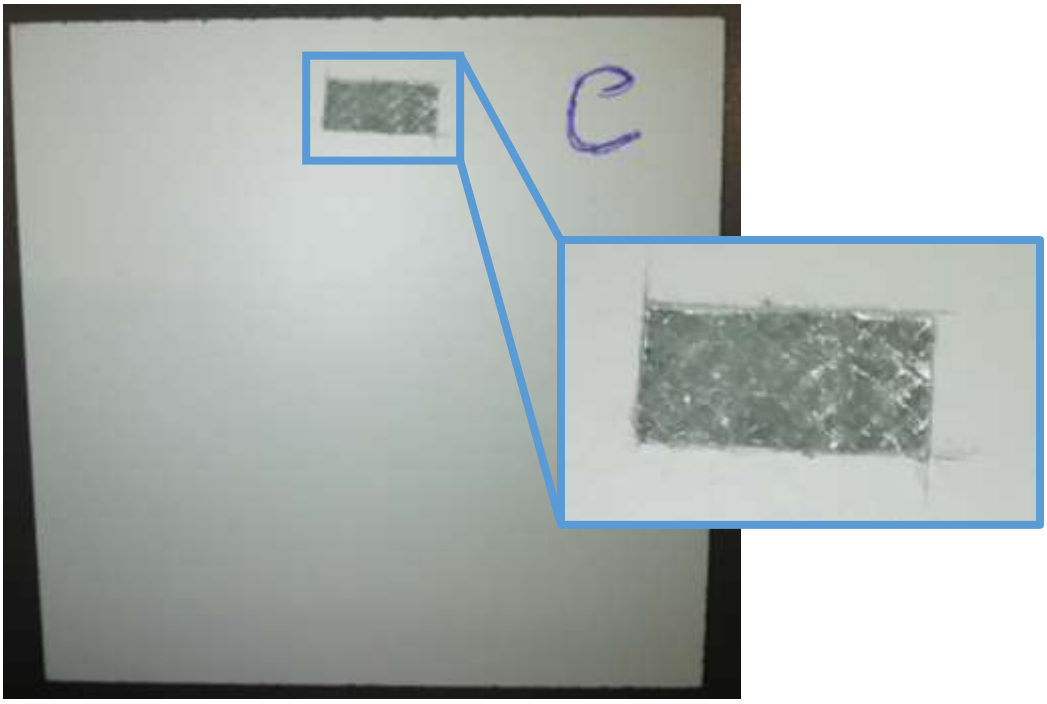

Figure 39 – T3C.

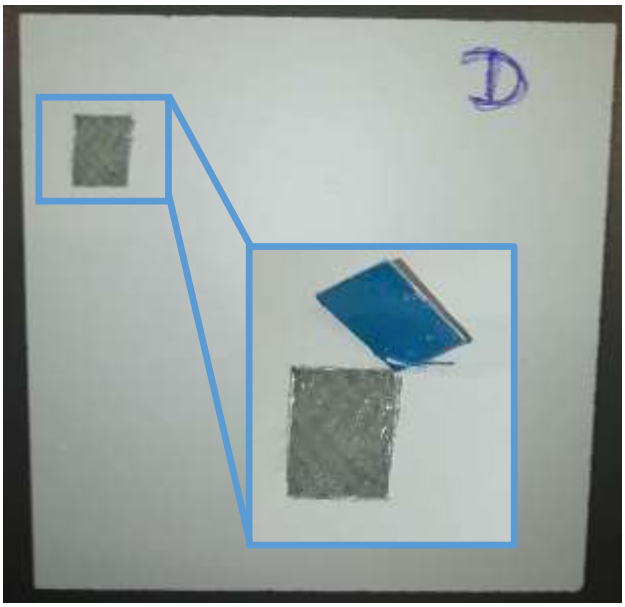

Figure 40 – T3D.

First conclusions

The selected process conditions and materials responded well to the infusion process. In addition, the integration of the dry coating during the infusion leads to great results, as the coating adheres well to the fibres and resin.

The application of the sensors after the infusion can be done after cutting a small window on the dry coating, accessing the FRP's surface and bonding the sensor with an adhesive. Four approaches were

This project has received funding from the European Union's Horizon 2020 research and innovation programme under grant agreement No 952966.

tested, however the best solutions - in terms of efficiency and potential use in larger parts - are the ones presented in T2A and T1C.

The embedment of the sensors within the infusion seems not to be the best solution: the accelerometer significantly disrupts the path of the fibres and leads to the formation of a void around the sensor; to access the strain gauge is necessary to cut and scrap the dry coating off, nonetheless it causes damage to the sensor's surface. Nevertheless, in order to verify if the achieved results in T2 were valid, it was decided to manufacture another sample (T3), including the embedded sensors and portion of tape.

With T3 it was proved that embedding the sensors within the infusion process between the dry coating and the GFRP composite does not lead to consolidated results. The presence of the accelerometer causes distortion of the fibres, which possibly affects its mechanical properties and structural function. The embedment of the strain gauge does not produce a significant distortion of the fibres around the sensor, leading to the formation of voids, however, if placed directly on the dry coating, it is not possible to cut the window on the coating and access the strain gauge's surface without damaging it, which is confirmed by the experiment of S3B. Conversely, when bonded to a small portion of tape, it is easier to cut the window on the dry coating to access the surface of the strain gauge (T3B_SG1). Nevertheless, resin flowed into the sensor-tape interface.

T3C and T3D proved that using tape to demarcate the positioning of the sensor on the dry coating and to assist the cutting of the window is a feasible strategy, since the dry coating does not adhere to the FRP composite and can be easily peeled off, instead of being necessary to scrap it off, which leaves residues on the FRP's surface and can cause damage to it.

In conclusion, considering the results of the experimental trials performed, the best approaches are the ones that comprise bonding the sensors after the manufacturing process, resourcing to:

- A small portion of tape and cutting the window using a box cutter;
- A Dremel;
- A CNC machine.

This project has received funding from the European Union's Horizon 2020 research and innovation programme under grant agreement No 952966.

3.5. FINAL SPECIMENS

3.5.1. Specimen 1

After performing a set of first experimental trials, the final specimens were produced, transferring the best concepts of the previous tests. In summary, only were produced samples for bonding the sensors after infusion (Option A), and a small portion of tape (the same area as the strain gauge) was placed between the dry coating and GF layers in each sample. The infusion procedure followed was the same as described above, however, it was manufactured a bigger part, covering almost all of the mould surface, as can be observed in Figure 41, and it was used a yellow dry coating, since it was the only one available in CORSO.

Figure 41 – Setup for the production of specimen A1.

The part, after curing, was demoulded and the results can be verified in **Figure 43**. It is not very clear in Figure (b), but it is worth mentioning that some resin flowed, by diffusion, through the dry coating, which did not happen in the production of the samples with the white dry coating. Nonetheless, this does not affect the properties of the FRP composite or compromise the bonding of the sensors but the quality of the yellow dry coating still need to be improved to avoid this phenomenon.

This project has received funding from the European Union's Horizon 2020 research and innovation programme under grant agreement No 952966.

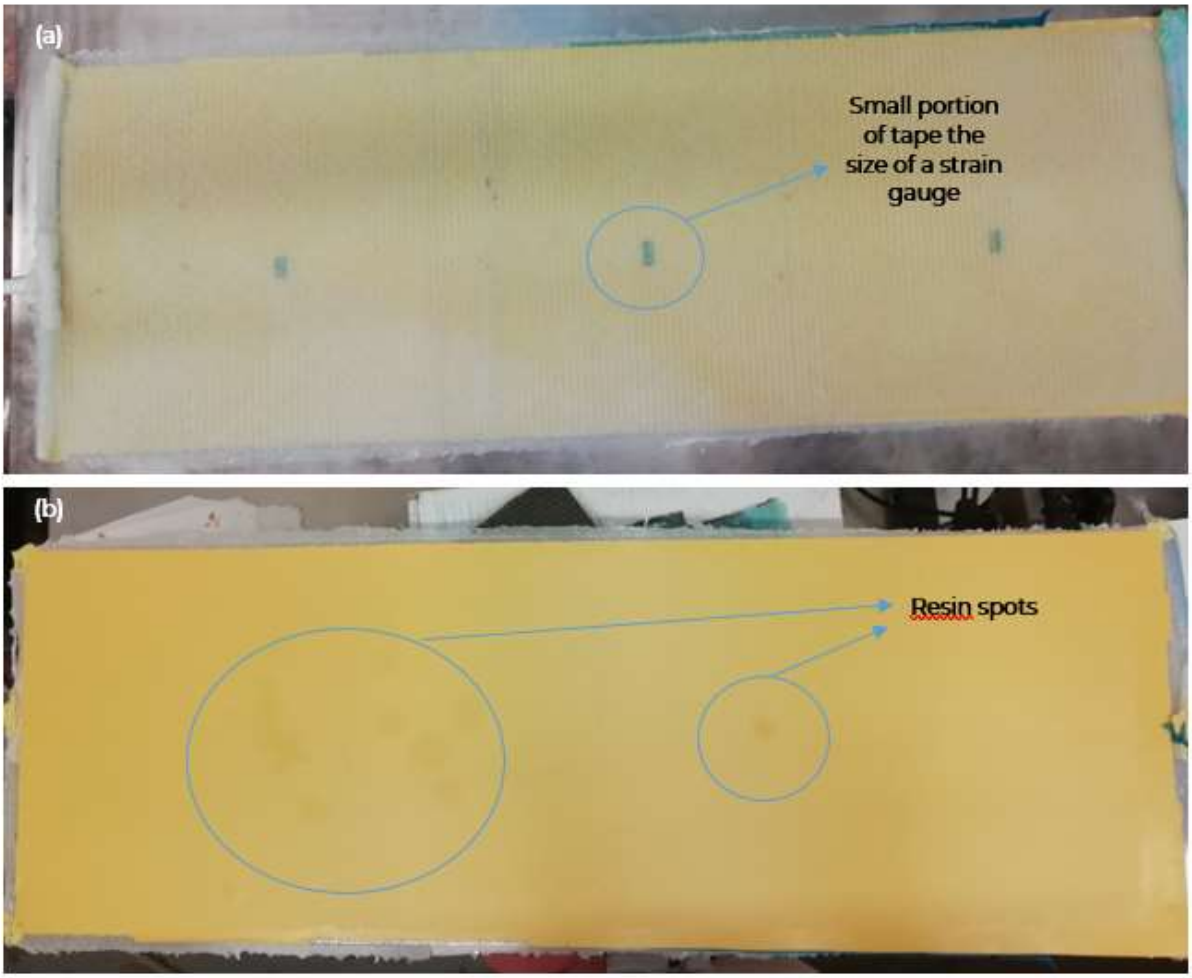

Figure 42 – Specimen S1. (a) FRP side. (b) Dry coating side.

Subsequently, S1 was cut in three samples with approximately 250 x 250 mm, using an abrasive disc. The main characteristics of each sample is documented in Table 13. Then, windows were opened on the dry coating with a box cutter, using the small portions of tape placed during the infusion process as reference marks – see Figure 44. The dry coating was peeled off and the strain gauges were bonded to the FRP's surface with M-Bond AE-10, as can be seen in Figure 45.

Table 13 – Characteristics of specimens S1_A, S1_B and S1_C.

Specimen S1	Infusion date	Demoulding date	Dimensions		Thickness (mm)
			Length (mm)	Width (mm)	
S1_A	2021-10-07	2021-10-11	250 ± 0.1	250 ± 0.1	4.2 ± 0.05
S1_B			250 ± 0.1	250 ± 0.1	4.2 ± 0.05
S1_C			250 ± 0.1	250 ± 0.1	4.2 ± 0.05

This project has received funding from the European Union's Horizon 2020 research and innovation programme under grant agreement No 952966.

Figure 43 – S1 after cutting, resulting in S1_A, S1_B and S1_C.

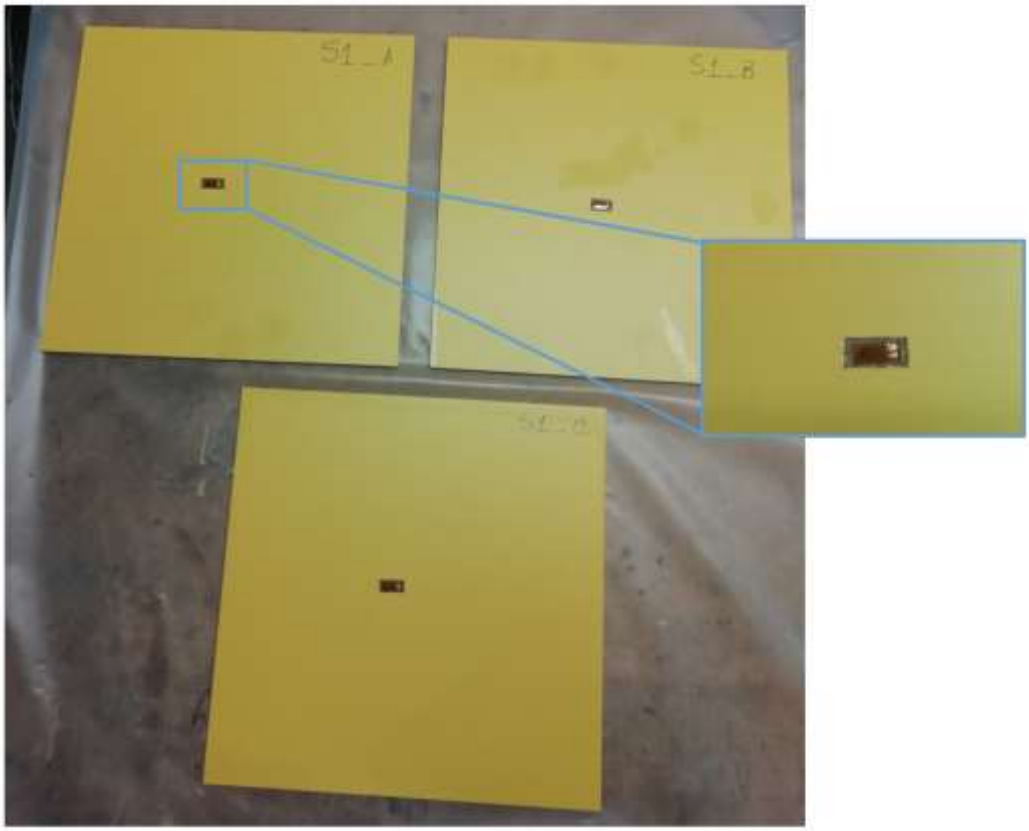

Figure 44 – Bonding of the strain gauges in samples S1_A, S1_B and S1_C.

This project has received funding from the European Union's Horizon 2020 research and innovation programme under grant agreement No 952966.

3.5.2. Specimen 2

For the production of specimen S2, which was intended for the bonding of the accelerometers, it was used the same setup and procedure as for the production of S1. Nonetheless, the portions of tape bonded to the dry coating prior to the infusion process were smaller than the ones placed in the previous specimen, once the area of accelerometers is inferior to the area of the strain gauges.

Figure 46 shows the specimen S2 after demoulding. This piece was then cut with an abrasive disc in three samples, resulting in S2_A, S2_B and S2_C, whose most relevant characteristics are gathered in Table 14. Figure 47 represents these specimens, including the open windows on the dry coating. Next, the accelerometers were bonded to the exposed FRP's surface in each specimen, as can be observed in Figure 48. It is worth noting that during the vacuum infusion process some resin also flowed through the yellow dry coating.

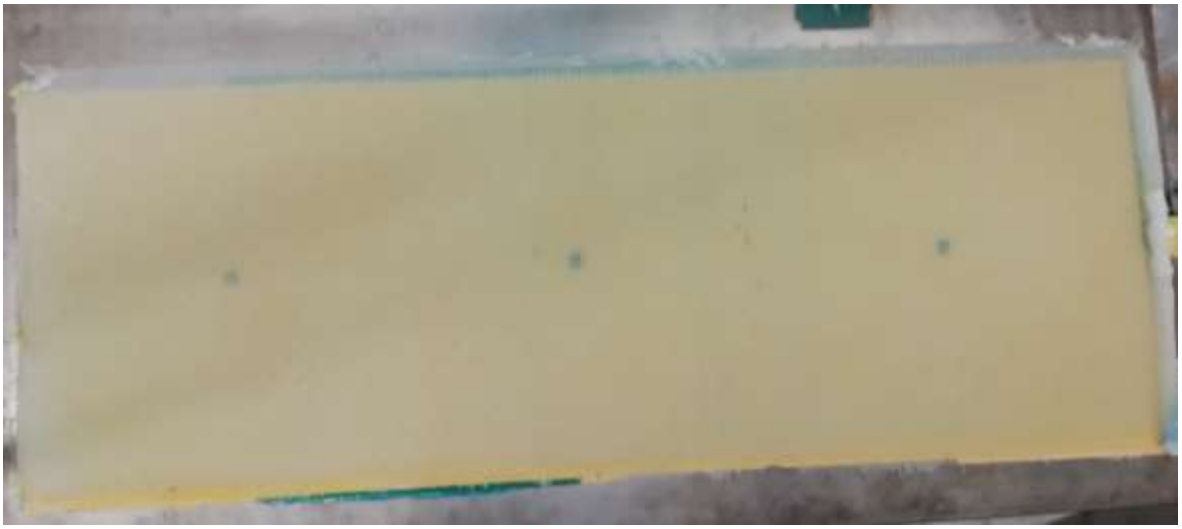

Figure 45 – Specimen S2.

Table 14 – Characteristics of specimens S2_A, S2_B and S2_C.

Specimen S2	Infusion date	Demoulding date	Dimensions		Thickness (mm)
			Length (mm)	Width (mm)	
S2_A	2021-10-11	2021-10-14	250 ± 0.1	250 ± 0.1	4.2 ± 0.05
S2_B			250 ± 0.1	250 ± 0.1	4.2 ± 0.05
S2_C			250 ± 0.1	250 ± 0.1	4.2 ± 0.05

This project has received funding from the European Union's Horizon 2020 research and innovation programme under grant agreement No 952966.

Figure 46 – S2 after cutting, resulting in S2_A, S2_B and S2_C.

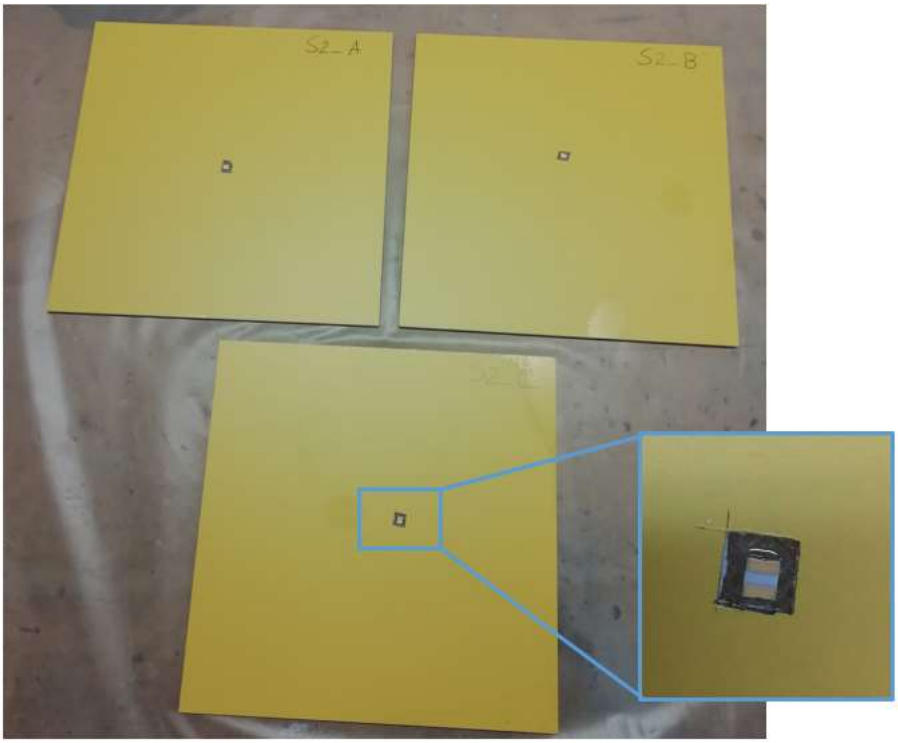

Figure 47 – Bonding of the strain gauges in samples S2_A, S2_B and S2_C.

This project has received funding from the European Union's Horizon 2020 research and innovation programme under grant agreement No 952966.

3.5.3. Final Remarks

With the development of this subtask, it was possible to conclude that the integration of the dry coating in the vacuum infusion process is a feasible concept, nonetheless, it must be carefully sealed and tested, in order to avoid resin flow to its surface. It was proved that the embedment of the sensors within the manufacturing process is very difficult, since the presence of a thick body as the accelerometer causes a significant disruption of the fibres path and the access to the strain gauge's surface possibly leads to its damage during the removal of the dry coating. Therefore, the best solution relies on applying the sensor after the vacuum infusion process – Option A.

Since the most effective and easy manner of opening a small window on the dry coating is by using a small portion of tape as a reference mark and a box cutter, this approach was implemented in both final production processes. However, the use of the box cutter is extremely dependent on the operator's skills and on the blade's quality. Subsequently, specimens S1 and S2 were cut in six samples with nearly 250 x 250 mm each. The small windows were cut and the sensors bonded to the composite's surface with a specific adhesive.

In summary, the process chain is the following:

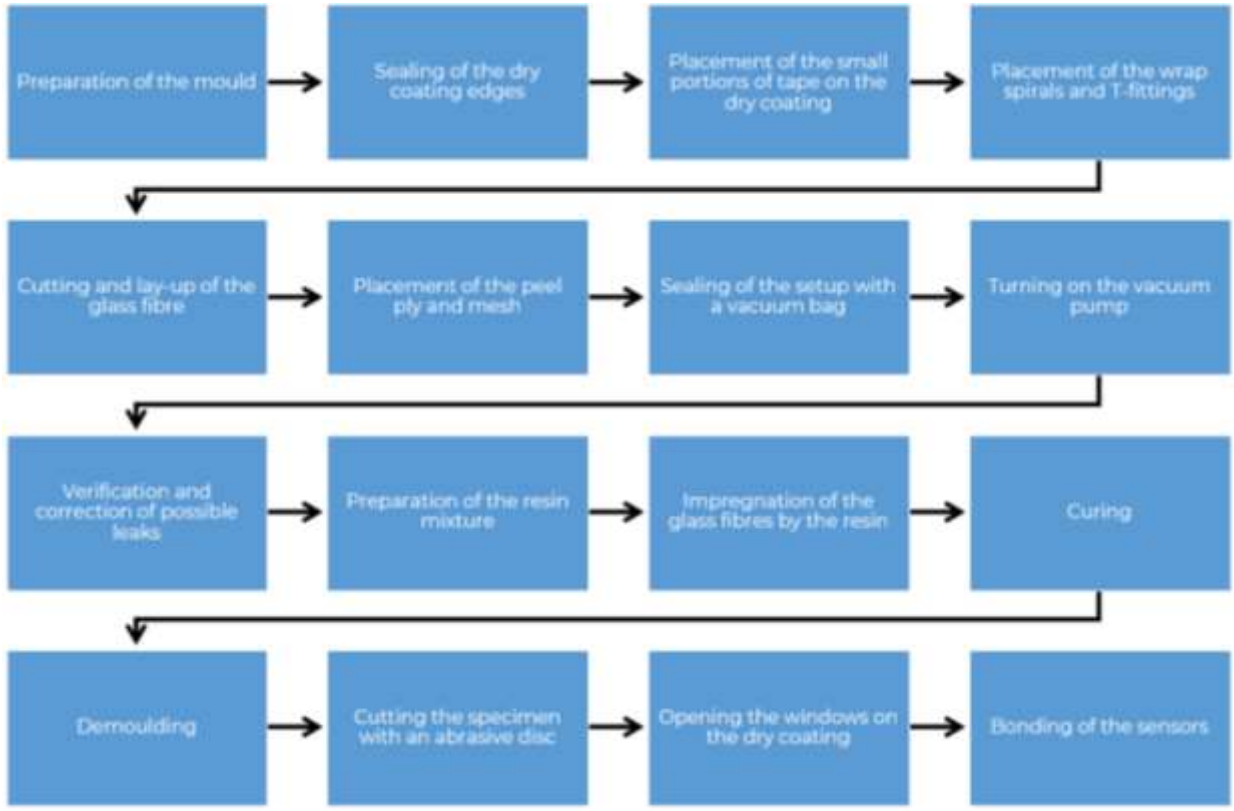

Figure 48 – Process chain for the production of the final specimens (best route).

The six specimens were then shipped to TSI's facilities, in Barcelona, to solder the cables to the sensors and to test their performance. It is worth mentioning that the exposed area around the sensor must be covered with a liquid/spray coating, in order to protect the FRP composite from the environmental conditions.

This project has received funding from the European Union's Horizon 2020 research and innovation programme under grant agreement No 952966.

3.6. TEST CAMPAING

A test campaign was carried out by TSI's engineering team to ensure that the performance of the FRP multifunctional materials is appropriate for the diagnosis of the structural integrity of the materials. Figure 50 presents a schematic representation of the plan for the development of the FRP multifunctional materials that has been divided into three engineering phases:

- In the first stage "Selection of the optimum manufacturing process", the FIBREGY consortium focused on the selection of the most appropriate process for the manufacturing of the FRP multifunctional materials.
- In the second phase "Analysis of the feasibility of the fabrication", a set of FRP multifunctional materials were manufactured by INEGI's research institute. To address this task, the accelerometers and strain gauge selected in the context of Task 2.5.1 are inserted in the dry-coating and FRP laminar interface as shown in the schematic description of Figure 50.
- In the third step "Verification of the FRP multifunctional materials in the laboratory", it has been proven the performance of the FRP multifunctional materials in the TSI laboratory by using a controlled pressure and vibration test to examine the sensitivity of the strain gauge and accelerometer.

Figure 49 – Flow chart for development of FRP multifunctional materials.

In the first stage, the consortium of the FIBREGY project has evaluated the potential of three manufacturing strategies for embedding the sensors selected in Task 2.5.1 into the FRP-multifunctional materials. The strategy selected for the FIBREGY consortium consisted of the integration of the sensor in the interface FRP tower-Dry Coating (referred to us as sensor position 2). This option was selected for the consortium for two main reasons: 1st) It is the most simple approach from the manufacturing point of view. 2nd) The integration of the sensor device into the FRP laminar material does not affect the mechanical performance of the FRP tower. More detailed information

on this initial stage can be found in Section 3.2 "Performance and diagnosis of multifunctional materials".

The primary aim of the second step consists of the fabrication of this new generation of FRP multifunctional materials by using the technology of infusion. With the aim to prove the concept, a set of FRP multifunctional materials were manufactured by INEGI's research institute with the above-mentioned configuration "sensor position 2". A digital photography of the six FRP multifunctional materials are given in **Figure 51**. For the sake of clarity, the inset of the figures shows a close-up photography of the strain gauges / accelerometers installed on the upper part of the FRP multifunctional materials.

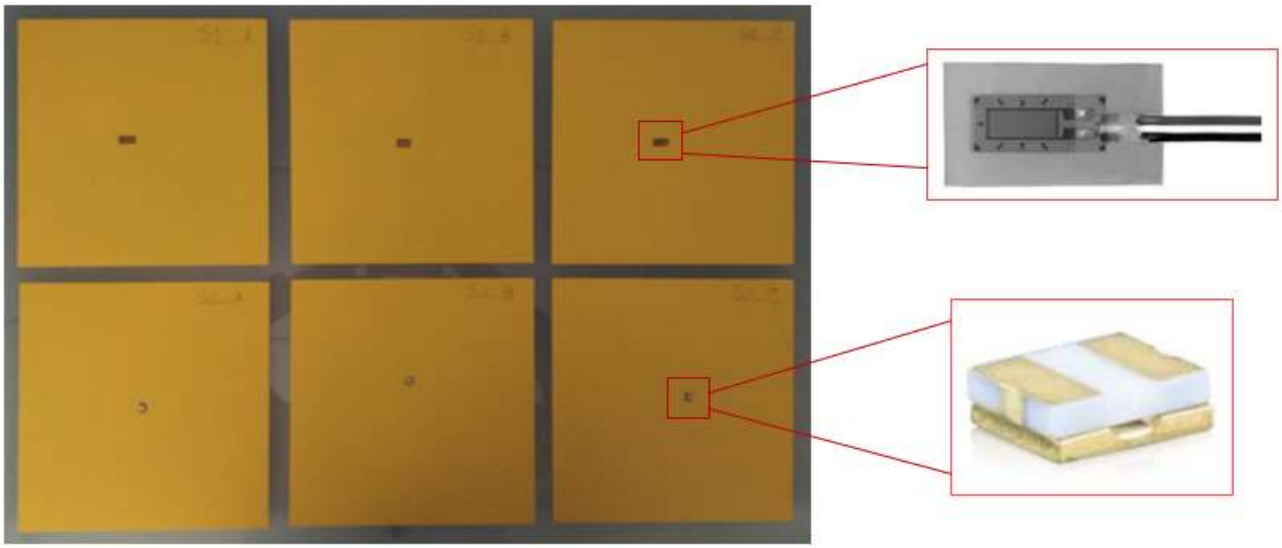

Figure 50 – Digital photography of the six FRP multifunctional materials manufactured by INEGI institute.

The final stage consisted on the verification of the FRP multifunctional materials performance in the laboratory. For such purpose, it has been proven the performance of the FRP multifunctional materials in TSI laboratory using a controlled pressure and vibration test in order to examine the sensitivity of the strain gauge and accelerometer.

- To evaluate the strain gauge's performance, the sensor electric responses exerted by a controlled pressure of 7424 Pa were recorded for 24 hours. As it is shown in **Figure 52**, the signals recorded by the sensor were stable and constant which verifies the correct performance of the sensor. The minimum variations of the strain levels recorded by the sensors are attributed to changes in Temperature.
- To evaluate the accelerometer's performance, the sensor electric responses were tested using a calibration vibration machine. The signal exerted by the vibration machine (input) is given in the red curve, while the signal recorded by the accelerometer (output) is provided in the blue curve (see **Figure 53**). The comparison of the signal (input-output) is in the range of 14.8 % which is within the range of sensor deviation. The Fast Fourier Transform spectrum of the vibratory signal recorded by the vibration machine and the sensor selected are given in **Figure 54**. The peak at 80 Hz is associated with the frequency of the vibration machine, while the peak at 50 Hz recorded for the accelerometers can be attributed to the electrical noise of the system.

This project has received funding from the European Union's Horizon 2020 research and innovation programme under grant agreement No 952966.

As a general conclusion, it is noticed that the functioning of the strain gauges and accelerometers embedded in the FRP plates is appropriate.

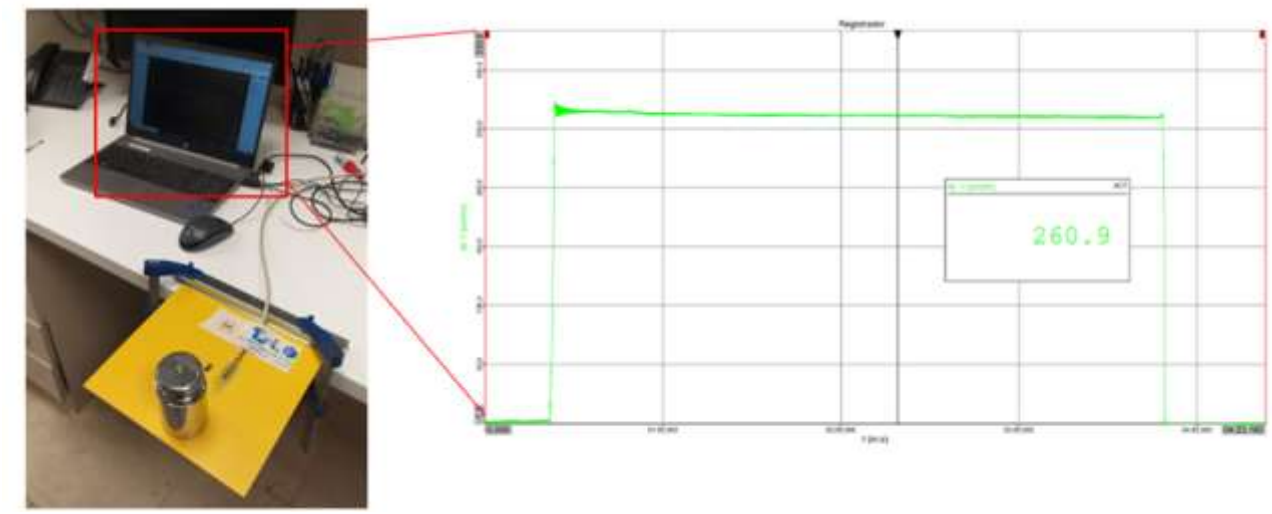

Figure 51 – Sensor electric output recorded for the strain gauge.

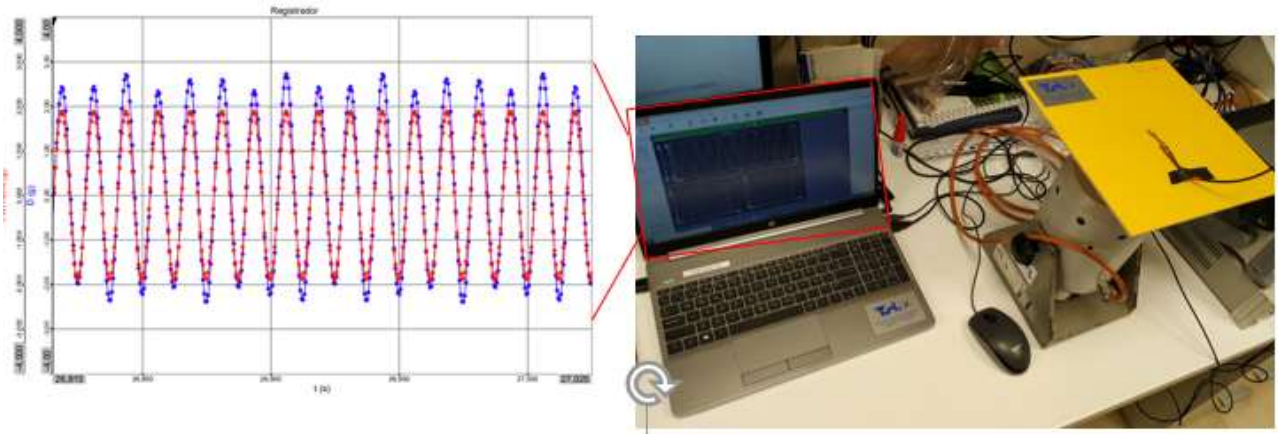

Figure 52 – Sensor electric output recorded for the accelerometer.

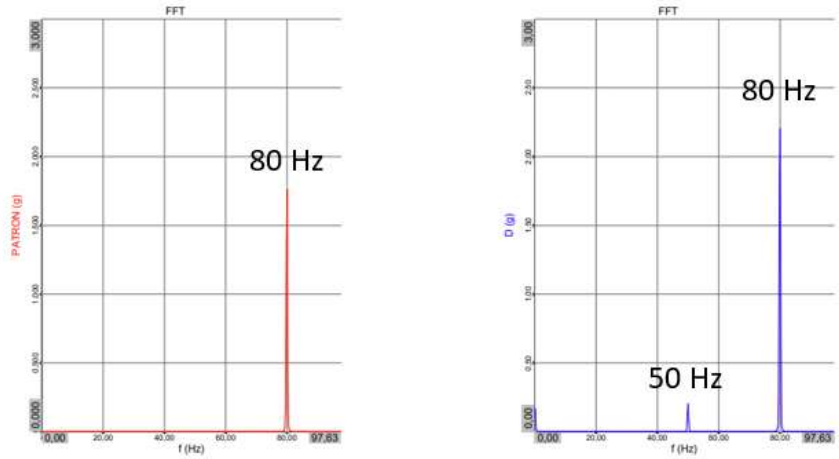

Figure 53 – FFT spectrum of the input of the vibration machine and output signal of the FRP multifunctional material of the sensor.

This project has received funding from the European Union's Horizon 2020 research and innovation programme under grant agreement No 952966.

TSI installed the accelerometers and strain gauges using the adhesive selected “M-Bond AE-10 Kit”. The adhesive tested works well in terms of strength. However, the exothermic reaction of the Curing Agent and the resin releases heat may affect negatively the performance of the piezoelectric accelerometers. This can be explained because piezoelectric materials are temperature dependent and therefore, any change in the temperature will result in a change in the sensitivity of the accelerometer. The change of sensor’s sensitivity can be reversible if the operation temperature varies in the range of operation of the sensor, or irreversible for higher temperatures. Therefore, it has been recommended for the consortium to watch out for this aspect and choose carefully the selection of the right adhesive for the installation of the sensors in the Structural Health Monitoring System envisaged in Task 4.4.

This project has received funding from the European Union's Horizon 2020 research and innovation programme under grant agreement No 952966.

4. DEVELOPMENT OF SHM METHODOLOGY FOR THE INSPECTION AND DIAGNOSIS OF FOWTs

The fact that the typical life span of a wind turbine is 20 years has been misinterpreted by the wind offshore owners, and therefore, the initial maintenance plans were based on the assumption that the structural components (tower, nacelle, and blades) of wind turbines were required limited or even no maintenance. Nevertheless, the lessons learned over the years is that the structural components of the wind turbines also fail due to multiple causes as manufacturing issues, lightning, foreign objects impacts, delamination, adhesive bonding, or problems in the modular connections. Thus, the development of structural health monitoring systems for the monitoring of the structural components of FOWTs is an area of potential interest for the offshore industry.

The final objective of Task 2.5 is the validation of a non-destructive SHM methodology for the inspection and diagnosis of the structural integrity of the 1:50 scale tower of the W2Power Wind Turbine. With respect to this, Task 2.5.3 looks at the two following aspects.

- Analysis of the feasibility of the shift of the natural frequencies, damping, and vibration mode shapes for the damage assessment of delamination failures in FRP-based towers. The main idea behind this task is to compare the modal parameters of medium-scaled specimens in pristine and damaged conditions with the purpose to evaluate the potential of the above-mentioned key performance indicators for the detection, quantification, and location of delamination damage. Further information about this research study can be found in Section 4.1.
- Evaluate the feasibility of a series of key performance indicators based on natural frequencies, damping, and mode shapes for the diagnosis of the tightening torques of the bolted joints of the W2Power tower connections. To achieve this goal, the effect of the tightening torques on the natural frequencies, damping, mode shapes of the towers has been investigated by the research team using a multidisciplinary approach. The results obtained in the experimental trials are detailed in Section 4.2.

This investigation is done with the paramount purpose to shed light on the basis for the structural health monitoring methodology developed for the monitoring of the 1:6 scale W2Power Platform installed in the PLOCAN site area at the Canary Islands.

This project has received funding from the European Union's Horizon 2020 research and innovation programme under grant agreement No 952966.

4.1. KEY PERFORMANCE INDICATORS FOR DETECTION, QUANTIFICATION, AND LOCALISATION OF TOWER STRUCTURAL DAMAGE

Most of the Floating Offshore Wind Turbines (FOWT) and Tidal platforms are designed with traditional materials like steel or concrete, however, the implementation of composite materials for the design and construction of Floating Offshore Wind Turbines and Tidal platforms will offer a large number of advantages like the absence to corrosion failures, reduction of maintenance costs, CAPEX, OPEX, and transportation costs.

- From the capital expenditures perspective, an interesting aspect derived from the application of FRP materials in shipbuilding is associated with the weight reduction in FOWT engineering structures. The vast experience of shipyards in the construction of small-length ships (below 500 GT) indicates that a significant weight reduction in the range of 30 % and 40 % can be accomplished by the massive employment of FRP materials. Similarly, if we look at larger length vessels (over 500 GT), the consortium of the FIBRESHIP project (1) demonstrated that a structural weight reduction of 45%, 33%, and 70% is achieved by the full application of lightweight materials in a 260 m length containership, a 204 m length Ro-Pax, and an 85 m length Fishing Research Vessel, respectively (11). Another positive effect is that the drastic weight reduction exerted by the implementation of FRP materials in the design of energy renewable platforms is expected to reduce the cost for the transportation, mooring, and commissioning of the turbine's foundation.
- From the operational costs point of view, corrosion failures are commonly appreciated on Floating Offshore Wind Turbine (FOWT) platforms due to the aggressive climate conditions of the sea, which represents approximately 60% of offshore maintenance costs in steel-based platforms (12). Therefore, one of the most relevant advantages of the application of composite materials in FOWTs is that they are not susceptible to the typical corrosion failures of metallic materials, which results in a better life cycle performance and a significant reduction of maintenance costs.
- From the environmental point of view, a remarkable benefit noted for the marine industry will be the reduction of fuel consumption and greenhouse gas emissions emitted during the transportation of the FOWTs, supporting the international effort of waterborne transport zero-emission industry.

A very frequent failure mode of Fibre Reinforced Polymer materials is the presence of delamination defects that severely affects the mechanical performance of these materials. The scientific and industrial community has reported a large number of non-destructive methods for the analysis of delamination defects in fiber-reinforced polymer (FRP) structures such as ultrasounds (13), thermography (13), acoustic emission (14), and vibration-based solutions (15), among others. Among the aforementioned techniques, Vibration-based SHM is a technique of special interest for the detection of delamination defects due to its advantages of being an economic, straightforward, and multidisciplinary approach that can be applied for different types of structural damage by operation and maintenance technicians.

This project has received funding from the European Union's Horizon 2020 research and innovation programme under grant agreement No 952966.

The main purpose of this investigation is to verify the feasibility of a non-destructive vibration-based methodology to identify the presence of interlaminar delamination defects in the FRP-based towers of the W2 Power Turbine Floating Offshore Platform. This strategy is based on the comparison of modal parameters of intact and damaged 1:50 scale FRP towers with different delamination scenarios.

4.1.1. Description of the FRP towers

In particular, the authors focused on the investigation of the feasibility of the modal parameters for the analysis of delamination defects in 1:50 scale towers of the Enerocean's innovative W2Power platform (12 MW). To achieve this goal, the natural frequencies, damping, and vibratory mode shapes are measured by the research team using a modal analysis non-destructive test. **Figure 55** displays a schematic description of the seven FRP specimens, which were manufactured by TUCO shipyards using the wet lay-up process. The intact FRP tower without the presence of delamination phenomena is referred to as healthy panel while the FRP towers with different delamination damage scenarios are known as damaged samples.

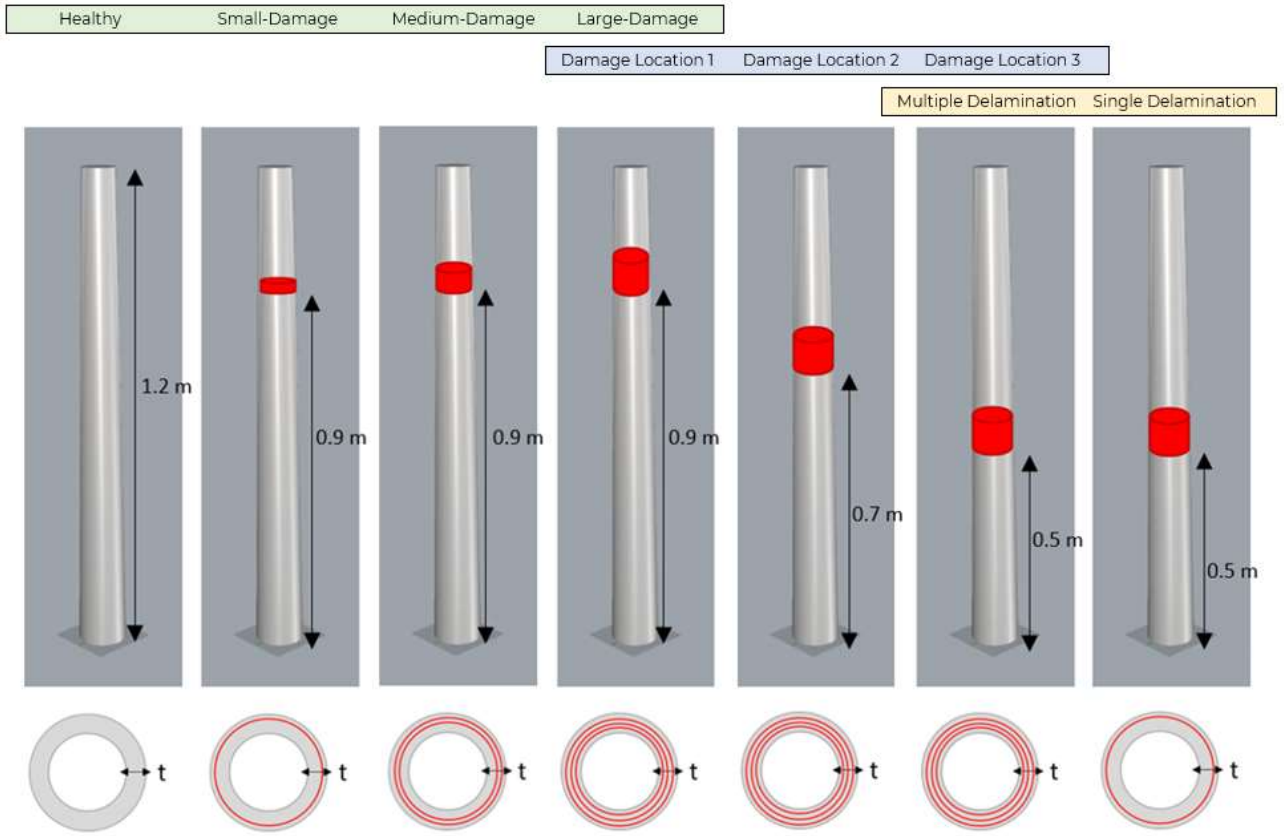

Figure 54: Schematic description of the seven FRP towers manufactured by TUCO shipyards. The red area of the frontal and superior views of the towers shows the location of the delamination regions in the FRP towers.

This project has received funding from the European Union's Horizon 2020 research and innovation programme under grant agreement No 952966.

The configuration of the towers is represented in Figure 55. The red area of the frontal and superior views of the towers shows the multiple locations of the delamination failures in the FRP towers

- The Healthy, Small-Damage, Medium-Damage, and Large-Damage towers are entitled in green in Figure 55: The main purpose of this experimental trial is to investigate the feasibility of the key performance indicators (KPI) to quantify the extension of delamination damage in the Towers.
- The towers with Damage Location 1, 2, and 3 are marked in blue in Figure 55: The paramount purpose for these three towers is to evaluate the feasibility of the KPI's to localise the delamination defects in the FRP towers.
- The towers with Single vs Multiple delaminations are named in orange in the tower (see Figure 55): The comparison of the KPI's for the FRP towers with single and multiple delamination defects is carried out to verify the capability of this non-destructive method to identify the typology of delamination.

The FRP towers were built at scale 1:50 with the dimensions given in Table 15. The resin system used for the fabrication of the composite laminates was a vinylester-based resin, while the fibers used as a reinforcement in the FRP panels are glass fiber (Hybon 2026 or Hybon 2002). The stacking sequence of the FRP laminates is [0/55, 0/-55,0/90] for a total number of 6 layers of unidirectional fibres. Eventually, the FRP towers with the dimensions and selected configuration were cured in an autoclave according to the process specifications provided by the material supplier.

	Height (h)	Bottom External Diameter (D_1)	Top External Diameter (D_2)	Thickness (t)
1:50	1200 mm	117 mm	84 mm	4 mm

Table 15 - Dimensions of the FRP towers at scale 1:50.

The delamination failures were introduced by inserting a "Teflon layer" in the interlaminar regions of the 1:50 scale FRP towers at the positions highlighted in red in Figure 55. The location of the delamination failures of the FRP towers is detailed in Table 16.

Name	Abbreviation	Length (l)	Number of layers delaminated (n)
Baseline	BL		
Small-Damage	D1	50 mm	1
Mid-Damage	D2	100 mm	2
Large-Damage	D3	150 mm	3
Location 2	D4	150 mm	3
Location 3	D5	150 mm	3
Single layer	D6	150 mm	1

Table 16: Definition of the delaminated regions in the FRP towers

This project has received funding from the European Union's Horizon 2020 research and innovation programme under grant agreement No 952966.

4.1.2. Description of the KPI parameters

A non-destructive free vibration test is used to acquire the modal parameters of the towers with and without internal delamination failures. A schematic of the experimental set-up is detailed in Figure 56. The experimental procedure can be divided into three steps: First, the manufactured towers with and without internal delamination defects are tested in free-free boundary conditions in the framework of the experimental campaign. Second, a sharp impact is applied to the upper positions of the FRP-based towers using a modal impact hammer in the position marked in red in the figure. Third, the vibration signals of the composite towers are recorded for 3 s in the range of frequencies (0-1000 Hz) using an array of four commercial accelerometers (Endevco, 44A16-1032). The measurement directions are detailed in the insets of Figure 56. This procedure was repeated five times to obtain a multiple number of realizations for each specimen.

The vibration-based strategy is based on the comparison of the modal parameters (natural frequencies, damping, and mode shapes) of FRP-based towers with different delamination scenarios. Here-below is provided a description of the procedures to extract the natural frequencies, damping, and mode shapes of the FRP towers with different levels of delamination damage.

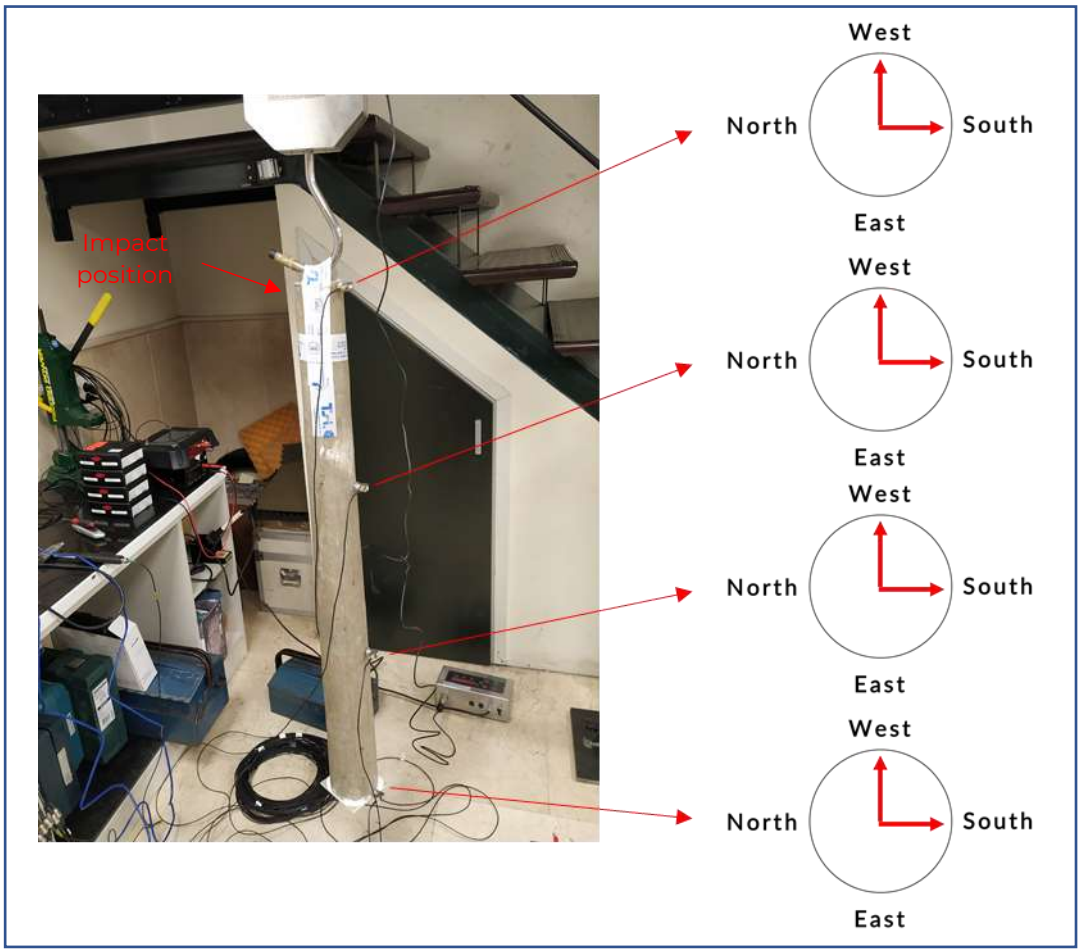

Figure 55: Description of the experimental trials in the TSI laboratory to obtain the modal parameters of the towers. The directions of the measurements are detailed in compass of the figure.

This project has received funding from the European Union's Horizon 2020 research and innovation programme under grant agreement No 952966.

Natural Frequencies

The natural frequencies of the composite towers with and without internal delamination failures are obtained via the Fast Fourier Transform on the recorded free vibration signals. The distinct peaks in the resulting spectrum are assumed to indicate the natural frequencies. A visual representation of the FFT spectrum acquired for the towers is depicted in Figure 57.

Damping

Damping can be defined as an indicator of the amount of energy that a material can dissipate, where higher damping values are associated with a greater capability for energy vibration dissipation. The damping is calculated to evaluate the ability of intact and damaged towers to dissipate vibrational energy during the resonance phenomena. For such purpose, the damping of the natural frequencies of the composite tower is determined through the half-power method through Equation (1).

$$\delta = \frac{w_3 - w_1}{2w_2} \quad (1)$$

Where w_1, w_2, and w_3 are the frequencies associated with the first, second, and third points of the frequency response function (FRF) as represented in Figure 58. It should be pointed out that the w_2 can be defined as the frequency of the resonant peak in the tower and $w_{1,3}$ stands for the points of the peak located 3 dB below the maximum amplitude.

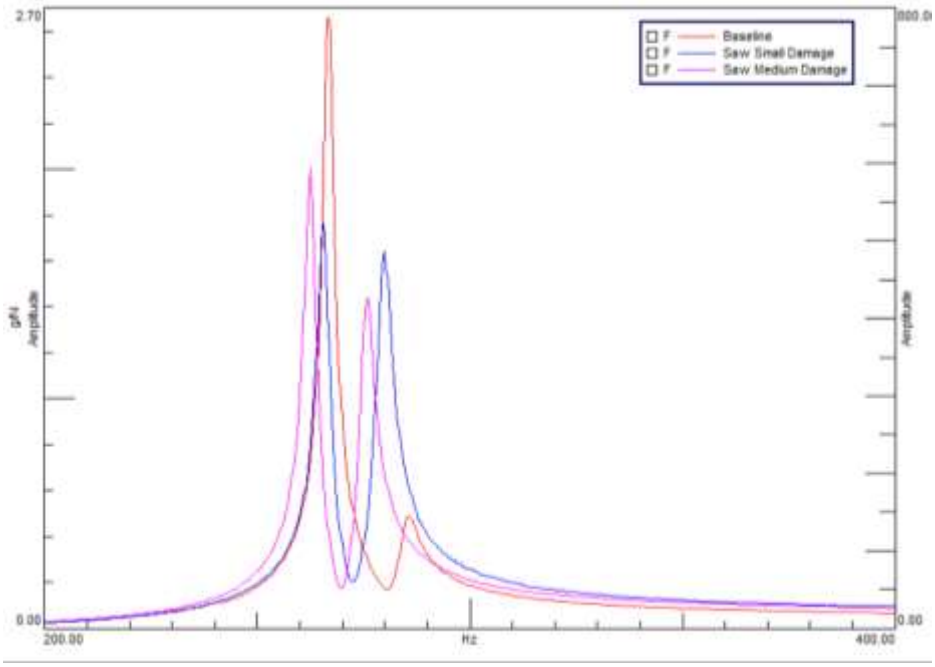

Figure 56: FFT spectrums of towers in intact state (red curve) and artificial damage (blue and pink curves). The peaks of the spectrum indicate the natural frequencies of the FRP towers.

This project has received funding from the European Union's Horizon 2020 research and innovation programme under grant agreement No 952966.

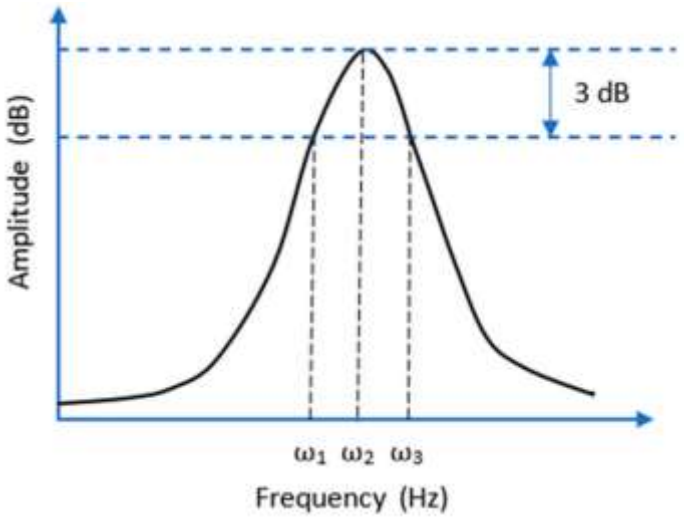

Figure 57: Description of the Half power damping method used for calculation of the damping loss factors.

Mode Shapes

The vibration mode shapes corresponding to the FRP towers were simulated using the modal analysis tool of the software Siemens LMS Test Lab. To address this task, the Fast Fourier Transform (FFT) spectrum characteristic for each measurement point is used to simulate the vibration mode shapes of the pristine and damaged towers. Figure 59 shows an example of one of the mode shapes of the intact FRP tower.

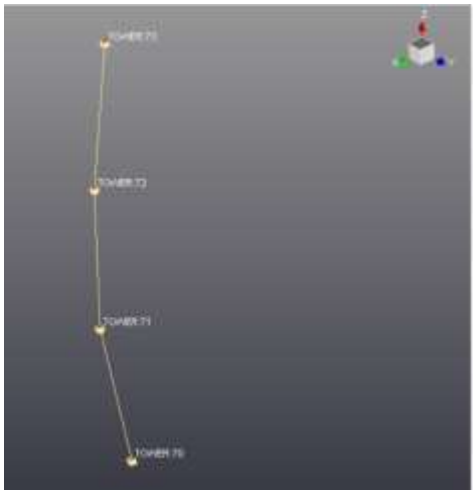

Figure 58: Representation of a Vibration Mode Shape of the FRP-based tower.

4.1.3. Results and Discussion

This section aims to analyse the feasibility of the shifts of the modal parameters for the detection, quantification, and location of delamination defects in FRP towers. The main purpose behind this is to find out if the shift of the natural frequencies, damping, and vibration mode shapes can be used as a diagnostic tool to evaluate the structural integrity of the FRP-based towers. For the sake of clarification, the paragraph is organized into three parts:

This project has received funding from the European Union's Horizon 2020 research and innovation programme under grant agreement No 952966.

- The first part is devoted to the analysis of the potential of the key performance indicators for the quantification of the delamination defects in the tower. The idea is to find out the potential of the modal parameters to estimate the extent/severity of the damage in the tower structure.
- The second part is focused on the location of delamination defects in the FRP towers with the aim to find out the capability of the KPIs for the identification of the localisation of the damage in the structure domain.
- The third part lies on the analysis of the KPIs for the identification of the type of damage (single vs multiple delaminations), which are two different typologies of delamination failures.

Analysis of the KPI's feasibility for the quantification of damage

This section looks at the influence of delamination defects on the modal parameters of the FRP tower. To address this investigation, the modal parameters for identical towers with three different damage states are compared in order to find out how the delamination breakages produce changes in the natural frequencies, damping, and mode shapes of the towers.

With respect to damage detection, the natural frequencies of the towers with four damage states (healthy, small-damage, medium-damage, and large-damage) are depicted in Figure 60. The results of the figure reveal that the clusters for the healthy tower are well separated from the observations of the delaminated towers. In particular, the natural frequencies of the pristine towers (290.82 ± 0.16 Hz) are greater than the natural frequencies of the damaged towers which vary in the range of frequencies between 263 and 280 Hz. Thus, it is noticed that the natural frequencies are an appropriate method to detect the presence of damage in the structure.

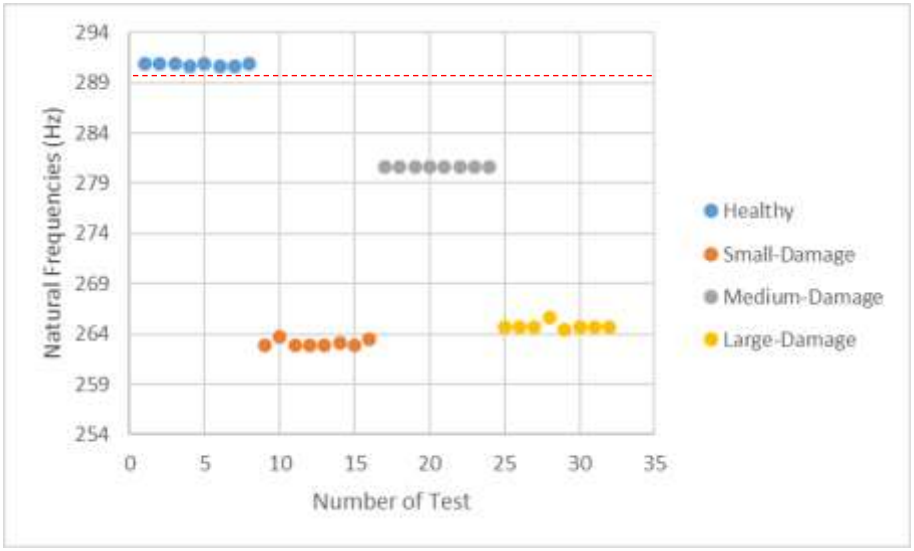

Figure 59: Evaluation of the capability of the natural frequencies to detect the presence of delamination defects in the intact and damage towers.

With respect to the damage quantification, the natural frequencies of the towers with small, medium and large delamination defects are in the range of 263.05 ± 0.37 Hz, 280.63 ± 00 Hz, and 264.77 ±

This project has received funding from the European Union's Horizon 2020 research and innovation programme under grant agreement No 952966.

0.36 Hz as detailed in the bar chart given in Figure 61. In general, it is known that the intensity of the natural frequency changes depends on the size of the delamination defect, and therefore, it is expected that larger delamination defects lead to higher decrements of the natural frequencies due to the greater loss of local stiffness. From the results, it can not be observed a clear relationship between the decrement of the natural frequencies and the extension of the delamination defects. From the authors point of view, this behaviour can be attributed to the fact that the weight and geometry of the four towers are not exactly identical due to the uncertainties of the manufacturing process, which limit the capabilities of this non-destructive methodology. Therefore, it can be concluded that the capabilities of the natural frequencies for the estimation of the severity of the delamination failures are not verified and validated for this set of trials.

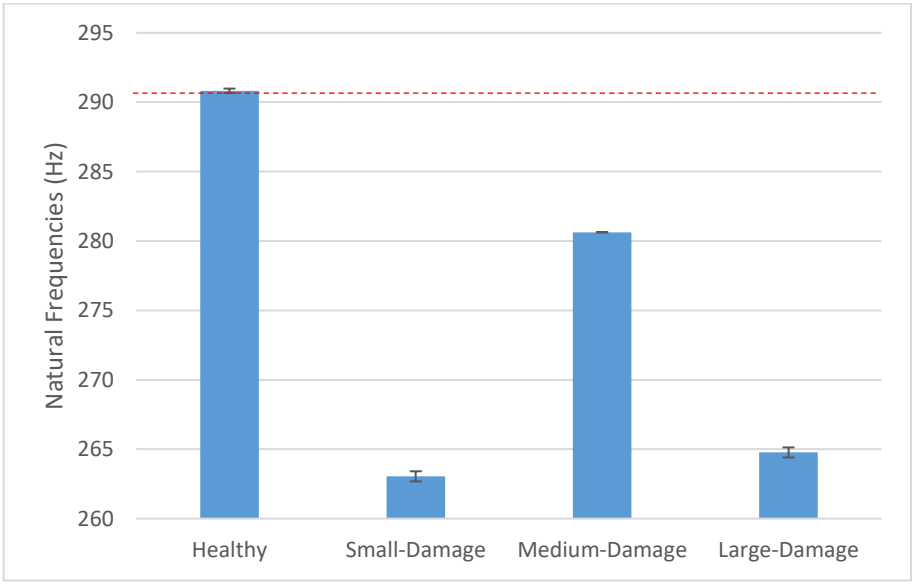

Figure 60: Effect of the delamination extension on the natural frequencies.

An additional effort was carried out to validate the capabilities of this NDT technology for the detection of delamination damage in the FRP towers. To carry out this task, an additional tower of 3.6 kg mass was damaged using a saw as shown in Figure 62.

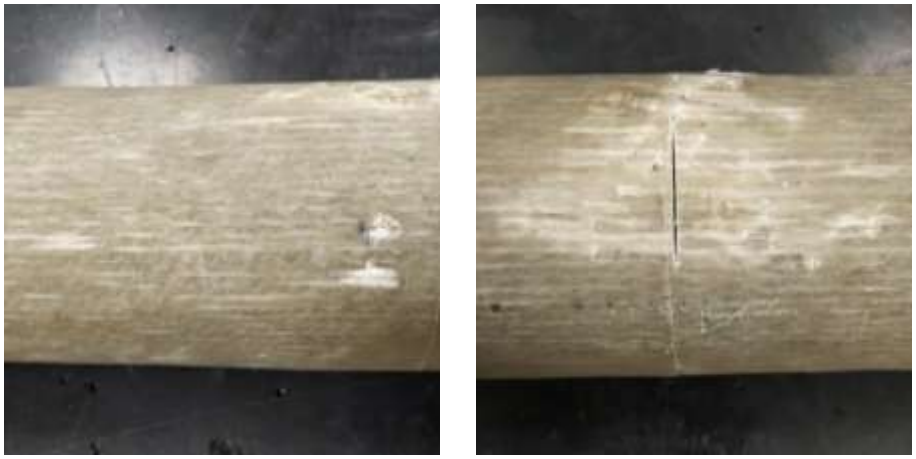

Figure 61: Digital photography of the healthy Tower (left) and Tower damaged by the saw (right).

This project has received funding from the European Union's Horizon 2020 research and innovation programme under grant agreement No 952966.

The natural frequencies of the towers with three damage states (healthy, small-damage saw, and medium-damage saw) are shown in Figure 63. From the results given in the figure, it can be seen that the results of the figure reveal that the clusters for the healthy tower are well separated from the observations of the delaminated towers. In particular, the natural frequencies of the towers with small, medium and large delamination defects are in the range of 284.81 ± 0.47 Hz, 279.69 ± 0.33 Hz, and 275.71 ± 0.28 Hz. This behaviour can be explained because the delamination damage causes a reduction of the local stiffness and therefore, the natural frequencies are lower. Based on these results, it can be said that the shift of the natural frequencies is a valid method for the estimation and quantification of the severity of the delamination failures

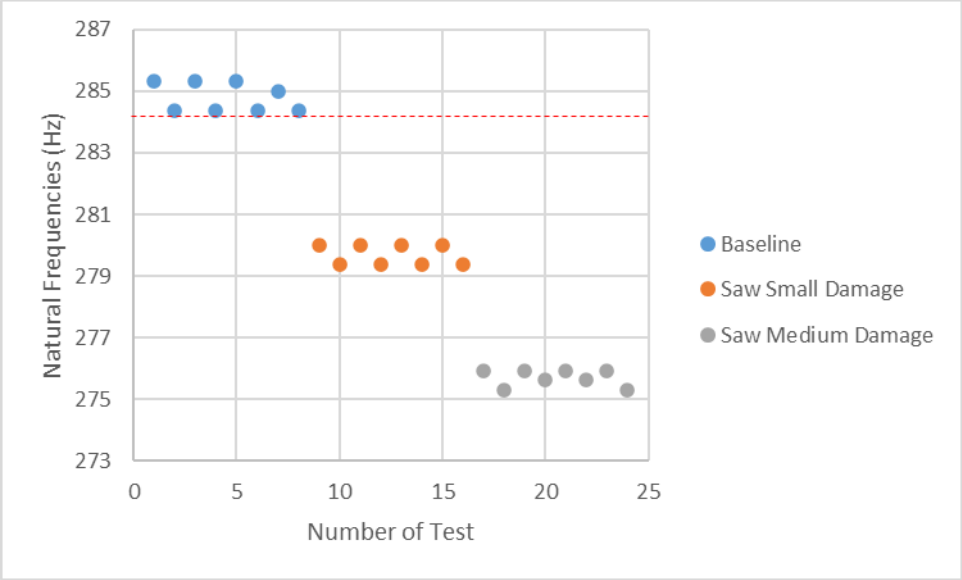

Figure 62: Evaluation of the capabilities of the natural frequencies to quantify the extension of delamination defects in intact and damage towers.

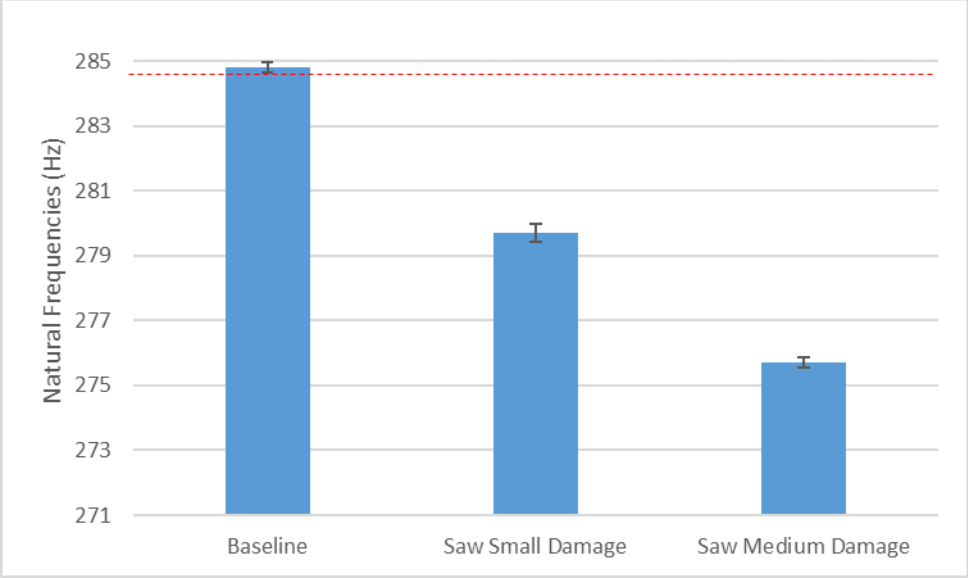

Figure 63: Effect of the delamination extension on the natural frequencies.

This project has received funding from the European Union's Horizon 2020 research and innovation programme under grant agreement No 952966.

In parallel, the feasibility of the damping for the detection and quantification of delamination defects was also investigated by the FIBREGY consortium. The mean value, standard deviation, and coefficient of variation of the natural frequencies and damping are given in Table 17 and 18, respectively. The measurements were repeated 8 times in order to obtain a multiple number of realizations for each measurement.

- If we look at the natural frequencies, the values of the natural frequencies show a high reproducibility with standard deviations in the range of ± 0.5 Hz and coefficient of variations in the range of 0.10-0.16 %, which is a good indicator that this key performance indicator is rather stable and can be considered reliable/credible.

Name	Mean Value (Hz)	S.D. Value (Hz)	C.V (%)
Healthy	284.81	0.47	0.16%
Saw Small Damage	279.69	0.33	0.12%
Saw Medium Damage	275.71	0.28	0.10%

Table 17: Analysis of the effect of the delamination extension on the damping of FRP materials.

- If we look at the damping, The values of the damping show a high variability with coefficients of variation in the range from 4 % to 10 %. Thus, the damping parameter is not recommended as key performance indicator for the detection of delamination defects.

Name	Mean Value (DL)	S.D. Value (DL)	C.V (%)
Healthy	0.94	0.14	10%
Saw Small Damage	0.65	0.02	4%
Saw Medium Damage	0.62	0.02	3%

Table 18: Analysis of the effect of delamination extension on the damping of the FRP materials.

Analysis of the KPI's feasibility for the localisation of damage

This section aims to study how the delamination location influences the modal parameters of the FRP tower. To carry out this investigation, the modal parameters of towers with identical size delamination defects (150 mm) ubicated at three different locations are extracted using the technique of modal analysis (see the exact position of the delamination defects in Figure 55). Figure 65 displays the results from the healthy tower, and from the towers with delamination defects in location 1, 2, and 3. The main outputs for the experimental trials can be drawn as follows:

- The measurements show that the clusters for the healthy tower are well separated from the clusters of the delaminated towers in damage locations 1, 2, and 3. Therefore, it is noticed that the network of clusters is able to distinguish the four different states tested in the tower.
- If we look at the results, the more drastic changes in the natural frequencies can be observed from the defects located in the upper section of the tower, which are in the range of 25 Hz, while the changes in the upper surfaces are around 5 Hz.

This project has received funding from the European Union's Horizon 2020 research and innovation programme under grant agreement No 952966.

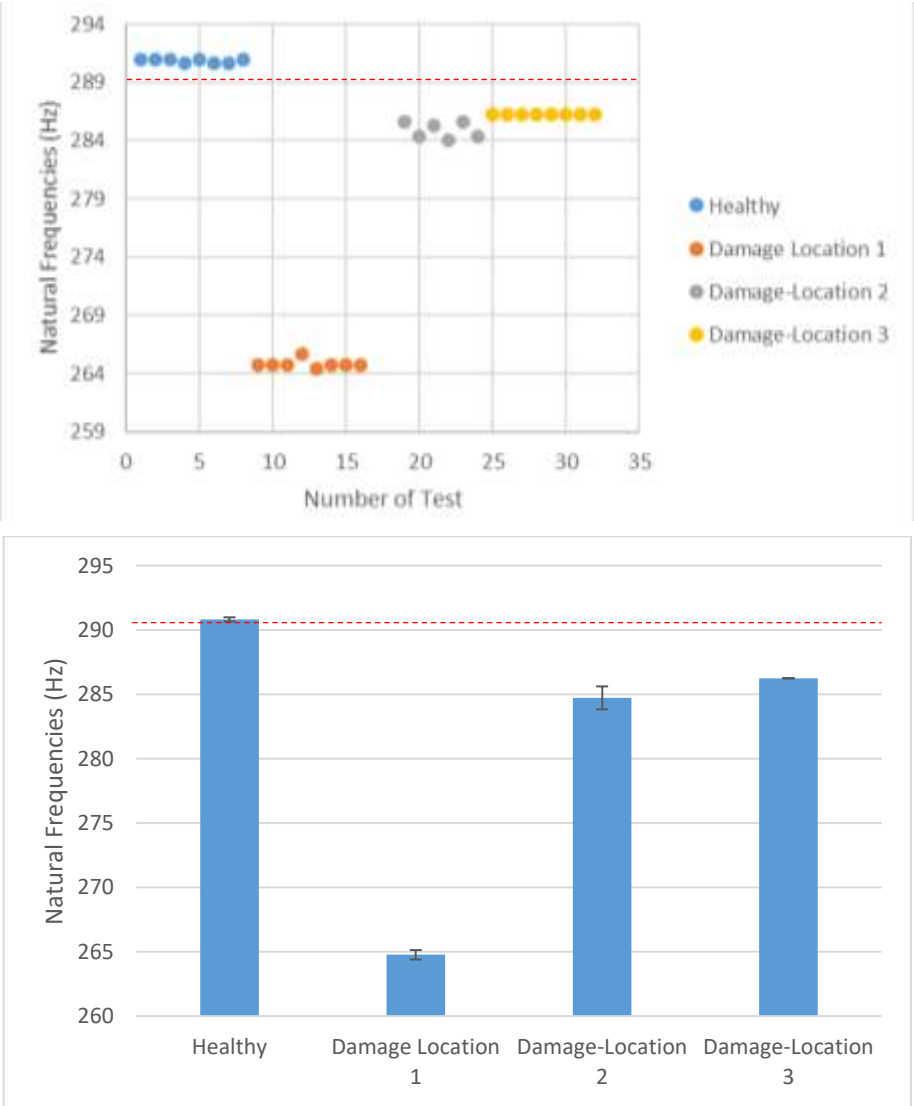

Figure 64 - Evaluation of the capabilities of the natural frequencies to localise the delamination defects in intact and damage towers.

In parallel, the feasibility of the damping for the localisation delamination defects was also investigated in this research study. The mean value, standard deviation, and coefficient of variation of the damping are given in Table 19. The measurements were repeated 8 times in order to obtain a multiple number of realizations for each measurement. As stated above, the damping parameter shows a high variability which leads to a high coefficient of variation, and therefore, this parameter is not recommended for the evaluation of the structural condition of the towers.

Name	Mean Value	S.D. Value	C.V (%)
Healthy	0.46	0.05	10%
Damage Location 1	0.58	0.14	25%
Damage Location 2	0.43	0.08	20%
Damage Location 3	1.62	1.66	102%

Table 19 - Analysis of the effect of the delamination location in the damping of FRP materials.

This project has received funding from the European Union's Horizon 2020 research and innovation programme under grant agreement No 952966.

Analysis of the KPI's feasibility for the identification of the type of damage

The last case scenario is devoted to the analysis of the feasibility of the KPI's for the analysis of different typology of delamination defects for two practical cases: 1st) single delamination referred to delamination in one interlaminar region, and 2nd) multiple delaminations referred to three interlaminar regions. The main question arises with respect to the capability of this non-destructive method to identify the typology of delamination failure.

For this particular case, the natural frequencies of the healthy tower are superior to the natural frequencies of the delaminated towers (see Figure 66). However, it has not been appreciated clear changes for the towers with single and multiple delamination defects. As a conclusion, it can be said that it is not possible to extract clear conclusions from the results of this experimental trial.

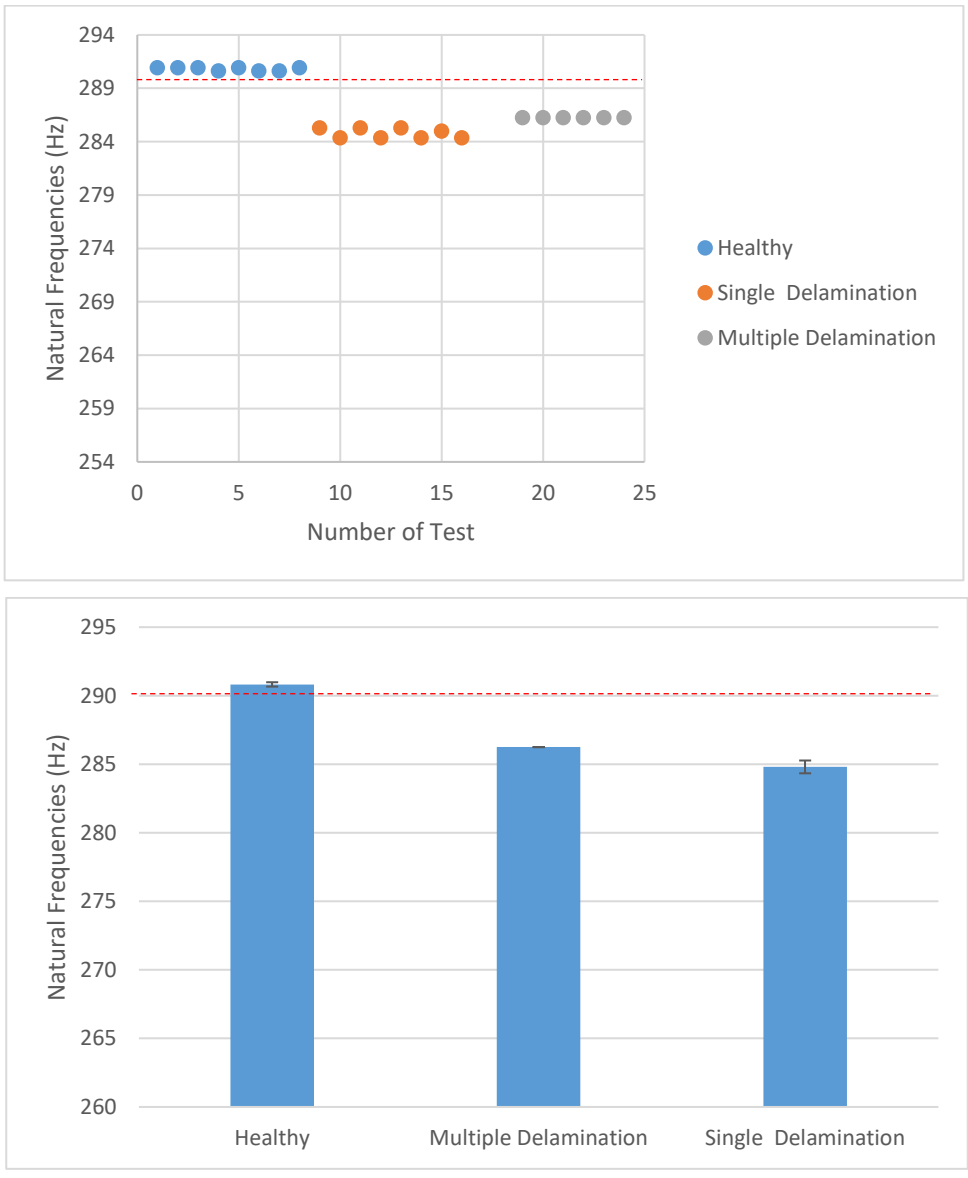

Figure 65: Effect of the delamination type on the natural frequencies of the towers.

This project has received funding from the European Union's Horizon 2020 research and innovation programme under grant agreement No 952966.

In parallel, the feasibility of the damping for the localisation delamination defects was also part of the investigation of this research study. The mean value, standard deviation, and coefficient of variation of the damping for the three towers are given in Table 20. In line with the above results, the damping parameter shows a large variability with coefficients of variation superior to the 20% and therefore, this parameter is not recommended for the evaluation of the structural condition of the towers.

Name	Mean Value	S.D. Value	C.V (%)
Healthy	0.46	0.05	10%
Multiple Delamination	0.46	0.08	20%
Single Delamination	1.62	1.66	102%

Table 20: Damping of the FRP towers with single and multiple delamination.

4.1.4. Conclusions

The main motivation of this research study is to investigate the feasibility of the natural frequencies, damping, and overall mode shapes for the detection, quantification, and localisation of tower structural damage in FRP-based towers. The fundamental idea behind a modal analysis is that the modal parameters (natural frequencies, damping, and vibration mode shapes) are functions of the physical properties of the composite structure (mass, damping, and stiffness). Therefore, changes in the physical properties of the material as per the example of stiffness reduction due to delamination breakages will cause changes in the modal characteristics.

- The main contribution of this research study is to prove that the shift of the natural frequencies can be used as a simple and cost-effective approach for the detection and quantification of delamination defects in the FRP-based towers used in the FOWTs. However, it should pointed out that the uncertanties of the manufacturing process in terms of mass, thickness and defects play a critical role on the efficiency of the technology.
- Apart from that, this paper investigates the changes of the damping due to the incorporation of delamination regions in the FRP towers. In general, the delamination defects tend to increase the damping of the towers because the delamination regions act as a dampers. However, the damping values present a large coefficient of variation, and therefore this key performance indicator is not recommended for the authors as a key performance indicators for the monitoring of the towers.
- Last, but not less important, the authors investigated the potential of the mode shapes for the detection of delamination defects. However, the authors of this paper discarded the variation of the mode shapes as a potential tool for the detection of delamination failures because it has not been apreciatted changes for the modes investigated in this research study.

This project has received funding from the European Union's Horizon 2020 research and innovation programme under grant agreement No 952966.

4.2. KEY PERFORMANCE INDICATORS FOR ANALYSIS OF THE INTEGRITY OF TOWER CONNECTIONS

The visual inspection of bolted joints in wind turbines is dangerous, expensive and impractical due to the non-possibility to access the platform by workboat in certain sea state conditions as well as the high costs derived from the transportation of maintenance technicians to offshore platforms located far away from the coast, especially if helicopters are involved. Consequently, the wind turbine operators have the need for simpler and less demanding techniques for the analysis of the bolts tightening.

Vibration-based structural health monitoring is one of the oldest and widely-used means for monitoring the health of onshore and offshore wind turbines. FIBREGY explored the potential applications of a Structural Health Monitoring technique for the evaluation of the integrity of FOWT towers connections. The core of this work is to find out if the modal parameters can be efficiently used as a key performance indicator (KPIs) for the assessment of joint bolts in a 1:50 scale tower of a Floating Offshore Wind Turbine (12 MW).

4.2.1. Methodology

The natural frequencies and damping of the towers were obtained by the research team using a vibration test. Figure 67 shows the steel-based tower tested in the framework of this experimental campaign. A detailed view of the connection tested can be seen in the inset of Figure 67. The tower consists of two parts which are a representation of the connection between the tower and the base of the offshore platform. This connection must be carefully controlled due to the fact that it is a critical point of the structure, which can lead to the entire collapse of the structure.

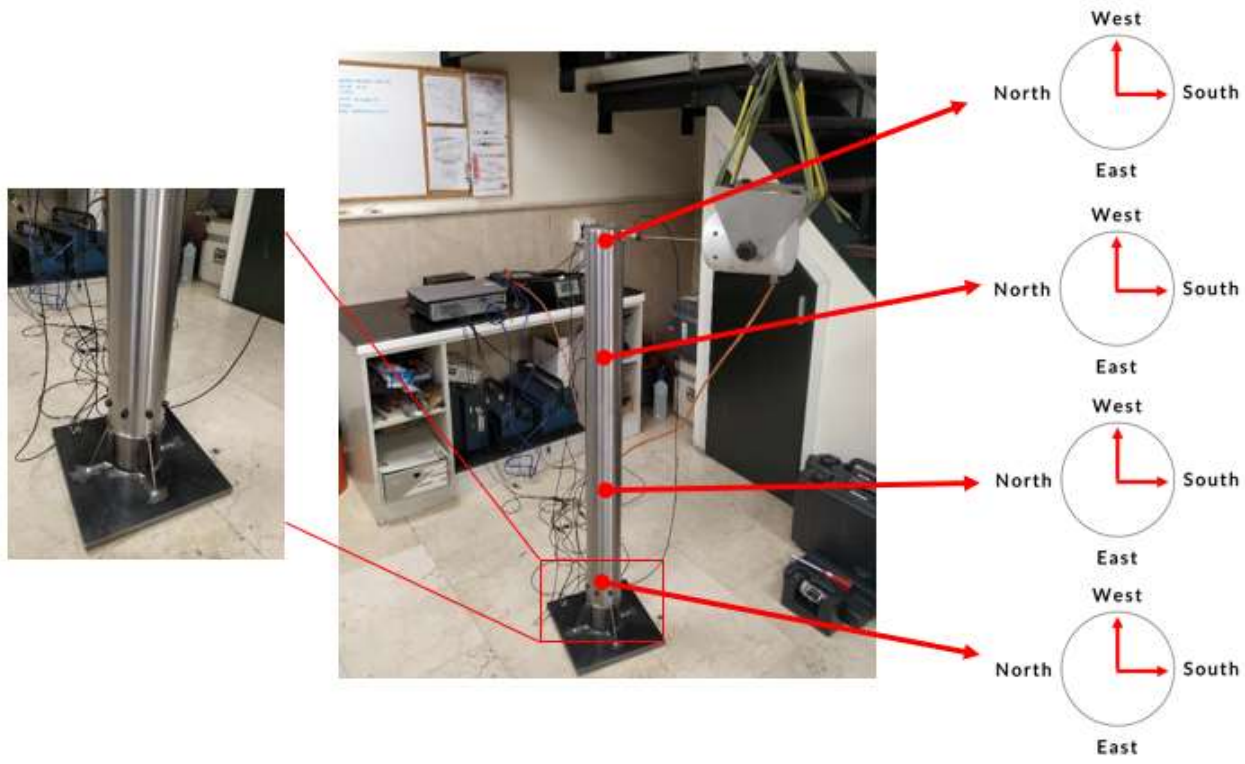

Figure 66: Schematic description of the non-destructive test used to test the connections integrity.

This project has received funding from the European Union's Horizon 2020 research and innovation programme under grant agreement No 952966.

The vibration test used for the analysis of the tightening torques of the 1:50 scale wind tower consists of three consecutive steps. Initially, an artificial excitation is introduced by means of commercial shaker mounted on the top of the tower. Subsequently, the vibration signals of the tower are measured by using an array of accelerometers at four different levels of the tower in the West and South directions. Eventually, the recorded signals of the sensors are used to calculate the modal parameters of the towers using the Software Siemens LMS.

The vibration-based strategy is based on the comparison of the modal parameters (natural frequencies, and damping) for various tightening torques (5 N/m, 6 N/m, 7 N/m, etc). The vibration signals of the composite towers are recorded for 3 s in the range of frequencies (0-1000 Hz) using an array of four commercial accelerometers (Endevco, 44A16-1032) placed at four different levels of the tower. This procedure was repeated five times to obtain a multiple number of realizations for each specimen.

4.2.2. Results and Discussion

This section shows and discusses the experimental results obtained from the modal analysis test detailed in Section 4.2.1. Initially, the effect of the number of loose bolts on the natural frequencies, and damping of the tower is analysed for several case scenarios (0, 1, 2, 3, 4, 5, 6, 7, and 8 bolts loosed). Secondly, the influence of the tightening torque on the modal parameters of the tower is investigated using the same non-destructive test for various cases (0 N/m, 5 N/m, 6 N/m, 7 N/m, etc.).

Case I: Effect of loosed bolts on the KPI's parameters

The main purpose of this experiment is to analyse if the modal parameter outputs are affected by the number of loose bolts of the tower connection. **Figure 68** (a) shows the natural frequencies for the multiple case scenarios tested in the tower. The graph reveals that the natural frequencies decrease as a function of the number of bolts loosed, which vary in the range from 0 to 8 bolts. Therefore, it can be clearly seen that the natural frequencies decrease from 20.48 ± 0.07 to 14.51 ± 0.02 when the number of loose bolts varies between 0 and 8. **Figure 68** (b) displays the natural frequencies of the tower as a function of the number of loose bolts. The graph includes the average natural frequencies and corresponding standard deviations for five repetitions of each boundary condition. The results show that the natural frequencies decrease gradually with the number of loose bolts. This behaviour can be explained by the fact that the stiffness of the tower is strongly affected by the number of loose bolts, which is dependent on the number of loose bolts. In other words, the union with more bolts leads to more stiffness, which results in an increment of the natural frequencies. From the results, it can also be deducted a linear correlation for the relationship between the natural frequencies and the number of loose bolts, with a Pearson of 0.97 and a sensitivity of 0.76 Hz is found on the measurement range.

As stated above, the damping of the natural frequencies is measured at different boundary conditions (see **Figure 69**). The main purpose is to investigate if the damping signals of the tower are dependent on the number of loose bolts. From the results, it can be seen that the damping increase gradually with the number of loose bolts, and therefore, the observed trend is that the damping increase when the number of loose bolts is increased. This behaviour can be explained by the fact that when the bolts are loose, the local frictions in the union of the tower are increased.

This project has received funding from the European Union's Horizon 2020 research and innovation programme under grant agreement No 952966.

(a)

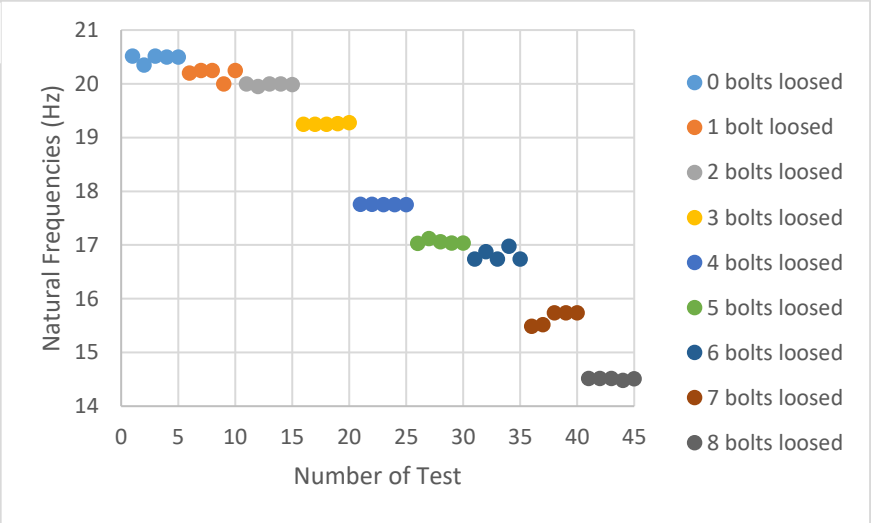

(b)

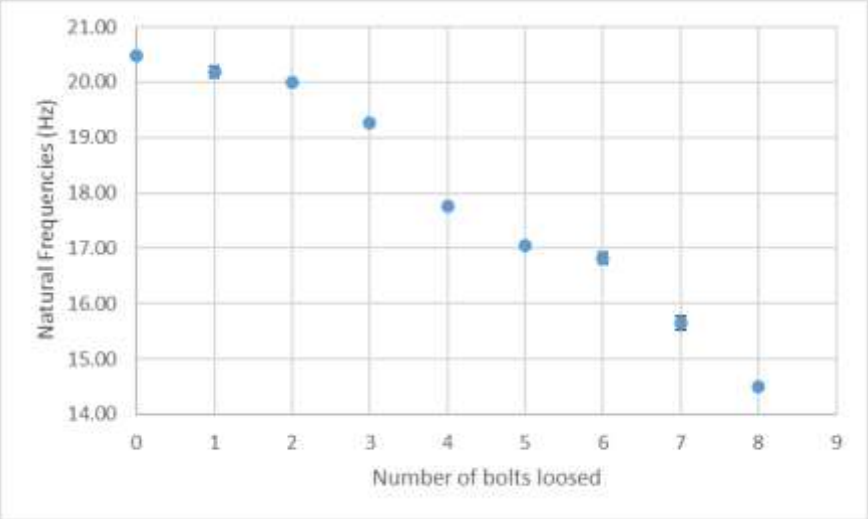

Figure 67: Influence of the number of loose bolts on the natural frequencies (a). Natural frequencies as a function of the number of bolts loosed (b).

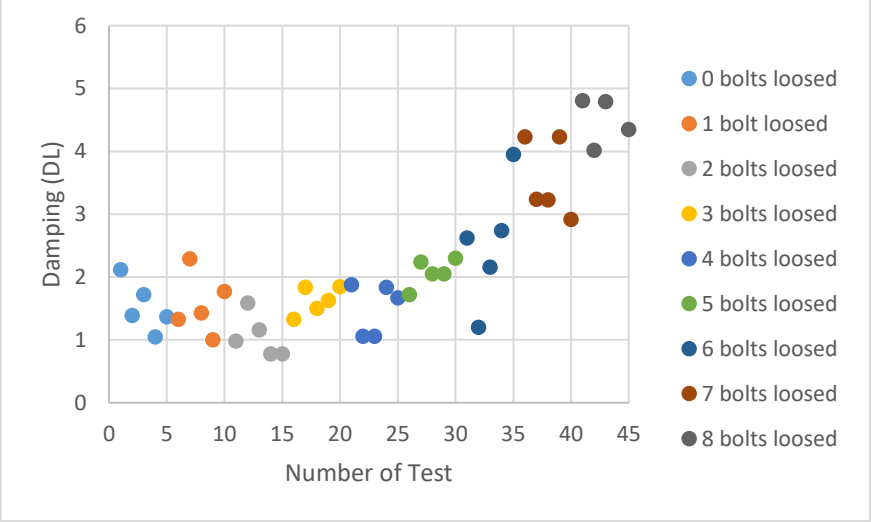

Figure 68: Effect of the number of loose bolts on the damping.

This project has received funding from the European Union's Horizon 2020 research and innovation programme under grant agreement No 952966.

Case II: Effect of the tightening torque on the KPI's parameters

The main objective of this experiment is to investigate the influence of the tightening torques on the modal parameters of a steel-based tower. For such purpose, the natural frequencies and damping of the tower are tested for various tightening torques which vary in the range from 0 N/m to 12 N/m.

Figure 70 shows the natural frequencies of the tower as a function of the tightening torque. The results given are the average natural frequencies and the corresponding standard deviations for the five measurements for each test. From Figure 70, it can be appreciated that the relationship between the natural frequencies and the tightening torque can be interpolated with two straight lines in the region from 0 to 7 N/m and another one between 7 to 12 N/m. The results display the natural frequencies increases at higher tensile forces of the bolts and finally saturates at 20.5 Hz. As a general rule, it can be said that the natural frequencies exhibit a very sensitive response to the applied tightening torque in the range from 0 to 7 N/m. However, in the region beyond 7 N/m, the natural frequencies reach a saturation point and it does not show good capabilities to distinguish in the range above 7 N/m.

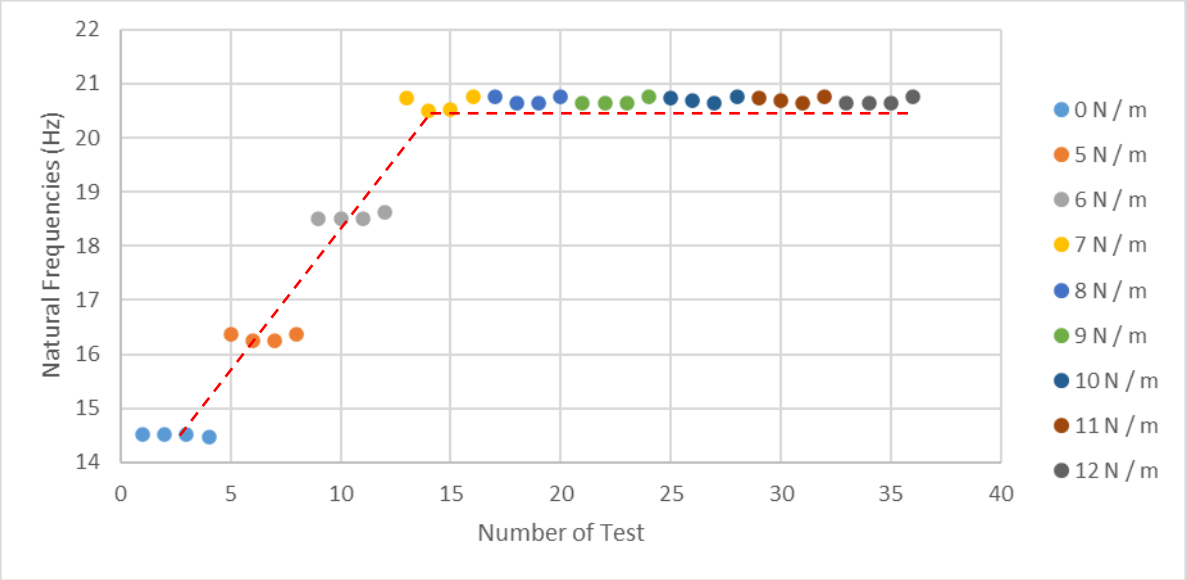

Figure 69: Effect of the tightening torque on the natural frequencies.

In parallel, the damping for the natural frequencies of the tower is measured at 0, 5, 6, 7, 8, 10, 11, 12 N/m as shown in Figure 71. As a general trend, it is appreciated that the damping tends to decrease for the towers with higher tensile strength, which can be attributed to the lower frictional levels of the bolts in the high-stress tensional bolt states. However, it is also observed a great level of dispersion for the results, which is an indicator of the high variability of the damping parameter. Thus, the authors of this study do not recommend that damping as a key performance indicator for the analysis of the tightening torques.

This project has received funding from the European Union's Horizon 2020 research and innovation programme under grant agreement No 952966.

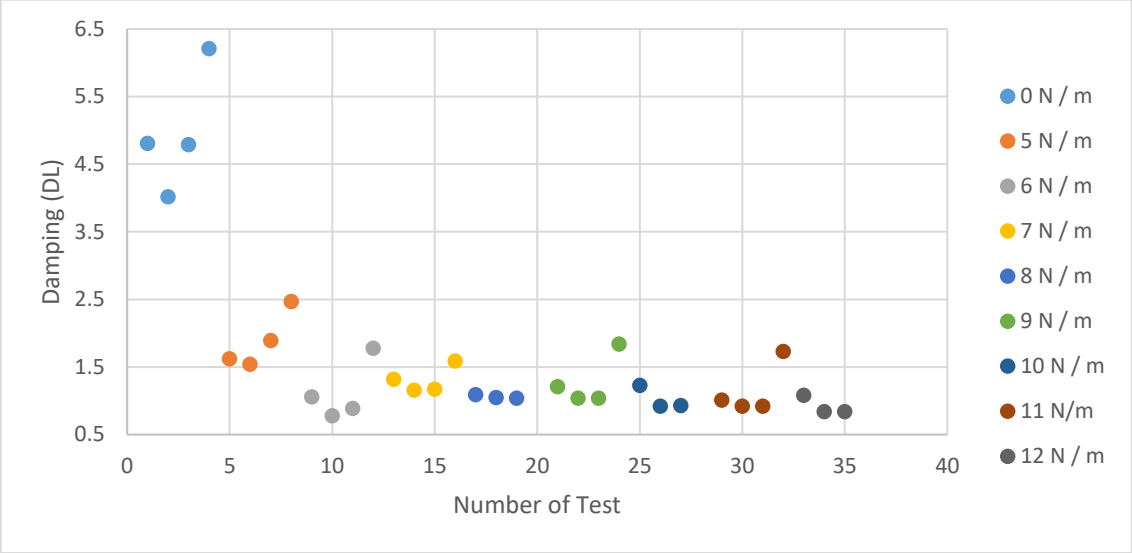

Figure 70: Effect of the damping on the tightening torque on the damping.

4.2.3. Conclusions

The FIBREGY project is conducting innovative research, where vibrations are utilized for estimation of the tightening torque of a 1:50 scale steel-based tower prototype.

- Initially, the effect of the number of loose bolts on the natural frequencies, and damping of the tower is analysed for multiple case scenarios (0, 1, 2, 3, 4, 5, 6, 7, and 8 bolts loosed) through a non-destructive test. The results reveal a direct relationship between the natural frequencies of the tower and the number of loose bolts, which demonstrates the sensitivity of this non-destructive method for the detection of loose bolts.

  In parallel, the authors investigated the relationship between the damping and the number of bolts loosed. The damping can be defined as the capability of a material to dissipate energy. For such a case, it can be observed that the damping increases gradually with the number of loose bolts, which might be attributed due to the local frictions exerted in the region of the connections between the tower and the base.

- Secondly, the influence of the tightening torque on the modal parameters of the tower is investigated using the same non-destructive test for various cases (0 N/m, 5 N/m, 6 N/m, 7 N/m, etc.) using a modal analysis test. From the results, it can be appreciated that the relationship between the natural frequencies and the tightening torque can be interpolated with two straight lines in the region from 0 to 7 N/m and another one between 7 to 12 N/m. As a general conclusion, it can be said that the natural frequencies exhibit a very sensitive response to the applied tightening torques in the range 0 - 7 N/m. However, the shift of the natural frequencies is not able to distinguish the tightening torques in the range above 7 N/m. Thus, it can be concluded that this method is limited to the region between 0 and 7 N/m.

  Apart from that, the research also focused on the relationship between damping and tightening torques. As mentioned above, the damping tends to be decreased with the increment of the tightening torque, however, this relationship is not clear due to the great dispersion of the data.

This project has received funding from the European Union's Horizon 2020 research and innovation programme under grant agreement No 952966.

The findings of this research carried out in the context of FIBREGY possess multiple implications for the assessment of the bolted joint integrity in multiple types of connections as tower-to-nacelle, modular, tower-to-column, tube-to-tube, etc.

This project has received funding from the European Union's Horizon 2020 research and innovation programme under grant agreement No 952966.

5. REFERENCES

1. *A novel piezoelectric thin film impact sensor: Application in non-destructive material discrimination.* **S. Joshi, G.M. Hedge, M.M. Nayak, K. Rajanna.** 272-282, s.l. : Sensors Actuators A Physics, 2013, Vol. 199.

2. *Flexible-foam-based capacitive sensor arrays for object detection at low cost.* **al., C. Metzger et.** 013506, s.l. : Applied Physics Letters, 2008, Vol. 92.

3. *Tactile sensor arrays using fiber Bragg grating sensors.* **312-327, s.l. : Sensors Actuators A Physics, 2006, Vol. 126.**

4. *Wearable triboelectric sensors for biomedical monitoring and human-machine interface.* X. Pu, S. An, Q. Tang, H. Guo, C. Hu. 102027, s.l. : iScience, 2021, Vol. 24.

5. *Hybrid resistive tactile sensing.* H. Zhang, E. So. 57-65, s.l. : IEEE Trans. Syst. Man Cybern. Part B, 2002, Vol. 32.

6. *Evaluation of air-bag electronic sensing system collision performance through laboratory simulation,.* D. Toomey, E. Winkel, R. Krishnaswami. s.l. : Proceedings of SAE World Congress and Exhibition, April 2015.

7. *Triboelectric sensor as a dual system for impact monitoring and prediction of the damage in composite structures* . C. Garcia, I. Trendafilova. 527-535, s.l. : Nano Energy, 2019, Vol. 60.

8. *Impact damage localisation with piezoelectric sensors under operational and environmental conditions.* M.S. Salmanpour, Z.S. Khodaei, M.H.F. Aliabadi. 1178, s.l. : Sensors, 2017, Vol. 17.

9. *Vibration Analysis Techniques included in the Predictive Maintance Plan of a Paper Machine.* Gutierrez, Paula Ibarrola. s.l. : E.T.S. de Ingeniería Industrial, Informática y de Telecomunicación (UPNA), 2019.

10. SUMMIT electronics. PCB Accelerometers . *https://www.summit.dk/en/products/pcb-accelerometers/#accordion1.* [Online]

11. FIBREGY consortium. *D2.10 - Engineering, production and life-cycle management for the complete construction of large-length FIBRE-based SHIPs.* 2020.

12. *Composites improving corrosion mitigation on offshore assets.* Offshore Magazine.

13. *Triboelectric sensor as a dual system for impact monitoring and prediction of the damage in composite structures.* Garcia, C. and Trendafilova, I. 527-535, s.l. : Nano Energy, 2019, Vol. 60.

14. *Delamination Detection in Polymeric Ablative Materals Using Pulse-Compression Thermography and Air-Coupled.* Laureti, S., et al. 2198, s.l. : Sensors, 2019, Vol. 19.

15. *Modeling of Acoustic Emission Signal Propagation in Waveguides.* Zelenyak, A.M., Hamstad, M.A. and Sause, M.G.R. 11805–11822, s.l. : Sensors, 2015, Vol. 15.

16. *Effect of delamination on the natural frequencies of Composite Laminates.* Pardoen, G.C. 1200–1215, s.l. : J. Compos. Mater, 1989, Vol. 23.

17. Schaaf, Kristin Leigh. *Composite materials with integrated embedded sensing networks.* s.l. : University of California, San Diego, 2008.

18. Meggitt. Extreme+ High Temperature Piezoelectric Accellerometer (E+HTPE). *https://www.meggitt.com/resources/product_sheets/2021/6245_DS_2021.pdf.* [Online]